Fall 11-2015

Lumped Parameter Model for a Self Powered Fontan Palliation of the Hypoplastic Left Heart Syndrome

Jang Ho Park
Embry-Riddle Aeronautical University

LUMPED PARAMETER MODEL FOR A SELF-POWERED FONTAN PALLIATION OF THE HYPOPLASTIC LEFT HEART SYNDROME

by

Jang Ho Park

A Thesis Submitted to the College of Engineering Department of Mechanical Engineering in Partial Fulfillment of the Requirements for the Degree of Master of Science in Mechanical Engineering

Embry-Riddle Aeronautical University
Daytona Beach, Florida
November 2015

LUMPED PARAMETER MODEL FOR A SELF POWERED FONTAN PALLIATION OF THE HYPOPLASTIC LEFT HEART SYNDROME

by

Jang Ho Park

This thesis was prepared under the direction of the candidate's Thesis Committee Chair, Dr. Eduardo A. Divo, Associate Professor, Daytona Beach Campus, and Thesis Committee Members Dr. Jean M. Dhainaut, Associate Professor, Daytona Beach Campus, and Dr. Victor Huayamave, Visiting Assistant Professor, Daytona Beach Campus, and has been approved by the Thesis Committee. It was submitted to the Department of Mechanical Engineering in partial fulfillment of the requirements for the degree of Master of Science in Mechanical Engineering

Thesis Review Committee:

Eduardo Divo, Ph.D.
Committee Chair

Jean-Michel Dhainaut, Ph.D.
Committee Member

Victor Huayamave, Ph.D.
Committee Member

Jean-Michel Dhainaut, Ph.D.
Graduate Program Chair,
Mechanical Engineering

Charles F. Reinholtz, Ph.D.
Department Chair,
Mechanical Engineering

Maj Mirmirani, Ph.D.
Dean, College of Engineering

Christopher Grant, Ph.D.
Associate Vice President of Academics

12/10/2015

Date

Acknowledgements

I would like to express thanks to my advisor Dr. Eduardo Divo for his guidance, encouragement and support throughout the thesis work. I would like to appreciate his expertise in the field which motivated me to work in this area of study and for his encouragement in me at every stage of the research.

I would like to show my gratitude to the professors who helped me by providing guidance throughout the thesis work. I would like to appreciate their encouragements as well as the information they provided me whenever I came across an obstacle.

I would like to thank Arnold Palmer Hospital for Children for providing expertise knowledge related to the content and ideas behind the research.

I would also like to thank my family and friends for their support and encouragement. I would specially like to thank my fiancé, Yue Hu for the support throughout the thesis work.

Abstract

Researcher: Jang Ho Park

Title: LUMPED PARAMETER MODEL FOR A SELF POWERED FONTAN PALLIATION OF THE HYPOPLASTIC LEFT HEART SYNDROME

Institution: Embry Riddle Aeronautical University

Year: 2015

Out of all newborn infants with congenital heart disease (CHD), 8% have a single functioning ventricle. The Fontan surgical procedure, where the superior and inferior venous returns are connected directly to the pulmonary arteries to allow the single functioning ventricle to perfuse the systemic circulation, has been around for decades, yet the patients who undergo this operation suffer from chronic illnesses and their survivability is less than 50% by adulthood [1-10]. Some suggest that the Fontan operation can be improved by implanting a synthetic pump. However, synthetic pumps also present some complications due to mechanical failure, risk of stroke, and risk of infection [23-30]. The purpose of this study is to numerically simulate the hemodynamics of a self-powered Fontan circulation aided by the reserve ventricular energy captured by the entrainment effect of an Injection Jet Shunt (IJS). A simulation is created to identify important physiological parameters caused be the IJS. By numerically approximating the solution using a lumped parameter model (LPM) of a single ventricle cardiovascular system, the physiological parameters can be approximated. Systemic flow, pulmonary flow, caval pressure and ratio between the pulmonary and systemic flows will be determined to verify whether the IJS is beneficial to the Fontan circulation.

Table of Contents

Table of Figures

Table of Tables

Introduction

Background

Out of all newborn infants with congenital heart disease (CHD), 8% have a single functioning ventricle [1-10]. Hypoplastic left heart syndrome (HLHS) is a heart defect where the left ventricle of the heart is atrophied and the aorta is underdeveloped before birth. In healthy babies, the left side of the heart receives oxygenated blood from the lungs and pumps into the rest of the body. With a defective left ventricle and malfunctioning aorta and mitral valve, the heart cannot circulate a sufficient amount of blood to the body and vital organs [68].

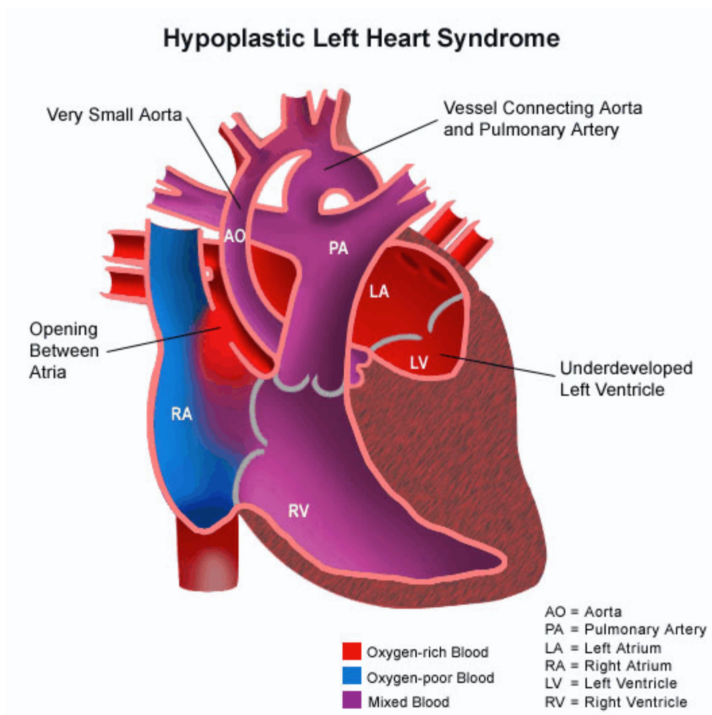

Figure 1 Hypo-plastic Left Heart Syndrome [1]

The right side of the heart is often used to pump the blood to the body for babies who suffer from HLHS. The objective of the stage 1 Norwood operation is to connect the single ventricle enabling a systemic circulation. The stage 1 Norwood procedure consists on implanting a shunt and opening the ductus arteriosus which connects the pulmonary artery and the descending aorta. By leaving the patent ductus arteriosus open and sealing off the left ventricle, the right ventricle becomes capable of supplying the blood to the systemic circulation. However, the blood flow towards the lungs are disrupted, which mandates an alternative path for the blood to pass through the lungs [53].

The stage 2 procedure, also known as Kawashima Procedure or Glenn procedure, is a procedure where venous flow is directed into the lungs. By using the superior vena cava (SVC) blood return from the upper body, blood is redirected to the lungs enabling the limitation of the disrupted blood flow to the lungs from the stage 1 Norwood procedure. However, patients still suffer from hypoxia since the inferior vena cava (IVC) blood return from the lower body isn't fed into the lungs to be oxygenated [69].

The Fontan procedure, also known as Kreutzer procedure, is a stage 3 procedure. This procedure involves the redirecting blood from IVC to the lungs. However, the poorly oxygenated blood from the SVC and IVC flows into the lungs without being pumped but is driven only by the pressure that is generated in the vessel. This corrects the problem of hypoxia and the right heart is capable of supplying blood to the entire human body [56].

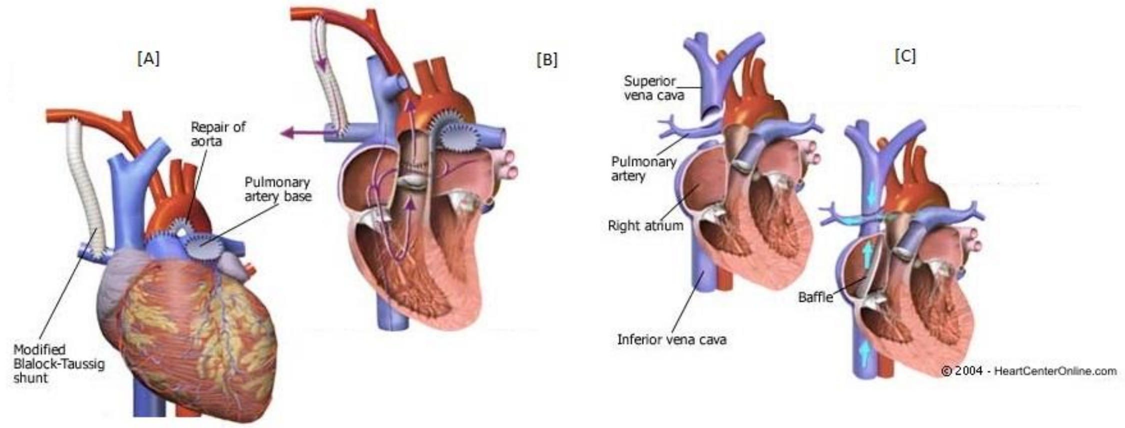

Figure 2 [A] Norwood Operation [B] Kawashima Operation [C] Fontan Operation [2,3,4]

Despite the fact of 3 stage procedure which has served as palliation for decades, less than 50% of the babies survive to adulthood due to chronic illnesses. In the Fontan circulation, the blood flows passively through the human body into the lungs due to the absence of the left heart. Over the past 3 decades, patients who have undergone the surgery have been improving due to the improvement in surgical procedures and pharmacological therapies. Since the original procedure of direct connection between the right atrium to pulmonary artery connection, there have been numerous alternative methods that were suggested to improve the circulation of blood throughout the human body as well as the surgical procedure itself [22].

Injection Jet Shunt (IJS)

In addition to the Fontan operation, a graft will be added from the ventricle or the aorta connecting to the pulmonary artery.

Figure 3 Injection Jet Shunt (IJS) Graft

The graft will directly assist the flow to the lungs from the ventricle or the aorta using the reserve mechanical energy from the heart itself and help the Fontan circulation. This graft will be called the Injection Jet System (IJS). The principle of IJS is used widely in the fluid mechanics industry, however, it has never been addressed to the Fontan circulation [31]. By successfully implementing the IJS, the Fontan circulation will have increase in pulmonary blood pressure and flow, better delivery of oxygen throughout the body and the lungs and decrease in pressure of the inferior vena cava. Due to the fact IJS system has never been validated in the Fontan circulation, the simulation will include the IJS being connected from the ventricle to the pulmonary artery to investigate the results before the CFD (computation fluid dynamics) models.

Mathematical Modeling

There are numerous methods that have been developed over the past decade to simulate the circulatory system of the heart. Due to the advance in computational simulation, experimental simulation and computational fluid dynamics can be used to simulate an approximation of the outcome. Before moving on to computational fluid dynamics, experimental simulation is made using mathematical approach in order to validate the parameters that will be used for computational fluid dynamics models.

The circulatory system of human body can be represented as a state-space model of a Resistance – Inductance – Capacitance circuit (RLC circuit). By solving the state-space variable, the pressure and the flow can be derived and approximated inside the circulatory system [34]. The human circulatory system can be simplified by using lumped parameter modeling. In this case, lumped parameter modeling can be used to model Fontan circulation. The Fontan circulation is initially designed to have 22 variables and IJS will be added. These variables will be solved using Runge-Kutta 4th order method (RK4). However, the lumped parameter model has been simplified so that there will be 12 different equations and IJS attached to it. The system of equations will be solved using the built in function ‘ode45’. This will allow the system of equations to be solved using Runge-Kutta 4th order method. After the system of equations are solved, a plot will be generated to demonstrate the pressure and flow at different points in the lumped parameter model.

After the plots are generated, flow measurements and pressure measurements will be taken to determine important parameters in the circuit and verify to validate the effect of Injection Jet system and compare the values without the Injection Jet System. The purpose of the simulation is to compare the values and check whether the flow and pressure values resides within the range

Methods

Cardiovascular system can be represented as a lumped parameter model using RLC circuit. The resistance resembles pressure, inductance resembles inertia of the flow and capacitance resembles the vessel compliance. This is called lumped parameter model. In a mathematical perspective of lumped parameter model, partial differential equations (PDE) of a space model are simplified to an ordinary differential equations (ODE) [34, 54, 70].

RL Circuits

Viscous vascular resistance (R), inertia of the flow (L) and flow rate (Q) are used to find the pressure difference (ΔP). The analogy to this comes from the idea behind Ohm's law.

$$\Delta P_{(t)} = L\frac{dQ_{(t)}}{dt} + RQ_{(t)} \quad \text{Equation 1}$$

Voltage (V) is the Potential difference which is equivalent to pressure difference (ΔP), current (I) is the flow rate (Q), L is the inertia of the flow and resistance (R) is the vascular resistance. The Ohm's law applies directly to the model of cardiovascular system either it is in series or parallel for the resistances to be calculated. The flow rate will be calculated over an inductor or inductance also known as the inertia of the flow.

The inductance works just like a resistance and will be combined together using Ohm’s law as well [34, 54, 70].

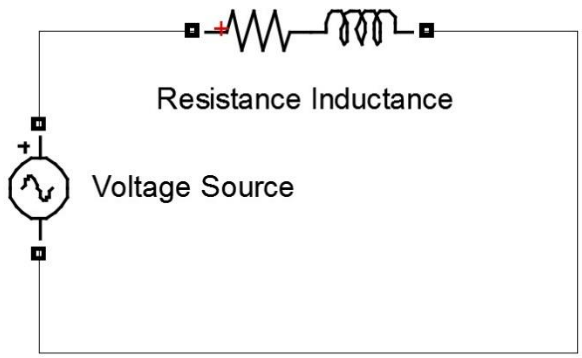

Figure 4 R (resistance) L (inductance) Circuit

In general, the solution of a linear variable coefficient, 1st order ODE:

$$\frac{\partial y_{(t)}}{\partial t} + F_{(t)} y_{(t)} = \ g_{(t)} \quad \text{Equation 2}$$

Found through an integration factor $I_{(t)}$ as:

$$y_{(t)} = \frac{1}{I_{(t)}} * \int I_{(t)*} g_{(t)} \, \partial t \quad \text{Equation 3}$$

So that

$$I_{(t)} = e^{\int F_{(t)} \partial t} \quad \text{Equation 4}$$

The RL circuit equation using the general solution of 1st order ODE can be expressed as:

$$\Delta P_{(t)} = L \frac{dQ_{(t)}}{dt} + RQ_{(t)} \quad \text{Equation 5}$$

Where general solution can be found as:

$$Q_{(t)} = \frac{\Delta P}{R} + C1 * e^{\frac{-R}{L}t} \quad \text{Equation 6}$$

RLC Circuits

The compliance of a vessel in a fluid lumped parameter model can be simulated by using a capacitor (C). A compliance is where the blood is stored and released over time. The flow rate (Q) flowing through the capacitor is related directly to the change in pressure (ΔP). The compliance can be measured directly through the change in volume and pressure in the vessel and the compliance is assumed as a constant [34, 54, 70].

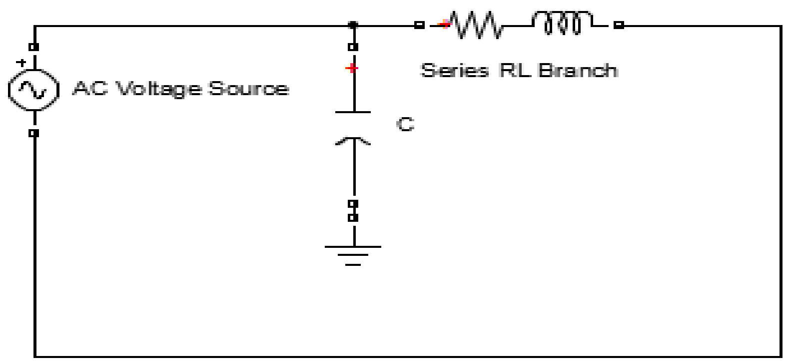

Figure 5 R (resistance) L (inductance) C (capacitance) Circuit

In a simple RLC circuit, the pressure drop across the RLC elements are given as:

$$L\frac{\partial Q_{(t)}}{\partial t} + RQ_{(t)} + \frac{1}{C}\int_{-\infty}^{t} Q_{(t)}\partial t = \Delta P_{(t)} \quad \text{Equation 7}$$

By differentiating the equation assuming the capacitance (C) is a constant:

$$L\frac{\partial^2 Q_{(t)}}{\partial t^2} + R\frac{\partial Q_{(t)}}{\partial t} + \frac{1}{C}Q_{(t)} = \frac{dP_{(t)}}{dt} \quad \text{Equation 8}$$

A second order constant coefficient liner ODE is generated.

In the RLC circuit, the circuit will contain a parallel compliance. On the node of separation, Kirchhoff's Current Law (KCL) will be applied. KCL states that the sum of currents flowing into that node is equal to the sum of currents flowing out of that node. This is equivalent to conservation of mass in fluids. In addition, since it is a close circuit with different pressure along the circuit, Kirchhoff's Voltage Law (KVL) states that the directed sum of pressure differences around a closed circuit is zero. This is equivalent to conservation of energy in fluids [34, 54, 70].

When solving the equation, the idea is to form a system of 1^{st} order ODEs. By forming 1^{st} order ODEs, the unknowns are the pressure associated with each compliance and the flow rates associated with each inductance. After applying KCL and KVL, a system of 1^{st} order ODE can be found. The system of 1^{st} order ODE can be expressed in a state variable matrix as:

$$\frac{\partial y}{\partial t} = [A]y + b \quad \text{Equation 9}$$

Where A is the state or system matrix and b is the input matrix.

In cardiovascular system, there are heart valves. The heart valves allows the blood to flow in one direction throughout the cardiovascular system. There are four valves in the cardiovascular systems. They are mitral valve, tricuspid valve, aortic valve and pulmonary valve. The mitral valve and tricuspid valve are between the upper atria and the lower ventricle. The aortic valve and pulmonary valve are the valves located near the arteries leaving the heart.

In the Fontan operation, due to the missing right heart, tricuspid valve and pulmonary valve are the ones that are operational. The valve can be represented by using a combination of diode and corresponding valve viscous resistance. A diode is an electrical element designed to allow flow in one direction as long as the pressure gradient is negative but block the flow in the opposite direction if the pressure gradient becomes positive. The valve will use Poiseuille's Law. The discontinuity can be formulated in terms of Heaviside step function (H) [34, 54, 70].

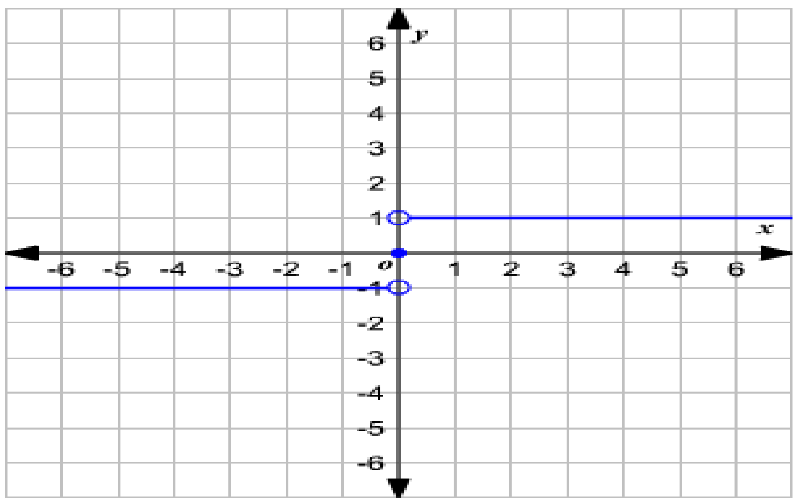

Figure 6 Heaviside Function to demonstrate the valves (diodes)

The valve formulation using Poiseuille's Law and the Heaviside function becomes as:

$$Q_{v(t)} = \left[\frac{P_{1(t)} - P_{2(t)}}{R_{valve}}\right] H\left(P_{1(t)} - P_{2(t)}\right) \quad \text{Equation 10}$$

By adding in the valves, the valve alters system of equation to become non-linear because of the presence of the Heaviside function (H) [34,70]. This alternates the state variable equation as series of non-linear system equations which can be represented as:

$$\frac{\partial y}{\partial t} = [A]_{(t)} y_{(t)} + b_{(y,t)} \quad \text{Equation 11}$$

However, the non-linear system can be replaced using two linear systems where the input matrix (b) is represented by an open valve or a closed valve. When the valve is open, the

Heaviside function (H) becomes 1 and when it is closed the Heaviside function (H) becomes 0.The system can be solved by using Runge-Kutta 4th order ODE (RK4) by switching the state depending on the condition of the Heaviside function [71].

Runge-Kutta method is a method in numerical analysis for controlling error. The idea is to compute two estimates of the solution at time step n+1. One using the original time step Δt and another using half of the original time step in two steps.

$$y_{n+1} = y_n + \frac{1}{6}(K_1 + 2 * K_2 + 2 * K_3 + K_4) \quad \text{Equation 12}$$

The value (y_{n+1}) is determined by y_n plus the weighted average of the four increments. The increments are K_1, K_2, K_3, and K_4. The increments are the product of the size of the interval and an estimation of the slope specified to the function using the right hand side of the function. K_1 is the increment based on the beginning interval and K_2 and K_3 are the increments based on the slope at midpoint and K_4 is the increment based on the endpoint. Since Runge-Kutta method is highly dependent on the size of the time step, it is important to pay attention while the incremental points are switching.

Since the cardiovascular system is homogeneous, where b = 0, it is important that the initial conditions y(0) are non-zero values otherwise the solution will result to be trivial solution which is zero. Therefore a good physiological starting value must be determined prior to solving the system of equations [71].

Ventricular Function through Time Varying Compliance

Time varying compliance is used to simulate the ventricles of the cardiovascular system. There are some important physiological parameters that must be determined which are the maximum (E_{max}) and minimum (E_{min}) elastance of the ventricle. The elastance of the ventricle ($E_{V(t)}$) is a measurable quantity which is the inverse of its compliance ($C_{V(t)}$). The elastance of the ventricle can be expressed in terms of maximum and minimum elastance as:

$$E_{V(t)} = \left((E_{max} - E_{min}) * E_{n(t_n)}\right) + E_{min} \quad \text{Equation 13}$$

Normalized elastance (E_n) is a non-dimensional elastance to curve fit the measured parameters throughout the heart cycle and t_n is a non-dimensional time according to E_n. Normalized elastance function is also known as the "Double Hill" function [34, 54, 70].

$$E_n(t_n) = 1.55 * \left[\frac{(\frac{t_n}{0.7})^{1.9}}{1+\left(\frac{t_n}{0.7}\right)^{1.9}}\right] * \left[\frac{1}{1+\left(\frac{t_n}{1.17}\right)^{21.9}}\right] \quad \text{Equation 14}$$

The normalized time parameter (t_n) is defined as:

$$t_n = \frac{t}{T_{max}} \quad \text{Equation 15}$$

Where t is time in seconds and T_{max} is the shifted heart cycle period defined as:

$$T_{max} = 0.2s + 0.15t_c \quad \text{Equation 16}$$

Where t_c is the standard heart cycle period in seconds (s) calculated through the heart rate (HR) in beats per minute (BPM) as:

$$t_c = \frac{60}{HR} \quad \text{Equation 17}$$

The Simulink diagram for the Time varying compliance looks like the following.

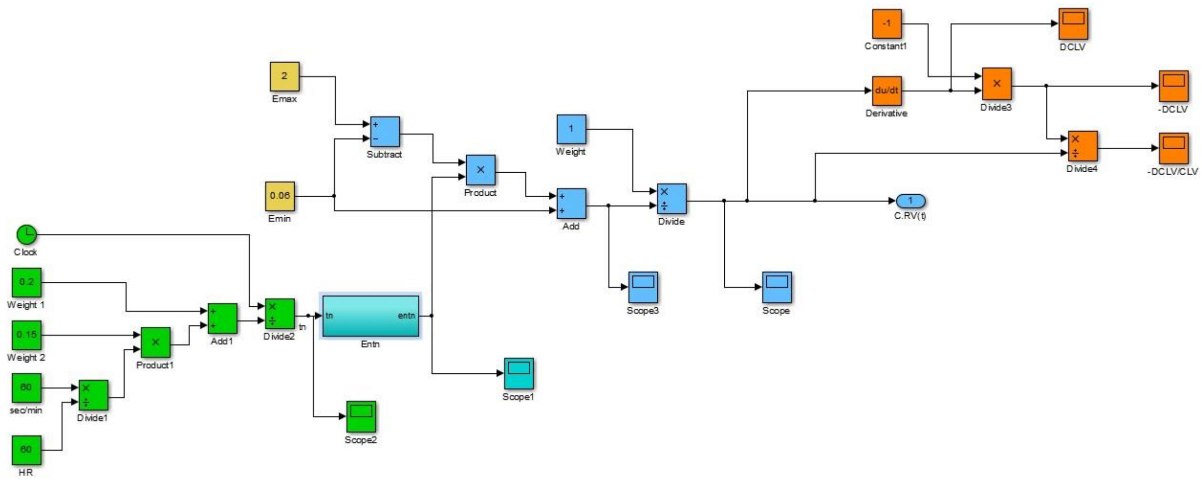

Figure 7 Time varying Compliance components

The reason we use a time varying compliance instead of a normal voltage source is due to the discontinuities that is caused by the valves. Since the function is discontinuous, it is better to use time varying compliance than a normal voltage source.

Fontan Circulation

In a Fontan circulation, the systemic venous return is connected to the pulmonary arteries without the interposition of a ventricle. In a Fontan circulation the post capillary energy is used to push the blood through the lungs. In other words, Fontan circulation cardiac output is no longer determined by the heart but by the pulmonary flow. The Fontan circulation can be simulated using a lumped parameter model. The lumped parameter model looks like the following:

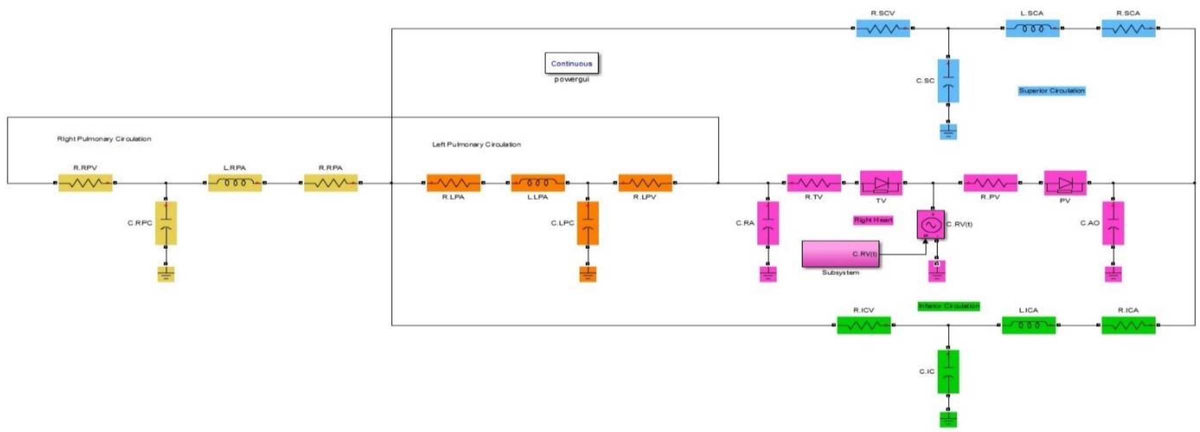

Figure 8. Lumped Parameter Model of Fontan Circulation

The lumped parameter model is made by using RLC circuit and a time varying compliance (capacitor). The vascular resistance (R), inductance (L) to measure the flow rate (Q), and compliance (C). The time varying compliance will represent the pulmonary flow which will allow the circulation in the system. There will be two diodes representing the two heart valves. The valves will be opened or closed depending on the Heaviside function and two state equation will be generated for each valve [34, 54, 70]. In total, there will be 4 matrices which will be dependent on the 2 valves with two states. The lumped parameter model will contain 12 degrees of freedom (DOF) which means there will be 12 state variables representing different pressure and flow rates. These state variables will be listed in a specific order **[**35-38**]**.

Injection Jet system

The principle of Injection Jet System is a mechanism that is used in the fluid mechanics industry. A graft is added to an existing tube. The graft will help the existing flow and push the flow to the region which is needed, in this case, the lungs. This is an alternative method and an easier solution compared to adding a synthetic heart pump.

The IJS will be originating from the ventricle, bifurcates with each tapered distal limb sutured into the pulmonary arteries in a way that the flow is directed parallel to the left and right pulmonary arteries. The energy and momentum generated from the graft will deliver the flow efficiently to the venous flow towards the lungs.

By adding the IJS, the lumped parameter model will contain 13 degree of freedom, 13 state variables, 7 equations related to the pressure of the Fontan circulation and 5 equations related to the flow of the circulation.

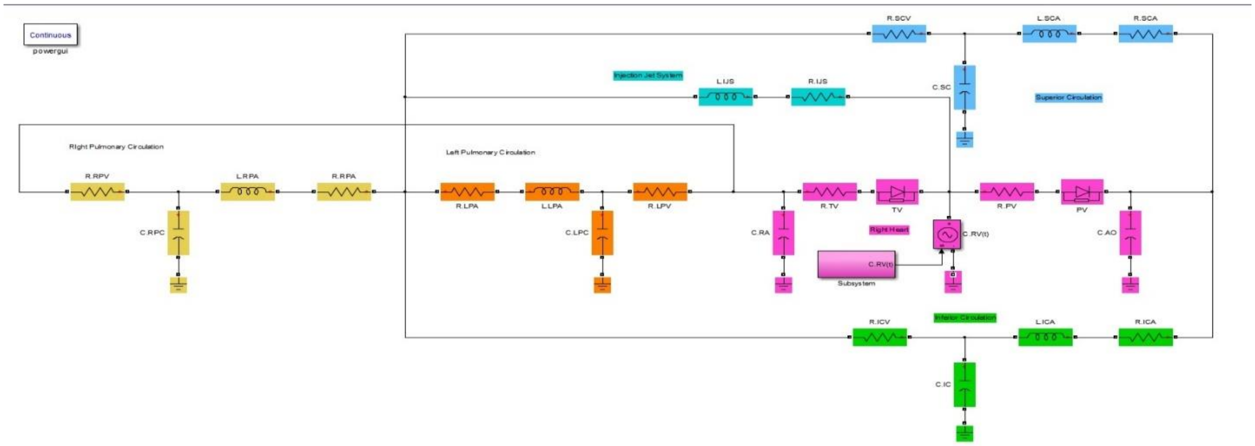

Figure 9. Lumped Parameter Model of Fontan Circulation with Injection Jet System

Simulation in MATLAB

The purpose of the simulation is to verify and validate the simplified model of the Fontan operation as well as to implement IJS into the Fontan circulation and check some physiological parameters associated with IJS. By quantifying the numerical values and validating the range of the values derived from the simulation, an assumption can be made and could validate whether the IJS implementation to the Fontan circulation is capable or not.

The simulation is divided into three parts. The first part consists the time varying compliance, the second part is the matrix consisting 4 cases depending on the valves open-closed conditions and the third part is using ode45 function to solve the state variable equation.

Valve	Tricuspid	Mitral
	Closed	Closed
	Open	Closed
	Closed	Open
	Open	Open

Table 1 State of Tricuspid and Mitral Valve

Time Varying Compliance

The time varying compliance is used to simulate the right ventricle of the circulation. The time varying compliance is written in MATLAB as a time dependent function. Determining the maximum and minimum elastance of the ventricle and the shifted heart cycle period to find the normalized elastance, the time varying compliance will be determined.

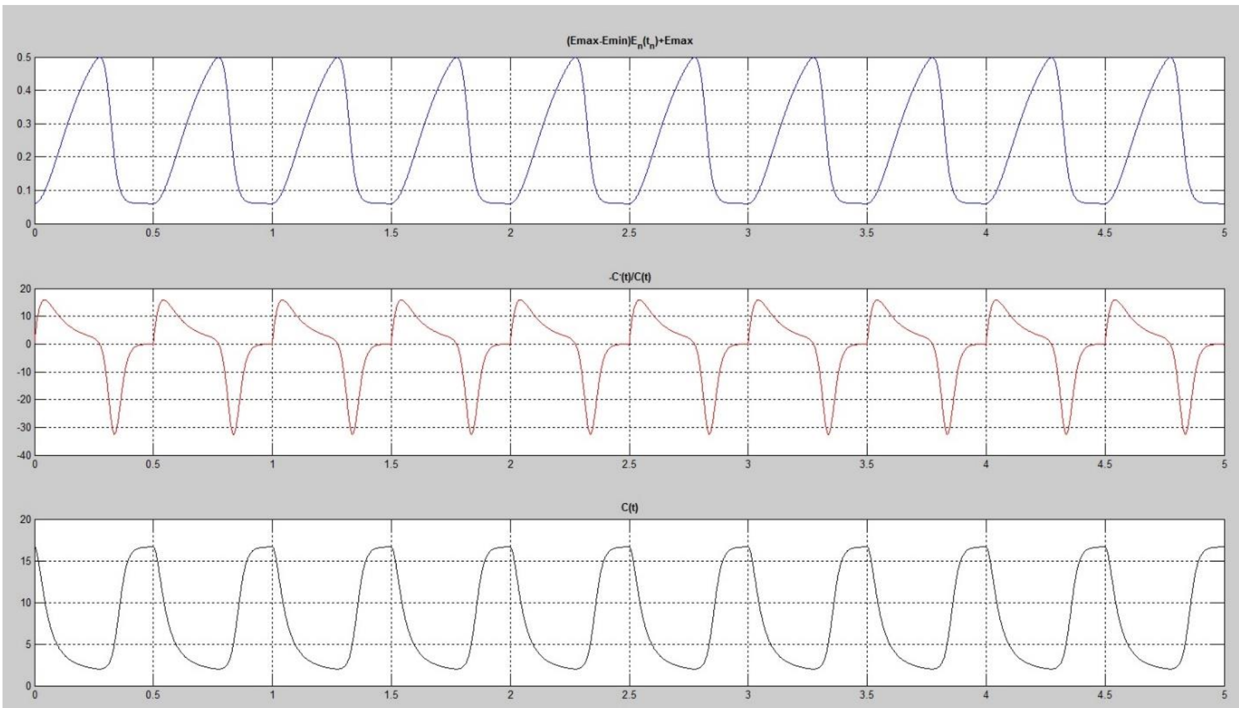

Figure 10 Time varying compliance elastance of the right ventricle and the derivative

The value of the elastance of the right ventricle is shown above and it is repeating between the maximum and minimum elastance. By using the equation:

$$E_{V(t)} = \left((E_{max} - E_{min}) * E_{n(t_n)}\right) + E_{min} \quad \text{Equation 18}$$

By taking the inverse of the elastance of the right ventricle, time varying compliance value, C(t) can be found. The derivative of the compliance is taken since it will be used throughout the mathematical calculation of the 2nd row vector of the system of equations.

Determining the State variables

The second part of the simulation is solving and determining the 13 state-variable equations. The equations are derived using Kirchhoff's current rule (KCL) and voltage rule (KVL). These equations will determine the pressure at each nodes and determine the flow over the inductors presented on the lumped parameter model. There will be 8 nodes that will measure the pressure at each nodes and 5 flow measurements over the inductor. In the circuit, there are 2 diodes that resembles the heart valve in the circuit. The valves will alternate between opening and closing depending on the pressure in the ventricle and the atrium. When the pressure of the ventricle is greater than the pressure of the atrium, the tricuspid valve opens. When the pressure of the atrium is greater than the pressure of the aorta, the pulmonary valves opens while the tricuspid closes. Depending on the state of the valves, there will be four states.

Therefore, four different matrices will be created depending on the states of these valves. In addition, since the valves will be closing and opening depending on the pressure of the ventricle, atrium and the aorta, there will be discontinuity while plotting of the result [34,54,70]. The lumped parameter model has been simplified from a 23 by 23 system of equation to a 13 by 13 system of equation.

The subclavian and the carotid arterial and venus bed has been simplified to superior circulation reducing 4 components into one singular component. The same simplification occurred with the lower body and coronary arterial and venus bed. Therefore 8 components has been reduced into 2 large components. In addition, the right and left pulmonary arterial and venus bed has been simplified into right and left pulmonary circulation reducing 4 components into 2 components as well as eliminating the flow on aorta. This simplification reduced the number of system of equations from 23 equations to 13 equations.

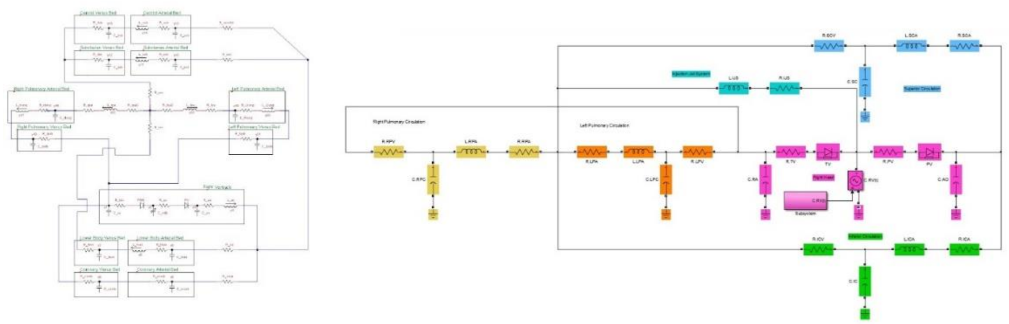

Figure 11 Comparison between Non-simplified and Simplifed Fontan Circulation

The 3D model of reduced circuit looks like the following.

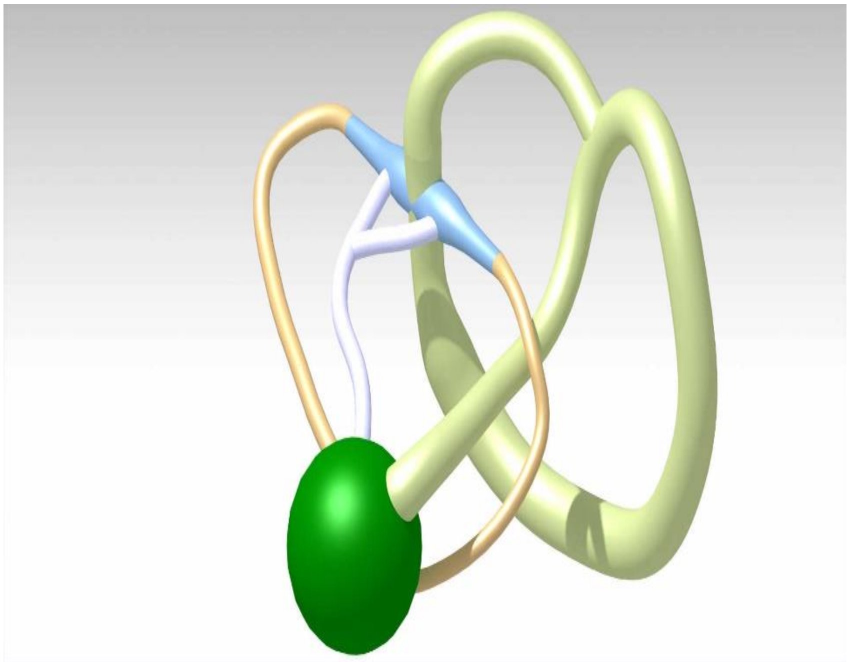

Figure 12 Simplified Model of Fontan Circulation with IJS

The green ball represents the right heart, the white section represents the IJS, the blue part represents the pulmonary arteries, the yellow region represents simplified aorta with the IVC and the SVC.

ODE45 in MATLAB

The last part of the simulation is using ode45 function which is a build in function for Runge-Kutta 4th order and 5th order approximation. By using this build in function, system of differential equations can be solved and approximate the solutions. The simulation will include two simulations with and without IJS system. The IJS is the new component that was suggested as a hypothetical solution for the Fontan operation. Comparisons will be made to identify the difference in flow and pressure according to the IJS. These value comparisons will be determined by changing Maximum and Minimum Elastance of Ventricle (Emax, Emin), resistance of IJS and heart rate (HR).

Solving Ordinary Differential Equations using MATLAB

An ordinary differential equation (ODE) is an equation that contains one independent variable and one or more derivatives with respect to that independent variable. In most cases, the independent variable is time. In the time domain, ODEs are initial value problems, so all conditions are specified at when time is zero. For example,

$$\frac{dy}{dx} = \frac{x}{y} \quad \text{Equation 19}$$

$$y(0) = 1 \quad \text{Equation 20}$$

$$y(x) = \sqrt{x^2} + 1 \quad \text{Equation 21}$$

The initial value of the function y is given when the time(x) is zero. The governing equation is $\frac{dy}{dx}$, y(x) value is the actual solution. This is an initial value problem. Matlab utilizes the built-in functions for the solution of the ODEs. Here are the most commonly used syntax.

```
[outputs] = function_name (inputs)
[time, state] = solver(@dstate, tspan, I.C,options)
```

The state represents the solution of ODEs which are the values of each state at given time. The solver represents the Matlab algorithm which is a built-in function that is determined by functions like ode23, ode45. @dstate handles the function that are containing the derivatives, tspan represents the time span and the intervals between each time period and I.Cs represents the initial conditions for the system in row or column.

ODEs are solved by computing the nearby values of y(x) using the information known and repeating over the time period. The built in solver function solve the ODEs and they have different orders. The higher order of ODE function reduces the error generated while solving the ODEs. However, time is compromised. As an example ode45 will have better accuracy in data compared to ode23. However, it will take shorter time to calculate ode23 than ode45. [74]

Solver	Accuracy	Description
ODE45	Medium	This should be the first solver you try
ODE23	Low	Less accurate than ODE45
ODE113	Low to High	For computational intensive problems
ODE15s	Low to Medium	Use if ode45 fails because the problem is stiff

Table 2 Types of ODE built-in functions in MATLAB

This table explains the accuracy of the MATLAB built-in solver functions and the descriptions.

The process of computing the nearby values using the information known is called numerical approximation. The table presents multiple methods or numerical approximation. ODE113 is Euler's method, ODE23 is Henn's method, and ODE45 is Runge-Kutta 4^{th} and 5^{th} order method.

While solving for the Fontan circulation, we are not dealing with a single ordinary differential equation but we are dealing with system of first order ordinary differential equations. [73] Often, engineering and science problems are governed by a system of coupled ordinary differential equations where the unknowns represent the state variable of specific instances in the field. Since using lumped parameter model to parameterize the problem, the current and voltages in the electric circuit represents the flow and pressure in a hydraulic system. Given the system of equations as

$$\frac{\boldsymbol{dy1(t)}}{\boldsymbol{dt}} = \boldsymbol{f1(t, y1, y2, y3}\ , \cdots \boldsymbol{yn}) \quad \text{Equation 22}$$

$$\frac{\boldsymbol{dy2(t)}}{\boldsymbol{dt}} = \boldsymbol{f2(t, y1, y2, y3}\ , \cdots \boldsymbol{yn}) \quad \text{Equation 23}$$

$$\frac{\boldsymbol{dyn(t)}}{\boldsymbol{dt}} = \boldsymbol{fn(t, y1, y2, y3}\ , \cdots \boldsymbol{yn}) \quad \text{Equation 24}$$

And set of initial conditions

$$\boldsymbol{y(0)} = \begin{matrix} \boldsymbol{y1(0)} \\ \boldsymbol{y2(0)} \\ \boldsymbol{yn(0)} \end{matrix} \quad = \quad \begin{matrix} \widehat{\boldsymbol{y1}} \\ \widehat{\boldsymbol{y2}} \\ \widehat{\boldsymbol{y3}} \end{matrix} \quad \text{Equation 25}$$

Which can be represented as a compact form

$$\dot{\boldsymbol{y}}(\boldsymbol{t}) = [\boldsymbol{A}(\boldsymbol{t})] * \{\boldsymbol{y}(\boldsymbol{t})\} + \{\boldsymbol{g}(\boldsymbol{t})\} \quad \text{Equation 26}$$

Where

$$\{\dot{\boldsymbol{y}}(\boldsymbol{t})\} = \begin{matrix} \frac{\boldsymbol{dy1(t)}}{\boldsymbol{dt}} \\ \vdots \\ \frac{\boldsymbol{dyn(t)}}{\boldsymbol{dt}} \end{matrix} \quad \boldsymbol{y(t)} = \begin{matrix} \boldsymbol{y1(t)} \\ \vdots \\ \boldsymbol{yn(t)} \end{matrix} \quad \boldsymbol{g(t)} = \begin{matrix} \boldsymbol{g1(t)} \\ \vdots \\ \boldsymbol{gn(t)} \end{matrix} \quad \text{Equation 27}$$

$$[\boldsymbol{A(t)}] = \begin{bmatrix} \boldsymbol{A1, 1(t)} & \cdots & \boldsymbol{A1, n(t)} \\ \vdots & \ddots & \vdots \\ \boldsymbol{An, 1(t)} & \cdots & \boldsymbol{An, n(t)} \end{bmatrix} \quad \text{Equation 28}$$

Where g(t) are forcing terms, $\mathbf{y(t)}$ are the initial conditions, $\dot{\mathbf{y}}\mathbf{(t)}$ are the governing equations and A(t) are constant coefficients. When the forcing term g(t) = 0, the solution is homogeneous. When a homogenous system of equations are presented, at least one of the initial conditions must be non-zero for the solution to be non-trivial meaning that y(t) ≠ 0.

In the simulation, Runge-Kutta method will be used to numerically approach the solution. The solution will converge to the answer and with correct time step applied with Runge-Kutta method, one can control the tolerance and precision of the solution. The general form of Runge-Kutta method looks like the following. [73]

$$\boldsymbol{K1} = \Delta \boldsymbol{t} * \boldsymbol{f}(\boldsymbol{yn}, \boldsymbol{tn}) \quad \text{Equation 29}$$

$$\boldsymbol{K2} = \Delta \boldsymbol{t} * \boldsymbol{f}\left(\boldsymbol{yn} + \tfrac{1}{2} K\boldsymbol{1}, \boldsymbol{tn} + \tfrac{1}{2}\Delta \boldsymbol{t}\right) \quad \text{Equation 30}$$

$$\boldsymbol{K3} = \Delta \boldsymbol{t} * \boldsymbol{f}\left(\boldsymbol{yn} + \tfrac{1}{2}\boldsymbol{K2}, \boldsymbol{tn} + \tfrac{1}{2}\Delta \boldsymbol{t}\right) \quad \text{Equation 31}$$

$$\boldsymbol{K4} = \Delta \boldsymbol{t} * \boldsymbol{f}(\boldsymbol{yn} + \boldsymbol{K3}, \boldsymbol{tn} + \boldsymbol{1}) \quad \text{Equation 32}$$

$$\boldsymbol{yn} + \boldsymbol{1} = \boldsymbol{yn} + \tfrac{\boldsymbol{1}}{\boldsymbol{6}} * (\boldsymbol{K1} + \boldsymbol{2} * \boldsymbol{K2} + \boldsymbol{2} * \boldsymbol{K3} + \boldsymbol{K4}) \quad \text{Equation 33}$$

This is the explicit form of equations for Runge-Kutta 4th order method. By applying these set of equation, numerical approximation can be performed for the solution for Fontan circulation. First, the equations have to be set up with unknowns using the lumped parameter model and generate the 12 equations and an equation for the Injection Jet System. The equations are listed below.

$$\boldsymbol{C_{RA}} * \frac{\boldsymbol{dP_{RA}(t)}}{\boldsymbol{dt}} = \boldsymbol{Q_{RA}(t)} \quad \text{Equation 34}$$

$$\frac{\boldsymbol{d}}{\boldsymbol{dt}}[\boldsymbol{C_{RV}(t)} * \boldsymbol{P_{RV}(t)}] = \boldsymbol{Q_{RV}(t)} \quad \text{Equation 35}$$

$$\boldsymbol{C_{AO}} * \frac{\boldsymbol{dP_{AO}(t)}}{\boldsymbol{dt}} = \boldsymbol{Q_{AO}(t)} \quad \text{Equation 36}$$

$$\boldsymbol{P_{AO}(t)} - \boldsymbol{P_{SC}}(t) = \boldsymbol{L_{SCA}} * \frac{\boldsymbol{dQ_{SCA}(t)}}{\boldsymbol{dt}} + \boldsymbol{R_{SCA}} * \boldsymbol{Q_{SCA}(t)} \quad \text{Equation 37}$$

$$\boldsymbol{C_{SC}} * \frac{\boldsymbol{dP_{SC}(t)}}{\boldsymbol{dt}} = \boldsymbol{Q_{SC}(t)} \quad \text{Equation 38}$$

$$\boldsymbol{P_{AO}(t)} - \boldsymbol{P_{IC}(t)} = \boldsymbol{L_{ICA}} * \frac{\boldsymbol{dQ_{ICA}(t)}}{\boldsymbol{dt}} + \boldsymbol{R_{ICA}} * \boldsymbol{Q_{ICA}(t)} \quad \text{Equation 39}$$

$$\boldsymbol{C_{IC}} * \frac{\boldsymbol{dP_{IC}(t)}}{\boldsymbol{dt}} = \boldsymbol{Q_{IC}(t)} \quad \text{Equation 40}$$

$$\boldsymbol{P_{J}(t)} - \boldsymbol{P_{LPC}(t)} = \boldsymbol{L_{LPA}} * \frac{\boldsymbol{dQ_{SCA}(t)}}{\boldsymbol{dt}} + \boldsymbol{R_{LPA}} * \boldsymbol{Q_{LPA}(t)} \quad \text{Equation 41}$$

$$C_{LPC} * \frac{dP_{LPC}(t)}{dt} = Q_{LPC}(t)$$ Equation 42

$$P_J(t) - P_{RPC}(t) = L_{RPA} * \frac{dQ_{RPA}(t)}{dt} + R_{RPA} * Q_{RPA}(t)$$ Equation 43

$$C_{RPC} * \frac{dP_{RPC}(t)}{dt} = Q_{RPC}(t)$$ Equation 44

$$C_J * \frac{dP_J(t)}{dt} = Q_J(t)$$ Equation 45

$$P_{RV}(t) - P_J(t) = L_{IJS} * \frac{dQ_{IJS}(t)}{dt} + R_{IJS} * Q_{IJS}(t)$$ Equation 46

These are the 13 equations with unknowns that needs to be solved using the Runge-Kutta method. After determining the equations, Kirchhoff's current rule (KCL) will be applied to determine the terms on the right hand side of the equations.

$$Q_{LPV}(t) + Q_{RPV}(t) = Q_{RA}(t) + Q_{TV}(t)$$ Equation 47

$$Q_{RA}(t) = Q_{LPV}(t) + Q_{RPV}(t) - Q_{TV}(t)$$ Equation 48

$$Q_{LPV}(t) = \frac{P_{LPC}(t) - P_{RA}(t)}{R_{LPV}}$$ Equation 49

$$Q_{RPV}(t) = \frac{P_{RPC}(t) - P_{RA}(t)}{R_{RPV}}$$ Equation 50

$$Q_{TV}(t) = \frac{P_{RA}(t) - P_{RV}(t)}{R_{TV}} H[P_{RA}(t) - P_{RV}(t)]$$ Equation 51

$$Q_{RA}(t) = \frac{P_{LPC}(t) - P_{RA}(t)}{R_{LPV}} + \frac{P_{RPC}(t) - P_{RA}(t)}{R_{RPV}} - \frac{P_{RA}(t) - P_{RV}(t)}{R_{TV}} H[P_{RA}(t) - P_{RV}(t)]$$ Equation 52

This is an example for using Kirchhoff's current rule on one the first node RA. By using Kirchhoff's current rule at all the nodes, the following equations can be determined.

$$\frac{dP_{RA}(t)}{dt} = \frac{P_{LPC}(t)-P_{RA}(t)}{R_{LPV}} + \frac{P_{RPC}(t)-P_{RA}(t)}{R_{RPV}} - \frac{P_{RA}(t)-P_{RV}(t)}{R_{TV}}\ H[\,P_{RA}(t) - P_{RV}(t)] \quad \text{Equation 53}$$

$$\frac{dP_{RV}(t)}{dt} = -\frac{1}{C_{RV}(t)} * \frac{dC_{RV}(t)}{dt} * P_{RV}(t) + \frac{P_{RA}(t)-P_{RV}(t)}{R_{TV}*C_{RV}(t)}\ H[\,P_{RA}(t) - P_{RV}(t)] - \frac{P_{RV}(t)-P_{AO}(t)}{R_{PV}*C_{RV}(t)}\ H[\,P_{RV}(t) - P_{AO}(t)] \quad \text{Equation 54}$$

$$\frac{dP_{AO}(t)}{dt} = \frac{P_{RV}(t)-P_{AO}(t)}{R_{PV}*C_{AO}(t)}\ H[\,P_{RV}(t) - P_{AO}(t)] - \frac{1}{C_{AO}} * Q_{SCA}(t) - \frac{1}{C_{AO}} * Q_{ICA}(t) \quad \text{Equation55}$$

$$\frac{dQ_{SCA}(t)}{dt} = \frac{1}{L_{SCA}} * P_{AO}(t) - \frac{1}{L_{SCA}} * P_{SC}(t) - \frac{R_{SCA}}{L_{SCA}} * Q_{SCA}(t) \quad \text{Equation 56}$$

$$\frac{dP_{SC}(t)}{dt} = \frac{1}{C_{SC}} * Q_{SCA}(t) - \frac{P_{sc}(t)-P_J(t)}{R_{SCV}*C_{SC}} \quad \text{Equation 57}$$

$$\frac{dQ_{ICA}(t)}{dt} = \frac{1}{L_{ICA}} * P_{AO}(t) - \frac{1}{L_{ICA}} * P_{IC}(t) - \frac{R_{ICA}}{L_{ICA}} * Q_{ICA}(t) \quad \text{Equation 58}$$

$$\frac{dP_{IC}(t)}{dt} = \frac{1}{C_{IC}} * Q_{ICA}(t) - \frac{P_{Ic}(t)-P_J(t)}{R_{ICV}*C_{IC}} \quad \text{Equation 59}$$

$$\frac{dQ_{LPA}(t)}{dt} = \frac{1}{L_{LPA}} * P_J(t) - \frac{1}{L_{LPA}} * P_{LPC}(t) - \frac{R_{LPA}}{L_{LPA}} * Q_{LPA}(t) \quad \text{Equation 60}$$

$$\frac{dP_{LPC}(t)}{dt} = \frac{1}{C_{LPC}} * Q_{LPA}(t) - \frac{P_{LPC}(t)-P_{RA}(t)}{R_{LPV}*C_{LPC}} \quad \text{Equation 61}$$

$$\frac{dQ_{RPA}(t)}{dt} = \frac{1}{L_{RPA}} * P_J(t) - \frac{1}{L_{RPA}} * P_{LPC}(t) - \frac{R_{RPA}}{L_{RPA}} * Q_{RPA}(t) \quad \text{Equation 62}$$

$$\frac{dP_{RPC}(t)}{dt} = \frac{1}{C_{RPC}} * Q_{RPA}(t) - \frac{P_{RPC}(t)-P_{RA}(t)}{R_{RPV}*C_{LPC}} \quad \text{Equation 63}$$

$$\frac{dP_J(t)}{dt} = \frac{P_{SC}(t)-P_J(t)}{R_{SCV}*C_J} + \frac{P_{IC}(t)-P_J(t)}{R_{ICV}*C_J} - \frac{1}{C_J} * Q_{LPA}(t) - \frac{1}{C_J} * Q_{RPA}(t) \quad \text{Equation 64}$$

These are the twelve equations without the Injection Jet system. Once the Injection Jet system is added into the circuit, equations (53) and (63) are modified.

$$\frac{dQ_{IJS}(t)}{dt} = -\frac{1}{L_{IJS}} * P_J(t) + \frac{1}{L_{IJS}} * P_{RV}(t) - \frac{R_{IJS}}{L_{IJS}} * Q_{IJS}(t) \quad \text{Equation 65}$$

$$\frac{dP_{RV}(t)}{dt} = -\frac{1}{C_{RV}(t)} * \frac{dC_{RV}(t)}{dt} * P_{RV}(t) + \frac{P_{RA}(t)-P_{RV}(t)}{R_{TV}*C_{RV}(t)}\ H[\,P_{RA}(t) - P_{RV}(t)] - \frac{P_{RV}(t)-P_{AO}(t)}{R_{PV}*C_{RV}(t)}\ H[\,P_{RV}(t) - P_{AO}(t)] - \frac{1}{C_{RV}(t)} * Q_{IJS}(t) \quad \text{Equation 66}$$

$$\frac{dP_J(t)}{dt} = \frac{P_{SC}(t)-P_J(t)}{R_{SCV}*C_J} + \frac{P_{IC}(t)-P_J(t)}{R_{ICV}*C_J} - \frac{1}{C_J} * Q_{LPA}(t) - \frac{1}{C_J} * Q_{RPA}(t) + \frac{1}{C_J} * Q_{IJS}(t) \quad \text{Equation 67}$$

In the equation (52), (53) and (54), there is a Heaviside function H, which will act as a valve. The value for the Heaviside function will be determined by 1 or 0. When H = 1, the valve is open and when H = 0, the valve is closed. Since 4 different cases are dealt due to the tricuspid valve and pulmonary valve, four different systems of ordinary differential equations must be solved. The equations are then simplified into the form of a 13x13 matrix in a descending order of the 13 equations. The matrix needs to be organized in the corresponding order in order moving up and down, left to right. The values are either pressure or flow inside the vessel. The pressure values will be represent with a P with the nodes and flow will be represented as Q with the nodes. The order of the 13 equations is represented below.

$$y = \begin{pmatrix} P_{RA} \\ P_{RV} \\ P_{AO} \\ Q_{SCA} \\ P_{SC} \\ Q_{ICA} \\ P_{IC} \\ Q_{LPA} \\ P_{LPC} \\ Q_{RPA} \\ P_{RPC} \\ P_{J} \\ Q_{IJS} \end{pmatrix}$$

Depending on the value of the Heaviside function, the valves will alter between open-closed phases. The 4 states are shown below.

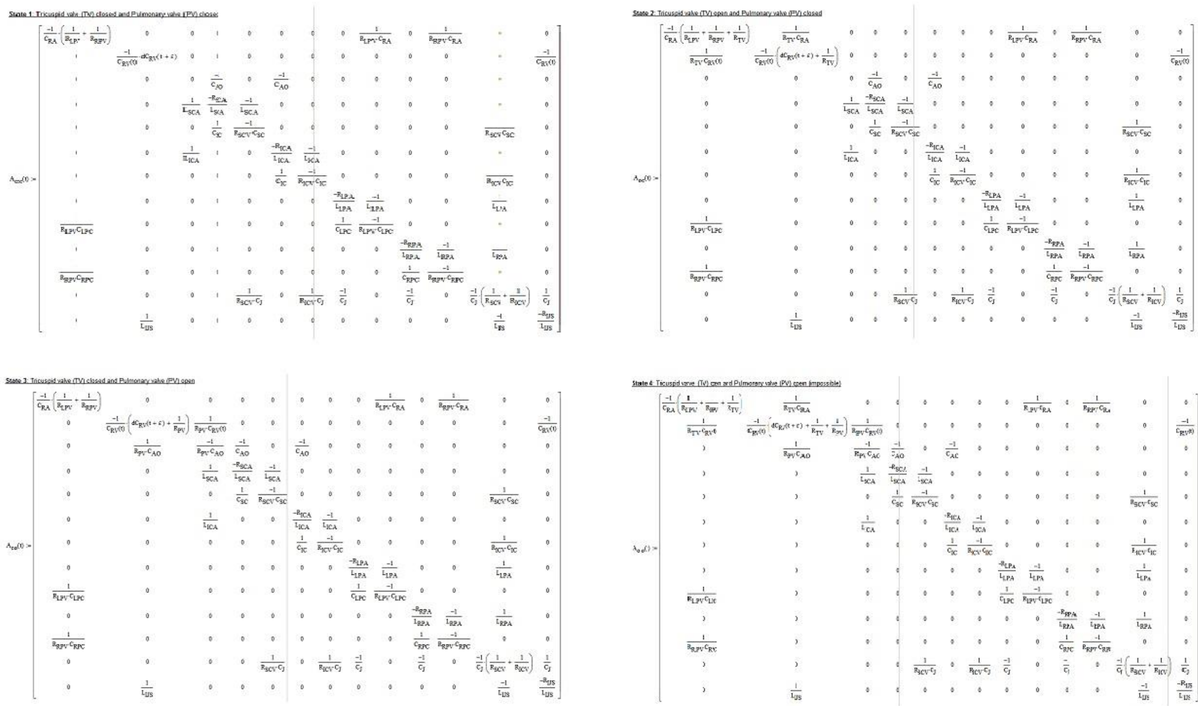

Figure 13 Four different states of system of equations with IJS

Listed in table 1, the four states are determined by the state of the valves. The matrix are determined by the 13 equations involving the Heaviside function. Direct comparison would be made with or without the IJS.

Comparison with Injection Jet Shunt (IJS)

While making comparison with and without the injection system there are several terms that needs to be discussed and be verified in the simulation. The main principle of injection jet system replies strictly on the principle of entrainment in the system. Entrainment is transportation of the fluid across the bodies. The entrainment occurs due to the injection jet system being added into the pulmonary connections toward the lungs. [72] The most common failure of Fontan circulation happens due to the high pressure in the inferior vena cava. The inferior vena cava come up from the lower part of the body and having high pressure can result in kidney failure and other illness. Therefore it is crucial to lower the pressure in inferior vena cava. The injection jet system will be added to the circulation as a method to reduce the pressure and aid the flow towards the lungs. The entrainments happens at the injection jet system and the two pulmonary vessels. A vacuum is created before the injection jet system pushing the flow to the lungs thus reducing the pressure in the inferior body. PICA and QICA will help us determine the values of the pressure in the inferior connection and the flow in the region. It is crucial to know the pressure in the inferior vena cava.

The injection jet system is a practice of Bernoulli's principle. In this case, it allows us to deliver concentrate blood flow towards the lungs. The drop in pressure caused by the increased velocity due to restriction pulls in the additional blood through the pulmonary vessels. The flow and its velocity will be influenced by the diameter of the jet orifice and the size of the entrainment port. These will allow the same outcome of increase flow in the pulmonary vessels. [72]

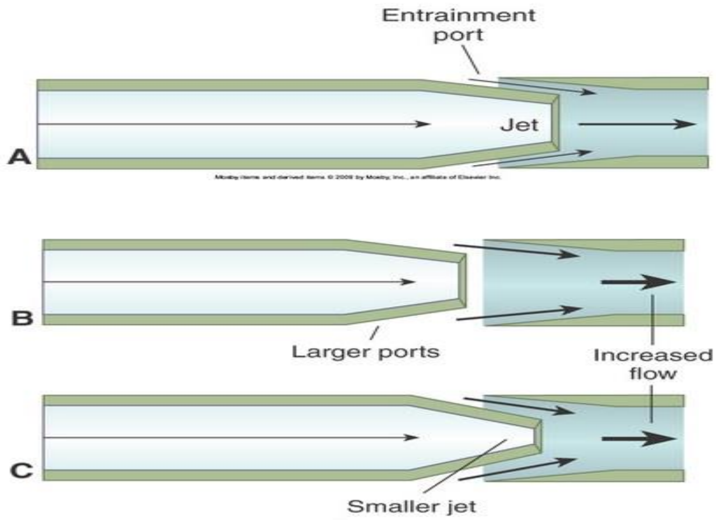

Figure 14 Entrainment ports and jet [5]

In case B, due to the large port, the entrainment port is bigger and in case C, the diameter of the jet is smaller. However, they result in increased flow over the region of the pulmonary vessel.

In addition, we will need to know the ratio of the flows in the inferior vena cava and superior vena cava respect to the pressure in the left and right pulmonary connections. The flows in the vena cava will be the flow leaving the heart and the pulmonary connections will be the flow coming in to the heart. Diving the two flows such as:

$$\frac{Q_{in}}{Q_{out}} = \frac{Q_{LPA}+Q_{RPA}}{Q_{SCA}+Q_{ICA}} < 1.5 \quad \text{Equation 68}$$

The ratio of the flow should be less than 1.5. By comparing the value with and without the injection system, we will be able to verify whether the flow has decreased or not.

Since we are adding the injection jet system, we will also need to verify the amount of flow that is delivered by the injection jet system to the lungs. Therefore we will be validating the amount of flow that is being transmitted by the injection jet graft. In addition, the flow at the junction of the IJS and the two vena cava and the pulmonary connections will be calculated to demonstrate the total flow at the junction.

Some initial values for the simulation will be adjusted due to the entrainment principle and due to the fact the problem is 1-D problem. In a 3-D problem where computation fluid dynamics (CFD) is used to evaluate the flows caused by the injection set system, in a 1-D problem, we have to have a forcing term of the resistance caused in the left and right pulmonary circulation. Since there should be a decrease in pressure, it will add a forcing term when IJS is added to the system. The initial value of the resistance in the left and right ventricle will be altered depending on the injection jet system. This will be discussed in depth in the results section of the report.

Results

The purpose of this simulation is to identify the effect of Injection Jet System (IJS) on the original Fontan Circulation. Depending on the patient's heart rate (HR), maximum and minimum elastance (Emax, Emin) the simulation will show how much additional flow is transmitted throughout the left and right pulmonary circulation. Comparison of different heart rate and elastance values will be made to identify whether the Injection Jet System will be helpful to Fontan circulation of not. After determining the 12x 12 system of equations for the original Fontan circulation and 13 x13 system of equations with the Injection Jet system added into the Fontan circulation, MATLAB was used to solve for the system of ordinary differential equations.

Time varying Compliance

The system of equation could be simplified in a form of a matrix consisting the same numbers of system of equations. The value inside the matrix are constants besides the time varying compliance which won't allow the usage of the built in functions in the MATLAB. Therefore the first step of the simulation is creating the time varying compliance and updating the value exactly identical to the times steps of the matrix so that the ode45 will be used later to solve the system of equations.

The time varying compliance can be made by the following codes.

```
1   Emax = 0.5;
2   Emin = 0.06;
3   HR = 120;
4   t = mod(t1,60/HR);
5   tn = @(t)  t./Tmax; % Normalized Time
6   En = @(t)
    1.55*(((tn(t)./0.7).^1.9)./(1+(tn(t)./0.7).^1.9)).*((1./(1+(tn(t)./1.17).^21.9)));
7   E  = @(t)  ((Emax - Emin) * En(t))+Emin;
8   C  = @(t) 1./E(t);          %reciprocal of E
9   CC = @(t,ts) diff(C(t))./(C(t(1:end-1))*ts); % dC./C
```

Table 3 Time varying compliance in Matlab

The Emax and Emin are elastance of the ventricle which are predetermined values as well as the heart rate, HR. Time will be determined by using modulo operation in line 4. This takes the initial time and final time and divide it by the time steps. In line 5, normal elastance is determined using the normalized time. The @ operator creates a function handle, which allows the function to be called in like variables. The function handle captures all the information about a function that MATLAB needs to execute the function. Typically, a function handle is passed in an argument list to other functions.

The receiving functions can then execute the function through the handle that was passed in. [74] By using function handle, it enables to pass function access information to other functions, reduces the number of files that define your functions and improves the performance of repeated operation by reducing the processing time. Since we will have to save the values and access the values of the time varying compliance throughout the computation of the matrix as well as the derivative of the time varying compliance, using the function handle simplifies and improves the performance of the computation. By doing this process, each value of the matrix will be updated according to the time step allowing the matrix to be in a form of constants.

Using ODE45 function and Heaviside Function

After declaring all the constants, a function will be created for the time-varying system of matrices. By solving for $\bar{y} = [A]*x + [b]$. This will solved by using ode45 function.

```
[time,p1]= ode45(dxcc,t_sim,x0);
valuescc = p1;
save p1
[time,p2]= ode45(dxco,t_sim,x0);
valuesco = p2;
save p2
[time,p3]= ode45(dxoc,t_sim,x0);
valuesoc = p3;
save p3
[time,p4]= ode45(dxoo,t_sim,x0);
valuesoo = p4;
save p4
```

Table 4Matlab code for ode45 operation

After solving the system of equation using ode45 function, each values will be saved in to file p1, p2, p3 and p4. These four files will be mounted to excel VBA in order to add the functionality of the valve to alternate between the open-closed and closed open cases.

The values of p1, p2, p3 and p4 will be mounted on the excel spreadsheet and will determine the state of each valves. The valve will be opening and closing depending on the pressure of the right atrium and right ventricle.

```
'Reads first value against second
If Cells(y, x).Value > Cells(y, x).Offset(0, 1).Value And Cells(y, x).Offset(0, 1).Value <= Cells(y, x).Offset(0, 2).Value Then
Dest.Cells(y, 2).Value = "AOC"
'Moves scan to ACO table by offset
x = 31

ElseIf Cells(y, x).Value <= Cells(y, x).Offset(0, 1).Value And Cells(y, x).Offset(0, 1).Value > Cells(y, x).Offset(0, 2).Value Then
Dest.Cells(y, 2).Value = "ACO"
'Moves scan to AOC table by offset
x = 17

ElseIf Cells(y, x).Value > Cells(y, x).Offset(0, 1).Value And Cells(y, x).Offset(0, 1).Value > Cells(y, x).Offset(0, 2).Value Then
Dest.Cells(y, 2).Value = "AOO"
'Moves scan to AOO table by offset
x = 45

Else
'if no condition is met, scan stays in ACC Table
Dest.Cells(y, 2).Value = "ACC"
x = 3

End If

'Once first value of each row is set, column loop iterates until empty cell is found
While Not IsEmpty(Cells(y, x).Offset(0, t))
Dest.Cells(y, 3).Offset(0, t).Value = Source.Cells(y, x).Offset(0, t).Value
```

Table 5 Defining the states of the valves depending on their pressure

In the code, assumption will be made that the valves are both closed at rest. This state of rest is called iso-volumetric contraction. The tricuspid valve will open when the pressure inside the right atrium is greater than the ventricle while the pulmonary valve remains closed. This process is called filling. After the process of filling both valves are closed again and it is called iso-volumetric relaxation. The pulmonary valve will open while the pressure in ventricle becomes greater than the aorta while the tricuspid valve closes. This process is called the relaxation. All of this is done by the execution of Heaviside function. The operation of Heaviside function was done through Excel. MATLAB was used to calculate system of ordinary differential equations and was saved to p1, p2, p3 and p4. The files are the 4 cases depending on the state of the tricuspid valve and the pulmonary valve. The phase of open-open is not feasible therefore the data from p4 will not be applicable for this application. The sets of values for 4 cases will be determined and will be put in a text file. MATLAB will retrieve the determined values after the Heaviside function and plot the results.

State of Heart

The human heart has multiple states. The heart can be healthy, can be slightly defected, severely defected. In the case of Fontan circulation and due to the patients who undergoes Fontan operation, the elastance of the ventricle values will be significantly low due to the heart being a defected heart. In addition since we will be dealing with a baby's heart which has a higher heart rate than an adult, the values of HR will be higher than a normal heart. The values that will be used for the simulation will be the following. The initial simulation will use maximum elastance to be 0.5, minimum elastance to be 0.06 and heart rate to be 120. In the simulation, the variables will be the maximum elastance and the heart rate. The minimum elastance does not alter the simulation. However the maximum elastance and the heart rate will alter the range of simulation. Comparisons will be made depending on the effects of increased maximum elastance and the heart rate to the initial simulation value. Evaluation will be made when the heart condition is slightly better or slightly worse than the initial condition to get a better idea of the condition of the patient.

Emax \ Heart Rate	140	120	100
0.75	0.75 \ 140	0.75 \ 120	0.75 \ 100
0.50	0.50 \ 140	0.50 \ 120	0.50 \ 100
0.25	0.25 \ 140	0.25 \ 120	0.25 \ 100

Table 6 Maximum Elastance and Heart Rate that will be used for comparison in the simulation.

A healthier heart of a baby will have a heart rate between 110 to 160 beats per minute (BPM). The maximum elastance of the heart would be higher when the heart is healthier and lower when the heart is ill. Values will be taken when the heart rate is between the range and out of the range to demonstrate the behavior of the pressure and flow in the circulation. In addition elastance values will be changed by 0.25 to determine a better functioning heart to a condition where the heart condition got worse. The comparisons will be made through excel and provide the values to see the flow ratios in the pulmonary circulation and the two vena cava as well as the flow influences by the injection jet system. [65, 68]

Without Injection Jet Shunt

General Information

The simulation is influenced by two major parameters which are the maximum elastance in the ventricle and the heart rate. The simulation will be created within the parameters of a malfunctioning heart of the babies and the two parameters will be controlled to see the difference when the heart is slightly healthier or slightly worse than the normal parameters. The value of the lumped parameter model will be addressed below.

```
%% Define Constants
%Resistance
RTV = 0.005;
RPV = 0.005;
RSCA = 2;
RICA = 1;
RSCV = 1;
RICV = 0.5;
RLPA = 0.1;
RLPV = 0.05;
RRPA = 0.1;
RRPV = 0.05;
%Inductance
LSCA = 0.001;
LICA = 0.001;
LLPA = 0.001;
LRPA = 0.001;
%Compliance
CRA = 4.4;
CAO = 0.08;
CSC = 2.66;
CIC = 2.66;
CLPC = 2.66;
CRPC = 2.66;
CJ = 0.1;
```

Table 7 Defined Constants for Fontan circulation lumped parameter model

These values have been predetermined before the creation of the simulations according to the parameters of a patient who had a Fontan operation. These values will be plugged into the 12x12 matrix of the system of equations and will be solved by using Runge-Kutta 4th order ordinary differential equation.

State 1: Tricuspid valve (TV) closed and Pulmonary valve (PV) closed

$$
A_{cc}(t) := \begin{bmatrix}
\frac{-1}{C_{RA}}\cdot\left(\frac{1}{R_{LPV}}+\frac{1}{R_{RPV}}\right) & 0 & 0 & 0 & 0 & 0 & 0 & 0 & \frac{1}{R_{LPV}\cdot C_{RA}} & 0 & \frac{1}{R_{RPV}\cdot C_{RA}} & 0 \\
0 & \frac{-1}{C_{RV}(t)}\cdot dC_{RV}(t+\varepsilon) & 0 & 0 & 0 & 0 & 0 & 0 & 0 & 0 & 0 & 0 \\
0 & 0 & 0 & \frac{-1}{C_{AO}} & 0 & \frac{-1}{C_{AO}} & 0 & 0 & 0 & 0 & 0 & 0 \\
0 & 0 & \frac{1}{L_{SCA}} & \frac{-R_{SCA}}{L_{SCA}} & \frac{-1}{L_{SCA}} & 0 & 0 & 0 & 0 & 0 & 0 & 0 \\
0 & 0 & 0 & \frac{1}{C_{SC}} & \frac{-1}{R_{SCV}\cdot C_{SC}} & 0 & 0 & 0 & 0 & 0 & 0 & \frac{1}{R_{SCV}\cdot C_{SC}} \\
0 & 0 & \frac{1}{L_{ICA}} & 0 & 0 & \frac{-R_{ICA}}{L_{ICA}} & \frac{-1}{L_{ICA}} & 0 & 0 & 0 & 0 & 0 \\
0 & 0 & 0 & 0 & 0 & \frac{1}{C_{IC}} & \frac{-1}{R_{ICV}\cdot C_{IC}} & 0 & 0 & 0 & 0 & \frac{1}{R_{ICV}\cdot C_{IC}} \\
0 & 0 & 0 & 0 & 0 & 0 & 0 & \frac{-R_{LPA}}{L_{LPA}} & \frac{-1}{L_{LPA}} & 0 & 0 & \frac{1}{L_{LPA}} \\
\frac{1}{R_{LPV}\cdot C_{LPC}} & 0 & 0 & 0 & 0 & 0 & 0 & \frac{1}{C_{LPC}} & \frac{-1}{R_{LPV}\cdot C_{LPC}} & 0 & 0 & 0 \\
0 & 0 & 0 & 0 & 0 & 0 & 0 & 0 & 0 & \frac{-R_{RPA}}{L_{RPA}} & \frac{-1}{L_{RPA}} & \frac{1}{L_{RPA}} \\
\frac{1}{R_{RPV}\cdot C_{RPC}} & 0 & 0 & 0 & 0 & 0 & 0 & 0 & 0 & \frac{1}{C_{RPC}} & \frac{-1}{R_{RPV}\cdot C_{RPC}} & 0 \\
0 & 0 & 0 & 0 & \frac{1}{R_{SCV}\cdot C_J} & 0 & \frac{1}{R_{ICV}\cdot C_J} & \frac{-1}{C_J} & 0 & \frac{-1}{C_J} & 0 & \frac{-1}{C_J}\cdot\left(\frac{1}{R_{SCV}}+\frac{1}{R_{ICV}}\right)
\end{bmatrix}
$$

Figure 15 Tricuspid valve closed - pulmonary valve closed for Fontan circulation without the IJS

The 4 cases of the 12x12 matrix are presented. The first case is when the tricuspid valve and the pulmonary valve are closed. The Heaviside functions does not exists since when the valves are closed, the value for the Heaviside functions becomes ‘0’ leaving the function without any terms.

State 2: Tricuspid valve (TV) open and Pulmonary valve (PV) closed

$$A_{oc}(t) := \begin{bmatrix}
\frac{-1}{C_{RA}}\cdot\left(\frac{1}{R_{LPV}}+\frac{1}{R_{RPV}}+\frac{1}{R_{TV}}\right) & \frac{1}{R_{TV}\cdot C_{RA}} & 0 & 0 & 0 & 0 & 0 & 0 & \frac{1}{R_{LPV}\cdot C_{RA}} & 0 & \frac{1}{R_{RPV}\cdot C_{RA}} & 0 \\
\frac{1}{R_{TV}\cdot C_{RV}(t)} & \frac{-1}{C_{RV}(t)}\cdot\left(dC_{RV}(t+\varepsilon)+\frac{1}{R_{TV}}\right) & 0 & 0 & 0 & 0 & 0 & 0 & 0 & 0 & 0 & 0 \\
0 & 0 & 0 & \frac{-1}{C_{AO}} & 0 & \frac{-1}{C_{AO}} & 0 & 0 & 0 & 0 & 0 & 0 \\
0 & 0 & \frac{1}{L_{SCA}} & \frac{-R_{SCA}}{L_{SCA}} & \frac{-1}{L_{SCA}} & 0 & 0 & 0 & 0 & 0 & 0 & 0 \\
0 & 0 & 0 & \frac{1}{C_{SC}} & \frac{-1}{R_{SCV}\cdot C_{SC}} & 0 & 0 & 0 & 0 & 0 & 0 & \frac{1}{R_{SCV}\cdot C_{SC}} \\
0 & 0 & \frac{1}{L_{ICA}} & 0 & 0 & \frac{-R_{ICA}}{L_{ICA}} & \frac{-1}{L_{ICA}} & 0 & 0 & 0 & 0 & 0 \\
0 & 0 & 0 & 0 & 0 & \frac{1}{C_{IC}} & \frac{-1}{R_{ICV}\cdot C_{IC}} & 0 & 0 & 0 & 0 & \frac{1}{R_{ICV}\cdot C_{IC}} \\
0 & 0 & 0 & 0 & 0 & 0 & 0 & \frac{-R_{LPA}}{L_{LPA}} & \frac{-1}{L_{LPA}} & 0 & 0 & \frac{1}{L_{LPA}} \\
\frac{1}{R_{LPV}\cdot C_{LPC}} & 0 & 0 & 0 & 0 & 0 & 0 & \frac{1}{C_{LPC}} & \frac{-1}{R_{LPV}\cdot C_{LPC}} & 0 & 0 & 0 \\
0 & 0 & 0 & 0 & 0 & 0 & 0 & 0 & 0 & \frac{-R_{RPA}}{L_{RPA}} & \frac{-1}{L_{RPA}} & \frac{1}{L_{RPA}} \\
\frac{1}{R_{RPV}\cdot C_{RPC}} & 0 & 0 & 0 & 0 & 0 & 0 & 0 & 0 & \frac{1}{C_{RPC}} & \frac{-1}{R_{RPV}\cdot C_{RPC}} & 0 \\
0 & 0 & 0 & 0 & \frac{1}{R_{SCV}\cdot C_J} & 0 & \frac{1}{R_{ICV}\cdot C_J} & \frac{-1}{C_J} & 0 & \frac{-1}{C_J} & 0 & \frac{-1}{C_J}\cdot\left(\frac{1}{R_{SCV}}+\frac{1}{R_{ICV}}\right)
\end{bmatrix}$$

Figure 16 Tricuspid valve open - pulmonary valve closed for Fontan circulation without the IJS

The second case is when the tricuspid valve is open and when the pulmonary valve is closed. We can see that the terms for the Heaviside function that governs the tricuspid valve is active. Since the valve is open the Heaviside is represented as ‘1’, thus allowing the term to be active. The Heaviside function is active through the first two lines of the matrix.

State 3: Tricuspid valve (TV) closed and Pulmonary valve (PV) open

$$
A_{co}(t) := \begin{bmatrix}
\frac{-1}{C_{RA}} \cdot \left(\frac{1}{R_{LPV}} + \frac{1}{R_{RPV}} \right) & 0 & 0 & 0 & 0 & 0 & 0 & 0 & \frac{1}{R_{LPV} \cdot C_{RA}} & 0 & \frac{1}{R_{RPV} \cdot C_{RA}} & 0 \\
0 & \frac{-1}{C_{RV}(t)} \cdot \left(dC_{RV}(t+\varepsilon) + \frac{1}{R_{PV}} \right) & \frac{1}{R_{PV} \cdot C_{RV}(t)} & 0 & 0 & 0 & 0 & 0 & 0 & 0 & 0 & 0 \\
0 & \frac{1}{R_{PV} \cdot C_{AO}} & \frac{-1}{R_{PV} \cdot C_{AO}} & \frac{-1}{C_{AO}} & 0 & \frac{-1}{C_{AO}} & 0 & 0 & 0 & 0 & 0 & 0 \\
0 & 0 & \frac{1}{L_{SCA}} & \frac{-R_{SCA}}{L_{SCA}} & \frac{-1}{L_{SCA}} & 0 & 0 & 0 & 0 & 0 & 0 & 0 \\
0 & 0 & 0 & \frac{1}{C_{SC}} & \frac{-1}{R_{SCV} \cdot C_{SC}} & 0 & 0 & 0 & 0 & 0 & 0 & \frac{1}{R_{SCV} \cdot C_{SC}} \\
0 & 0 & \frac{1}{L_{ICA}} & 0 & 0 & \frac{-R_{ICA}}{L_{ICA}} & \frac{-1}{L_{ICA}} & 0 & 0 & 0 & 0 & 0 \\
0 & 0 & 0 & 0 & 0 & \frac{1}{C_{IC}} & \frac{-1}{R_{ICV} \cdot C_{IC}} & 0 & 0 & 0 & 0 & \frac{1}{R_{ICV} \cdot C_{IC}} \\
0 & 0 & 0 & 0 & 0 & 0 & 0 & \frac{-R_{LPA}}{L_{LPA}} & \frac{-1}{L_{LPA}} & 0 & 0 & \frac{1}{L_{LPA}} \\
\frac{1}{R_{LPV} \cdot C_{LPC}} & 0 & 0 & 0 & 0 & 0 & 0 & \frac{1}{C_{LPC}} & \frac{-1}{R_{LPV} \cdot C_{LPC}} & 0 & 0 & 0 \\
0 & 0 & 0 & 0 & 0 & 0 & 0 & 0 & 0 & \frac{-R_{RPA}}{L_{RPA}} & \frac{-1}{L_{RPA}} & \frac{1}{L_{RPA}} \\
\frac{1}{R_{RPV} \cdot C_{RPC}} & 0 & 0 & 0 & 0 & 0 & 0 & 0 & 0 & \frac{1}{C_{RPC}} & \frac{-1}{R_{RPV} \cdot C_{RPC}} & 0 \\
0 & 0 & 0 & 0 & \frac{1}{R_{SCV} \cdot C_J} & 0 & \frac{1}{R_{ICV} \cdot C_J} & \frac{-1}{C_J} & 0 & \frac{-1}{C_J} & 0 & \frac{-1}{C_J} \cdot \left(\frac{1}{R_{SCV}} + \frac{1}{R_{ICV}} \right)
\end{bmatrix}
$$

Figure 17 Tricuspid valve closed - pulmonary valve open for Fontan circulation without the IJS

The third case is when the tricuspid valve is closed and the pulmonary valves are opened. When the pulmonary valve is opened, the second and third term gets modified due to the Heaviside function. However the Heaviside term for the tricuspid valve is canceled since the valve is closed.

State 4: Tricuspid valve (TV) open and Pulmonary valve (PV) open (impossible)

$$A_{oo}(t) := \begin{bmatrix} \frac{-1}{C_{RA}}\cdot\left(\frac{1}{R_{LPV}}+\frac{1}{R_{RPV}}+\frac{1}{R_{TV}}\right) & \frac{1}{R_{TV}\cdot C_{RA}} & 0 & 0 & 0 & 0 & 0 & 0 & \frac{1}{R_{LPV}\cdot C_{RA}} & 0 & \frac{1}{R_{RPV}\cdot C_{RA}} & 0 \\ \frac{1}{R_{TV}\cdot C_{RV}(t)} & \frac{-1}{C_{RV}(t)}\cdot\left(dC_{RV}(t+\varepsilon)+\frac{1}{R_{TV}}+\frac{1}{R_{PV}}\right) & \frac{1}{R_{PV}\cdot C_{RV}(t)} & 0 & 0 & 0 & 0 & 0 & 0 & 0 & 0 & 0 \\ 0 & \frac{1}{R_{PV}\cdot C_{AO}} & \frac{-1}{R_{PV}\cdot C_{AO}} & \frac{-1}{C_{AO}} & 0 & \frac{-1}{C_{AO}} & 0 & 0 & 0 & 0 & 0 & 0 \\ 0 & 0 & \frac{1}{L_{SCA}} & \frac{-R_{SCA}}{L_{SCA}} & \frac{-1}{L_{SCA}} & 0 & 0 & 0 & 0 & 0 & 0 & 0 \\ 0 & 0 & 0 & \frac{1}{C_{SC}} & \frac{-1}{R_{SCV}\cdot C_{SC}} & 0 & 0 & 0 & 0 & 0 & 0 & \frac{1}{R_{SCV}\cdot C_{SC}} \\ 0 & 0 & \frac{1}{L_{ICA}} & 0 & 0 & \frac{-R_{ICA}}{L_{ICA}} & \frac{-1}{L_{ICA}} & 0 & 0 & 0 & 0 & 0 \\ 0 & 0 & 0 & 0 & 0 & \frac{1}{C_{IC}} & \frac{-1}{R_{ICV}\cdot C_{IC}} & 0 & 0 & 0 & 0 & \frac{1}{R_{ICV}\cdot C_{IC}} \\ 0 & 0 & 0 & 0 & 0 & 0 & 0 & \frac{-R_{LPA}}{L_{LPA}} & \frac{-1}{L_{LPA}} & 0 & 0 & \frac{1}{L_{LPA}} \\ \frac{1}{R_{LPV}\cdot C_{LPC}} & 0 & 0 & 0 & 0 & 0 & 0 & \frac{1}{C_{LPC}} & \frac{-1}{R_{LPV}\cdot C_{LPC}} & 0 & 0 & 0 \\ 0 & 0 & 0 & 0 & 0 & 0 & 0 & 0 & 0 & \frac{-R_{RPA}}{L_{RPA}} & \frac{-1}{L_{RPA}} & \frac{1}{L_{RPA}} \\ \frac{1}{R_{RPV}\cdot C_{RPC}} & 0 & 0 & 0 & 0 & 0 & 0 & 0 & 0 & \frac{1}{C_{RPC}} & \frac{-1}{R_{RPV}\cdot C_{RPC}} & 0 \\ 0 & 0 & 0 & 0 & \frac{1}{R_{SCV}\cdot C_J} & 0 & \frac{1}{R_{ICV}\cdot C_J} & \frac{-1}{C_J} & 0 & \frac{-1}{C_J} & 0 & \frac{-1}{C_J}\cdot\left(\frac{1}{R_{SCV}}+\frac{1}{R_{ICV}}\right) \end{bmatrix}$$

Figure 18 Tricuspid valve open - pulmonary valve open for Fontan circulation without the IJS

The fourth case, which is practically impossible, is when the two valves are open. You can see that the first three rows of the matrix has the Heaviside term on the first 3 columns of the matrix. These set of matrix will be alternating depending on the pressure difference in the ventricle and the aorta.

Simulation Results

Results of the simulation was generated using the built-in function ODE45 in Matlab. The function is also called as Runge-Kutta 4^{th} order and 5^{th} order approximation function.

```
[time,p1]= ode45(dxcc,t_sim,x0);
valuescc = p1;
save p1
[time,p2]= ode45(dxco,t_sim,x0);
valuesco = p2;
save p2
[time,p3]= ode45(dxoc,t_sim,x0);
valuesoc = p3;
save p3
[time,p4]= ode45(dxoo,t_sim,x0);
valuesoo = p4;
save p4
```

Table 8 Matlab code for ode45 operation

Since the syntax of the order we used was [time, data location of columns], the plots were generated by using the plot function with the same order of syntax. Since p1, p2,p3 and p4 has been combined into the file called data due to the different states in the circulation, by simply changing the column values depending on the different nodes, the following sets of data were generated.

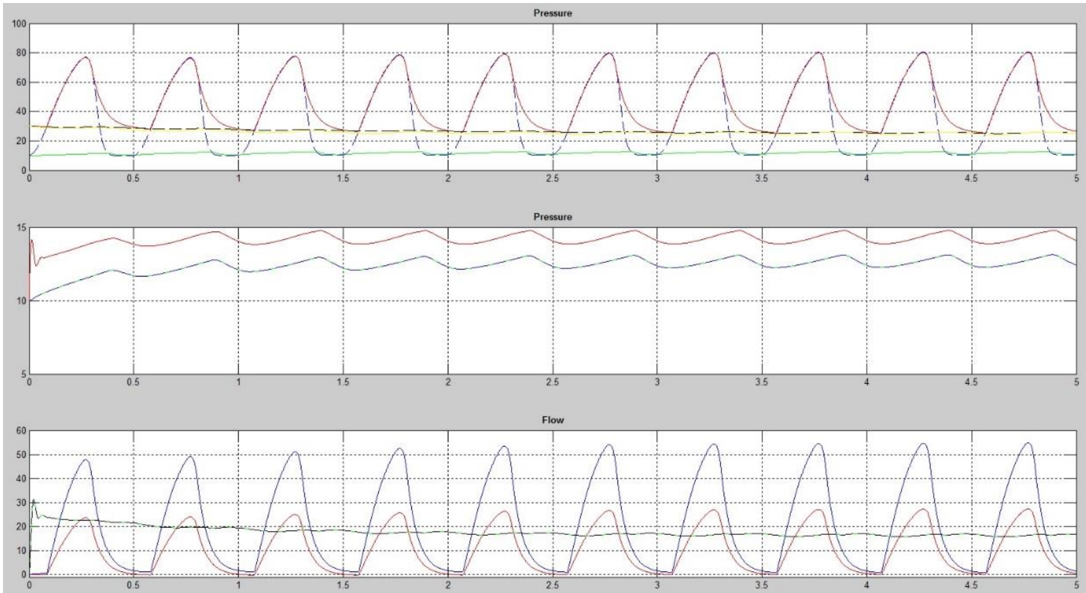

Figure 19 Pressure and Flow values without IJS

The following data was generated for the case where the maximum elastance of the ventricle is 0.5, minimum elastance of 0.06 and heart rate of 120 bpm. The format of the syntax in order to generate the graph is shown next to the graphs. The comparison of the data sets will be made through excel. In addition, the value of the systemic flow, pulmonary flow and caval pressure will be found in comparison.

With Injection Jet Shunt

General Information

When injection jet system is introduced into the system of the Fontan circulation, the graft is added between the pulmonary valve and the two pulmonary circulation. This changes the values inside the original matrix of the Fontan matrix but also adds an extra row and column to the matrix making it 13x13 matrix. A new term 'QIJS', which is the flow of IJS will be introduced into the system of equations. These system of equations are shown below.

State 1: Tricuspid valve (TV) closed and Pulmonary valve (PV) closed

$$
A_{cc}(t) := \begin{bmatrix}
\frac{-1}{C_{RA}}\cdot\left(\frac{1}{R_{LPV}}+\frac{1}{R_{RPV}}\right) & 0 & 0 & 0 & 0 & 0 & 0 & 0 & \frac{1}{R_{LPV}\cdot C_{RA}} & 0 & \frac{1}{R_{RPV}\cdot C_{RA}} & 0 & 0 \\
0 & \frac{-1}{C_{RV}(t)}\cdot dC_{RV}(t+\varepsilon) & 0 & 0 & 0 & 0 & 0 & 0 & 0 & 0 & 0 & 0 & \frac{-1}{C_{RV}(t)} \\
0 & 0 & 0 & \frac{-1}{C_{AO}} & 0 & \frac{-1}{C_{AO}} & 0 & 0 & 0 & 0 & 0 & 0 & 0 \\
0 & 0 & \frac{1}{L_{SCA}} & \frac{-R_{SCA}}{L_{SCA}} & \frac{-1}{L_{SCA}} & 0 & 0 & 0 & 0 & 0 & 0 & 0 & 0 \\
0 & 0 & 0 & \frac{1}{C_{SC}} & \frac{-1}{R_{SCV}\cdot C_{SC}} & 0 & 0 & 0 & 0 & 0 & 0 & \frac{1}{R_{SCV}\cdot C_{SC}} & 0 \\
0 & 0 & \frac{1}{L_{ICA}} & 0 & 0 & \frac{-R_{ICA}}{L_{ICA}} & \frac{-1}{L_{ICA}} & 0 & 0 & 0 & 0 & 0 & 0 \\
0 & 0 & 0 & 0 & 0 & \frac{1}{C_{IC}} & \frac{-1}{R_{ICV}\cdot C_{IC}} & 0 & 0 & 0 & 0 & \frac{1}{R_{ICV}\cdot C_{IC}} & 0 \\
0 & 0 & 0 & 0 & 0 & 0 & 0 & \frac{-R_{LPA}}{L_{LPA}} & \frac{-1}{L_{LPA}} & 0 & 0 & \frac{1}{L_{LPA}} & 0 \\
\frac{1}{R_{LPV}\cdot C_{LPC}} & 0 & 0 & 0 & 0 & 0 & 0 & \frac{1}{C_{LPC}} & \frac{-1}{R_{LPV}\cdot C_{LPC}} & 0 & 0 & 0 & 0 \\
0 & 0 & 0 & 0 & 0 & 0 & 0 & 0 & 0 & \frac{-R_{RPA}}{L_{RPA}} & \frac{-1}{L_{RPA}} & \frac{1}{L_{RPA}} & 0 \\
\frac{1}{R_{RPV}\cdot C_{RPC}} & 0 & 0 & 0 & 0 & 0 & 0 & 0 & 0 & \frac{1}{C_{RPC}} & \frac{-1}{R_{RPV}\cdot C_{RPC}} & 0 & 0 \\
0 & 0 & 0 & 0 & \frac{1}{R_{SCV}\cdot C_J} & 0 & \frac{1}{R_{ICV}\cdot C_J} & \frac{-1}{C_J} & 0 & \frac{-1}{C_J} & 0 & \frac{-1}{C_J}\cdot\left(\frac{1}{R_{SCV}}+\frac{1}{R_{ICV}}\right) & \frac{1}{C_J} \\
0 & \frac{1}{L_{IJS}} & 0 & 0 & 0 & 0 & 0 & 0 & 0 & 0 & 0 & \frac{-1}{L_{IJS}} & \frac{-R_{IJS}}{L_{IJS}}
\end{bmatrix}
$$

Figure 20 Tricuspid valve closed - pulmonary valve closed for Fontan circulation with the IJS

Like the 12x12 matrix without the injection jet system, when the injection jet system is introduced to the system as an extra component, the size of the matrix has increased by 1 row and 1 column and some additional values have been introduced to the system. The resistance of the vessel IJS, and inductance of the IJS value has been added as new constants. This state represents the case when both tricuspid and the pulmonary valves are closed.

State 3: Tricuspid valve (TV) closed and Pulmonary valve (PV) open

$$A_{co}(t) := \left[\begin{array}{ccccccccccccc}
\frac{-1}{C_{RA}}\cdot\left(\frac{1}{R_{LPV}}+\frac{1}{R_{RPV}}\right) & 0 & 0 & 0 & 0 & 0 & 0 & 0 & \frac{1}{R_{LPV}\cdot C_{RA}} & 0 & \frac{1}{R_{RPV}\cdot C_{RA}} & 0 & 0 \\
0 & \frac{-1}{C_{RV}(t)}\cdot\left(dC_{RV}(t+\varepsilon)+\frac{1}{R_{PV}}\right) & \frac{1}{R_{PV}\cdot C_{RV}(t)} & 0 & 0 & 0 & 0 & 0 & 0 & 0 & 0 & 0 & \frac{-1}{C_{RV}(t)} \\
0 & \frac{1}{R_{PV}\cdot C_{AO}} & \frac{-1}{R_{PV}\cdot C_{AO}} & \frac{-1}{C_{AO}} & 0 & \frac{-1}{C_{AO}} & 0 & 0 & 0 & 0 & 0 & 0 & 0 \\
0 & 0 & \frac{1}{L_{SCA}} & \frac{-R_{SCA}}{L_{SCA}} & \frac{-1}{L_{SCA}} & 0 & 0 & 0 & 0 & 0 & 0 & 0 & 0 \\
0 & 0 & 0 & \frac{1}{C_{SC}} & \frac{-1}{R_{SCV}\cdot C_{SC}} & 0 & 0 & 0 & 0 & 0 & 0 & \frac{1}{R_{SCV}\cdot C_{SC}} & 0 \\
0 & 0 & \frac{1}{L_{ICA}} & 0 & 0 & \frac{-R_{ICA}}{L_{ICA}} & \frac{-1}{L_{ICA}} & 0 & 0 & 0 & 0 & 0 & 0 \\
0 & 0 & 0 & 0 & 0 & \frac{1}{C_{IC}} & \frac{-1}{R_{ICV}\cdot C_{IC}} & 0 & 0 & 0 & 0 & \frac{1}{R_{ICV}\cdot C_{IC}} & 0 \\
0 & 0 & 0 & 0 & 0 & 0 & 0 & \frac{-R_{LPA}}{L_{LPA}} & \frac{-1}{L_{LPA}} & 0 & 0 & \frac{1}{L_{LPA}} & 0 \\
\frac{1}{R_{LPV}\cdot C_{LPC}} & 0 & 0 & 0 & 0 & 0 & 0 & \frac{1}{C_{LPC}} & \frac{-1}{R_{LPV}\cdot C_{LPC}} & 0 & 0 & 0 & 0 \\
0 & 0 & 0 & 0 & 0 & 0 & 0 & 0 & 0 & \frac{-R_{RPA}}{L_{RPA}} & \frac{-1}{L_{RPA}} & \frac{1}{L_{RPA}} & 0 \\
\frac{1}{R_{RPV}\cdot C_{RPC}} & 0 & 0 & 0 & 0 & 0 & 0 & 0 & 0 & \frac{1}{C_{RPC}} & \frac{-1}{R_{RPV}\cdot C_{RPC}} & 0 & 0 \\
0 & 0 & 0 & 0 & \frac{1}{R_{SCV}\cdot C_J} & 0 & \frac{1}{R_{ICV}\cdot C_J} & \frac{-1}{C_J} & 0 & \frac{-1}{C_J} & 0 & \frac{-1}{C_J}\cdot\left(\frac{1}{R_{SCV}}+\frac{1}{R_{ICV}}\right) & \frac{1}{C_J} \\
0 & \frac{1}{L_{IJS}} & 0 & 0 & 0 & 0 & 0 & 0 & 0 & 0 & 0 & \frac{-1}{L_{IJS}} & \frac{-R_{IJS}}{L_{IJS}}
\end{array}\right]$$

Figure 21 Tricuspid valve open - pulmonary valve closed for Fontan circulation with the IJS

In state two, the tricuspid valve opens and the pulmonary valve remains shut. This applies the exact same principle with the state where the injection jet system is not introduced into the system.

State 3 and state 4 applies exactly same as the state 3 and 4 when injection jet system has not been introduced. The only difference between the two sets of matrix is the last column vector and the last row vector since the IJs has been added. Addition of the IJS changes the equation for PRV and QJ. In addition another set of equation ‘QIJS’ is introduced to the system.

State 2: Tricuspid valve (TV) open and Pulmonary valve (PV) closed

$$A_{oc}(t) := \begin{bmatrix} \frac{-1}{C_{RA}}\cdot\left(\frac{1}{R_{LPV}}+\frac{1}{R_{RPV}}+\frac{1}{R_{TV}}\right) & \frac{1}{R_{TV}\cdot C_{RA}} & 0 & 0 & 0 & 0 & 0 & 0 & \frac{1}{R_{LPV}\cdot C_{RA}} & 0 & \frac{1}{R_{RPV}\cdot C_{RA}} & 0 & 0 \\ \frac{1}{R_{TV}\cdot C_{RV}(t)} & \frac{-1}{C_{RV}(t)}\cdot\left(dC_{RV}(t+\varepsilon)+\frac{1}{R_{TV}}\right) & 0 & 0 & 0 & 0 & 0 & 0 & 0 & 0 & 0 & 0 & \frac{-1}{C_{RV}(t)} \\ 0 & 0 & 0 & \frac{-1}{C_{AO}} & 0 & \frac{-1}{C_{AO}} & 0 & 0 & 0 & 0 & 0 & 0 & 0 \\ 0 & 0 & \frac{1}{L_{SCA}} & \frac{-R_{SCA}}{L_{SCA}} & \frac{-1}{L_{SCA}} & 0 & 0 & 0 & 0 & 0 & 0 & 0 & 0 \\ 0 & 0 & 0 & \frac{1}{C_{SC}} & \frac{-1}{R_{SCV}\cdot C_{SC}} & 0 & 0 & 0 & 0 & 0 & 0 & \frac{1}{R_{SCV}\cdot C_{SC}} & 0 \\ 0 & 0 & \frac{1}{L_{ICA}} & 0 & 0 & \frac{-R_{ICA}}{L_{ICA}} & \frac{-1}{L_{ICA}} & 0 & 0 & 0 & 0 & 0 & 0 \\ 0 & 0 & 0 & 0 & 0 & \frac{1}{C_{IC}} & \frac{-1}{R_{ICV}\cdot C_{IC}} & 0 & 0 & 0 & 0 & \frac{1}{R_{ICV}\cdot C_{IC}} & 0 \\ 0 & 0 & 0 & 0 & 0 & 0 & 0 & \frac{-R_{LPA}}{L_{LPA}} & \frac{-1}{L_{LPA}} & 0 & 0 & \frac{1}{L_{LPA}} & 0 \\ \frac{1}{R_{LPV}\cdot C_{LPC}} & 0 & 0 & 0 & 0 & 0 & 0 & \frac{1}{C_{LPC}} & \frac{-1}{R_{LPV}\cdot C_{LPC}} & 0 & 0 & 0 & 0 \\ 0 & 0 & 0 & 0 & 0 & 0 & 0 & 0 & 0 & \frac{-R_{RPA}}{L_{RPA}} & \frac{-1}{L_{RPA}} & \frac{1}{L_{RPA}} & 0 \\ \frac{1}{R_{RPV}\cdot C_{RPC}} & 0 & 0 & 0 & 0 & 0 & 0 & 0 & 0 & \frac{1}{C_{RPC}} & \frac{-1}{R_{RPV}\cdot C_{RPC}} & 0 & 0 \\ 0 & 0 & 0 & 0 & \frac{1}{R_{SCV}\cdot C_J} & 0 & \frac{1}{R_{ICV}\cdot C_J} & \frac{-1}{C_J} & 0 & \frac{-1}{C_J} & 0 & \frac{-1}{C_J}\cdot\left(\frac{1}{R_{SCV}}+\frac{1}{R_{ICV}}\right) & \frac{1}{C_J} \\ 0 & \frac{1}{L_{IJS}} & 0 & 0 & 0 & 0 & 0 & 0 & 0 & 0 & 0 & \frac{-1}{L_{IJS}} & \frac{-R_{IJS}}{L_{IJS}} \end{bmatrix}$$

Figure 22 Tricuspid valve closed - pulmonary valve open for Fontan circulation with the IJS

State 4: Tricuspid valve (TV) open and Pulmonary valve (PV) open (impossible)

$$A_{oo}(t) := \begin{bmatrix} \frac{-1}{C_{RA}}\cdot\left(\frac{1}{R_{LPV}}+\frac{1}{R_{RPV}}+\frac{1}{R_{TV}}\right) & \frac{1}{R_{TV}\cdot C_{RA}} & 0 & 0 & 0 & 0 & 0 & 0 & \frac{1}{R_{LPV}\cdot C_{RA}} & 0 & \frac{1}{R_{RPV}\cdot C_{RA}} & 0 & 0 \\ \frac{1}{R_{TV}\cdot C_{RV}(t)} & \frac{-1}{C_{RV}(t)}\cdot\left(dC_{RV}(t+\varepsilon)+\frac{1}{R_{TV}}+\frac{1}{R_{PV}}\right) & \frac{1}{R_{PV}\cdot C_{RV}(t)} & 0 & 0 & 0 & 0 & 0 & 0 & 0 & 0 & 0 & \frac{-1}{C_{RV}(t)} \\ 0 & \frac{1}{R_{PV}\cdot C_{AO}} & \frac{-1}{R_{PV}\cdot C_{AO}} & \frac{-1}{C_{AO}} & 0 & \frac{-1}{C_{AO}} & 0 & 0 & 0 & 0 & 0 & 0 & 0 \\ 0 & 0 & \frac{1}{L_{SCA}} & \frac{-R_{SCA}}{L_{SCA}} & \frac{-1}{L_{SCA}} & 0 & 0 & 0 & 0 & 0 & 0 & 0 & 0 \\ 0 & 0 & 0 & \frac{1}{C_{SC}} & \frac{-1}{R_{SCV}\cdot C_{SC}} & 0 & 0 & 0 & 0 & 0 & 0 & \frac{1}{R_{SCV}\cdot C_{SC}} & 0 \\ 0 & 0 & \frac{1}{L_{ICA}} & 0 & 0 & \frac{-R_{ICA}}{L_{ICA}} & \frac{-1}{L_{ICA}} & 0 & 0 & 0 & 0 & 0 & 0 \\ 0 & 0 & 0 & 0 & 0 & \frac{1}{C_{IC}} & \frac{-1}{R_{ICV}\cdot C_{IC}} & 0 & 0 & 0 & 0 & \frac{1}{R_{ICV}\cdot C_{IC}} & 0 \\ 0 & 0 & 0 & 0 & 0 & 0 & 0 & \frac{-R_{LPA}}{L_{LPA}} & \frac{-1}{L_{LPA}} & 0 & 0 & \frac{1}{L_{LPA}} & 0 \\ \frac{1}{R_{LPV}\cdot C_{LPC}} & 0 & 0 & 0 & 0 & 0 & 0 & \frac{1}{C_{LPC}} & \frac{-1}{R_{LPV}\cdot C_{LPC}} & 0 & 0 & 0 & 0 \\ 0 & 0 & 0 & 0 & 0 & 0 & 0 & 0 & 0 & \frac{-R_{RPA}}{L_{RPA}} & \frac{-1}{L_{RPA}} & \frac{1}{L_{RPA}} & 0 \\ \frac{1}{R_{RPV}\cdot C_{RPC}} & 0 & 0 & 0 & 0 & 0 & 0 & 0 & 0 & \frac{1}{C_{RPC}} & \frac{-1}{R_{RPV}\cdot C_{RPC}} & 0 & 0 \\ 0 & 0 & 0 & 0 & \frac{1}{R_{SCV}\cdot C_J} & 0 & \frac{1}{R_{ICV}\cdot C_J} & \frac{-1}{C_J} & 0 & \frac{-1}{C_J} & 0 & \frac{-1}{C_J}\cdot\left(\frac{1}{R_{SCV}}+\frac{1}{R_{ICV}}\right) & \frac{1}{C_J} \\ 0 & \frac{1}{L_{IJS}} & 0 & 0 & 0 & 0 & 0 & 0 & 0 & 0 & 0 & \frac{-1}{L_{IJS}} & \frac{-R_{IJS}}{L_{IJS}} \end{bmatrix}$$

Figure 23 Tricuspid valve open - pulmonary valve open for Fontan circulation with the IJS

When Injection set system is added into the system, it was mentioned that due to the training effect of the entrainment, there will be a pressure drop in the area where the injection jet system is added. This pressure drop can be programmed in a three dimensional computational fluid dynamics simulation model. However, it is impossible to design the pressure drop in a one dimensional problem. Therefore, we will be forcing that the pressure drop in the vessel is approximately 0.01 mmHg and there for we will be subtracting 0.09 mmHg from 0.1 mmHg which were the initial value of RRPA and RRPA which are the pressure of left and right pulmonary circulation.

Simulation Results

In order to get the results, ode45 function has been used with exact same codes from table 8. This will solve the system of equations and display the values of pressure and flow corresponding to different maximum elastance and the heart rate. The initial condition of the patient is provided with the maximum elastance of 0.5, minimum elastance of 0.06 and heart rate of 120 bpm.

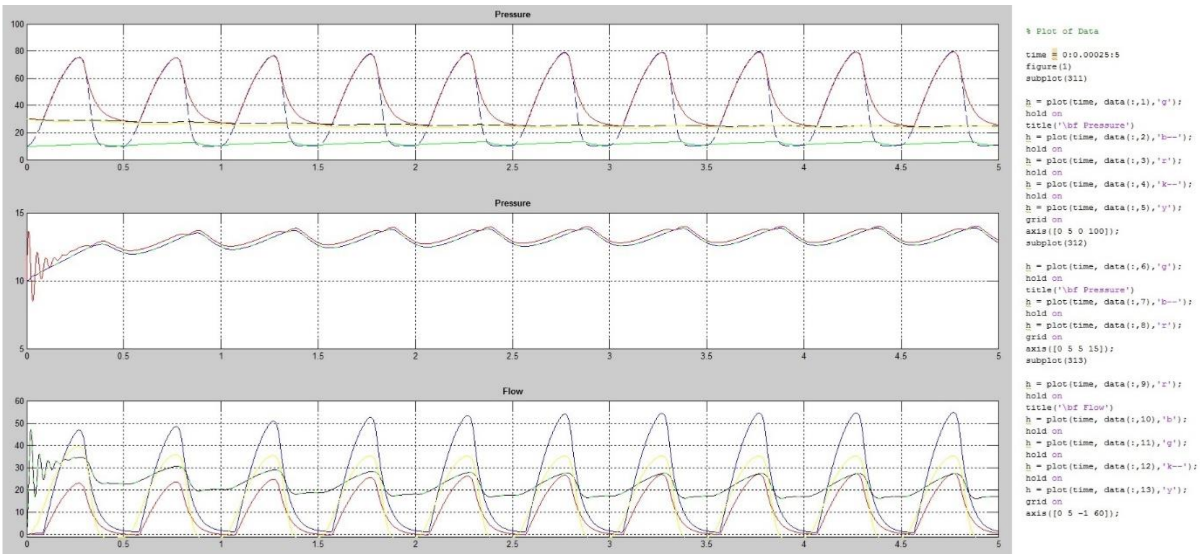

Figure 24 Fontan circulation with Injection Jet System

With the injection jet system added into the Fontan circulation there are changes to the pressure at the junction and also a new flow has been added into the circuit. In addition, we will be taking the sum of the points of the last cycle, taking an average to determine the flow or pressure of each points. This will validate the difference of injection jet system compared to the circulation without the injection jet system.

Comparison

Comparison of the data will be made through excel after importing the data points from MATLAB. The comparison of the data will be made between the data point with and with injection jet system depending on the heart rate and elastance as well as to the general parameter model which had the heart rate of 120bpm, Maximum elastance of 0.5. When the resistance of injection jet system changes, the value of caval pressure, systemic flow and pulmonary flow changes along with the flow of the injection jet system. In the simulation, the value of caval pressure and the ratio of systemic flow over pulmonary flow is extremely critical. The ideal caval pressure range is below 15mmHg and it should show that it is decreasing depending on the maximum elastance and the resistance of the injection jet system. The values that will be used to make comparison would be 0.75, 0.50, 0.25 for the maximum elastance and 140bpm, 120bpm and 100bpm for the heart rate and 1mmHg, 2mmHg and 3mmHg for the resistance of the injection jet system. The systemic flow and pulmonary flow values will be found by using the last cycle of the generated graphs as well as the caval pressure and the flow in injection jet system.

Case 1: Heart Rate 140, Maximum Elastance 0.75

Without Injection Jet System

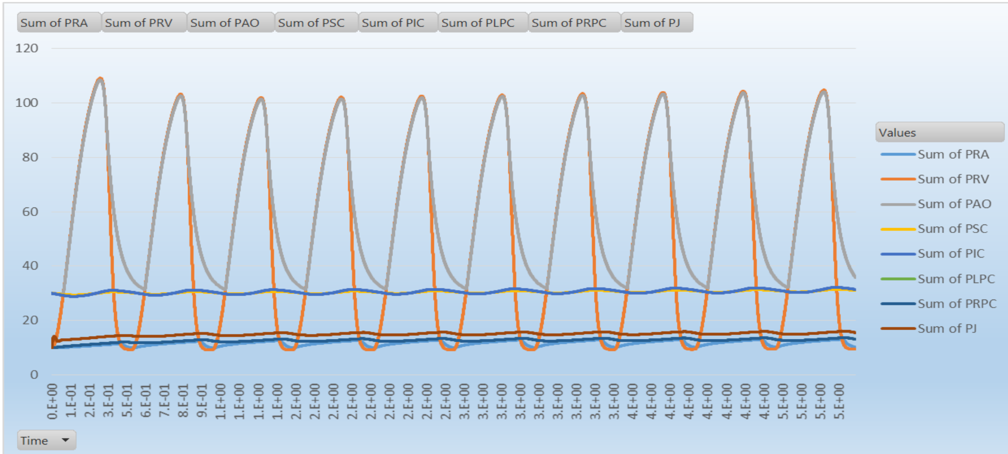

Figure 25 Pressure Summary for Maximum Elastance of 0.75, Minimum Elastance of 0.06 and Heart Rate of 140 bpm

The change in heart rate will affect the change in time since the heart rate will be divided by the number of samples of the last period to determine the flow going in to the ventricle, going out of the ventricle and the combined pressure at the junction by the pulmonary circulation. The caval pressure in the vena cava is 15.447 mmHg.

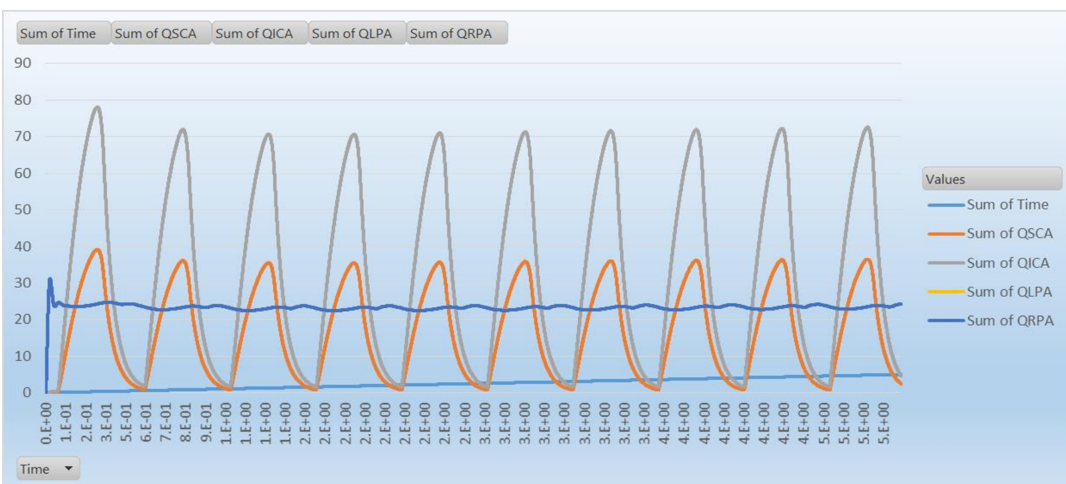

Figure 26 Flow Summary for Maximum Elastance of 0.75, Minimum Elastance of 0.06 and Heart Rate of 140 bpm

The flow in the circuit with the injection jet system will depend on the systemic flow which is Qout and pulmonary flow which is Qin. Flow leaving the ventricle is 2.913 mmHg/ml and flow entering the ventricle is approximately 2.821mmHg/ml. The ratio of the systemic flow over pulmonary flow is 0.968.

With Injection Jet System

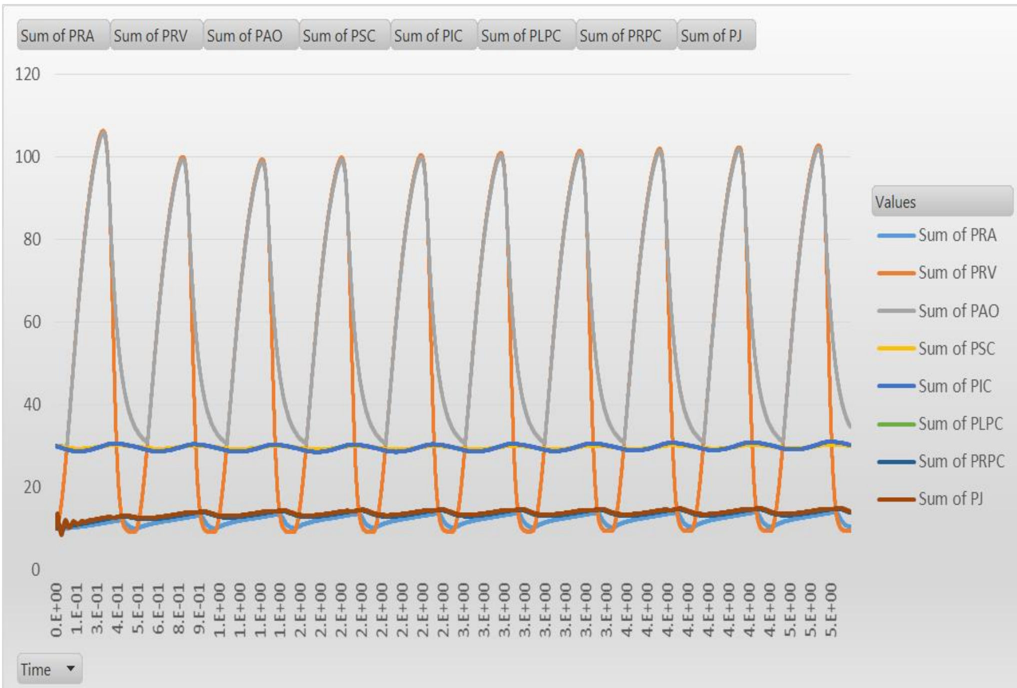

Figure 27 Pressure Summary for Maximum Elastance of 0.75, Minimum Elastance of 0.06 and Heart Rate of 140 bpm

The injection jet system has been added into the system. By adding the injection jet system, the caval pressure is 14.243mmHg.

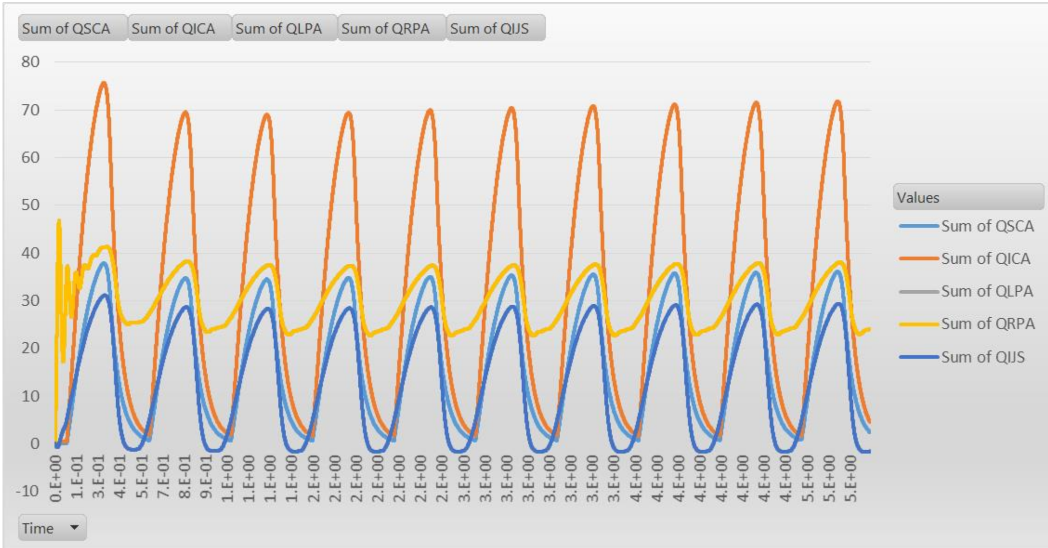

Figure 28 Flow Summary for Maximum Elastance of 0.75, Minimum Elastance of 0.06 and Heart Rate of 140 bpm

The injection jet system has been added and the flow for the injection jet system was 0.759mmHg/ml. In addition the systemic flow is 2.924mmHg/ml and the pulmonary flow is 3.598mmHg. The ratio of the systemic pressure to pulmonary pressure is 1.231.

Comparison

QSYSTEMIC	2.924	mmHg/ml
QSYSTEMIC (NO IJS)	2.913	mmHg/ml
QPULMONARY	3.598	mmHg/ml
QPULMONARY(NO IJS)	2.821	mmHg/ml
QP/QS	1.230506	
QP/QS (NO IJS)	1	
PCAVAL	14.243	mmHg
PCAVAL (NO IJS)	15.447	mmHg
QIJS	0.759	mmHg/ml

Table 9 Heart Rate =140bpm, Maximum Elastance = 0.75, Resistance of IJS = 3

The resistance of Injection Jet is set at 3mmHg. The flow of the systemic circulation is 2.913mmHg/ml and 2.821mmHg/ml without the Injection Jet System. Flow of the systemic circulation is 2.924mmHg/ml and pulmonary circulation is 3.598mmHg/ml with the Injection Jet System. The Injection Jet System added more flow to the systemic circulation as well as the pulmonary circulation. In addition the Injection Jet System had a flow rate of 0.759mmHg/ml. The ratio of the systemic flow to the pulmonary flow resulted to be 1.23 with the injection jet system. However the ratio was 0.968 without the Injection Jet System. The ratio of the systemic flow and pulmonary flow is within the range of 1.20 and 1.50 which is the ideal range.

The caval pressure is 14.243mmHg with the Injection jet system and the caval pressure without the injection jet system is 15.447mmHg. The caval pressure with the injection jet system should be less than the caval pressure without the injection jet system.

RIJS = 2			RIJS = 1		
QSYSTEMIC	2.869	mmHg/ml	QSYSTEMIC	2.726	mmHg/ml
QPULMONARY	3.899	mmHg/ml	QPULMONARY	4.735	mmHg/ml
QP/QS	1.359		QP/QS	1.736	
PCAVAL	14.497	mmHg	PCAVAL	15.174	mmHg
QIJS	1.113	mmHg/ml	QIJS	2.09	mmHg/ml

Table 10 Heart Rate =140bpm, Maximum Elastance = 0.75, Resistance of IJS = 2 (Left) and Heart Rate =140bpm, Maximum Elastance = 0.75, Resistance of IJS = 1(right)

The resistance of the Injection Jet is set at 2mmHg.The flow of the systemic circulation is 2.869 mmHg/ml and the flow of the pulmonary circulation is 3.899. The ratio of the pulmonary circulation to the systemic circulation is 1.36. The value resides within the range of 1.25 to 1.5. The flow of Injection Jet system is 1.11 mmHg/ml. The caval pressure is 14.497 mmHg which is also within the range between 12.5 and 15.0.

The resistance of the Injection Jet is set at 1mmHg. The flow of the systemic circulation is 2.726 mmHg/ml and the flow of the pulmonary circulation is 4.735. The ratio of the pulmonary circulation to the systemic circulation is 1.73. The value resides above the range of 1.25 and 1.5 which is not good for the patient. The flow of Injection Jet system is 2.09 mmHg/ml. The caval pressure is 15.174 which is also above 15 which is above the range.

Case 2: Heart Rate 120, Maximum Elastance 0.75

Without Injection Jet System

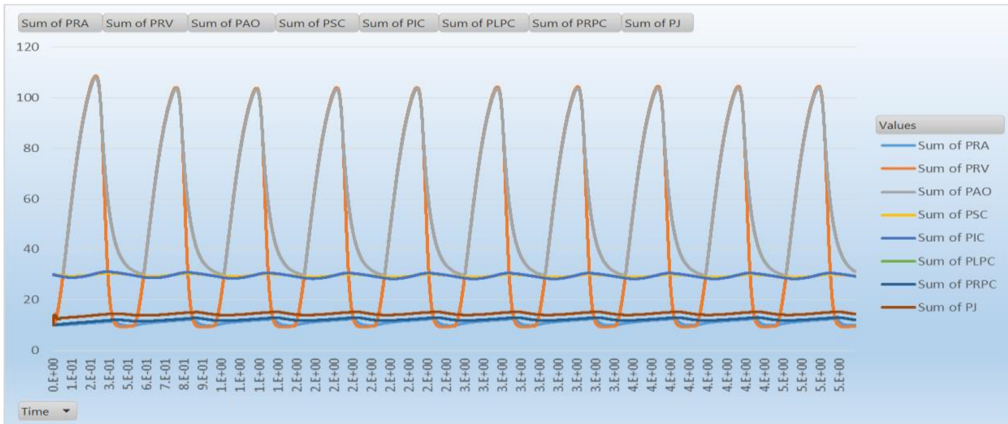

Figure 29 Pressure Summary for Maximum Elastance of 0.75, Minimum Elastance of 0.06 and Heart Rate of 120 bpm

With the change in heart rate to 120bpm, we can tell that the interval between each beat has reduced. However the values and the shape of the function remains identical. The caval pressure is 14.621mmHg.

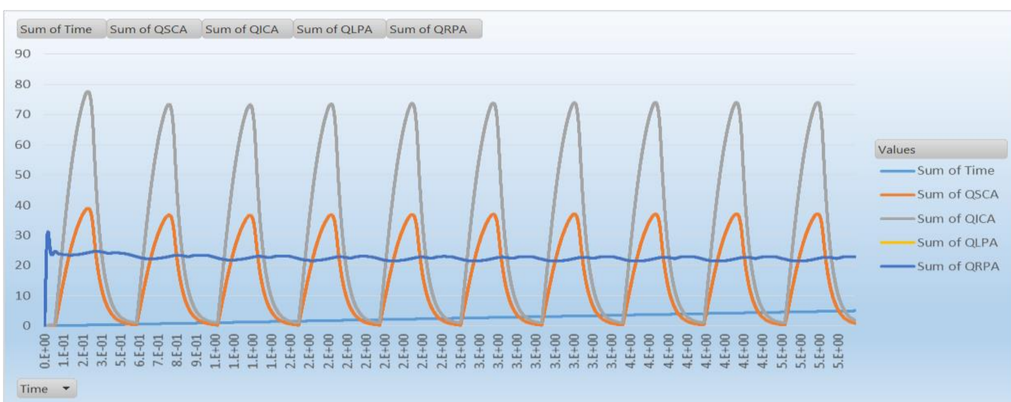

Figure 30 Flow Summary for Maximum Elastance of 0.75, Minimum Elastance of 0.06 and Heart Rate of 120 bpm

The systemic flow is 2.676 mmHg/ml and the pulmonary flow is 2.674 mmHg/ml. The ratio of the systemic pressure over pulmonary pressure is 0.99.

With Injection Jet System

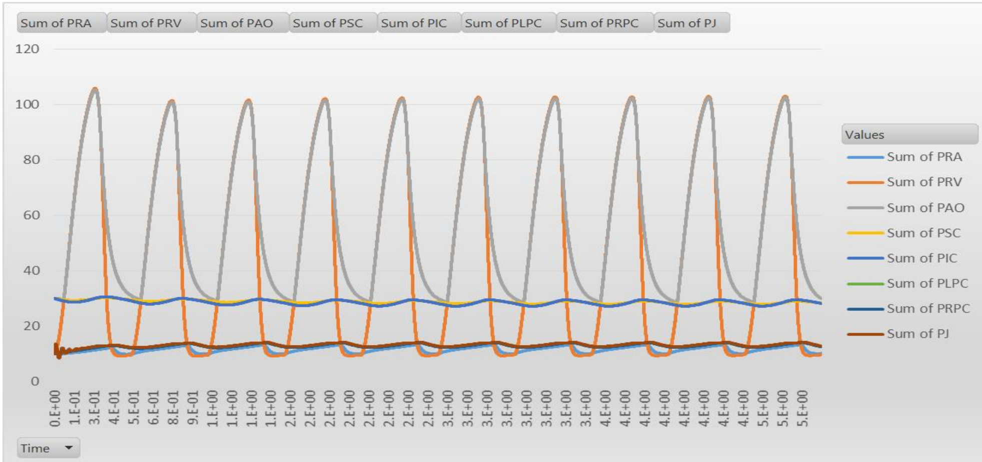

Figure 31 Pressure Summary for Maximum Elastance of 0.75, Minimum Elastance of 0.06 and Heart Rate of 120 bpm

When the injection jet system is added, the caval pressure is 13.413 mmHg.

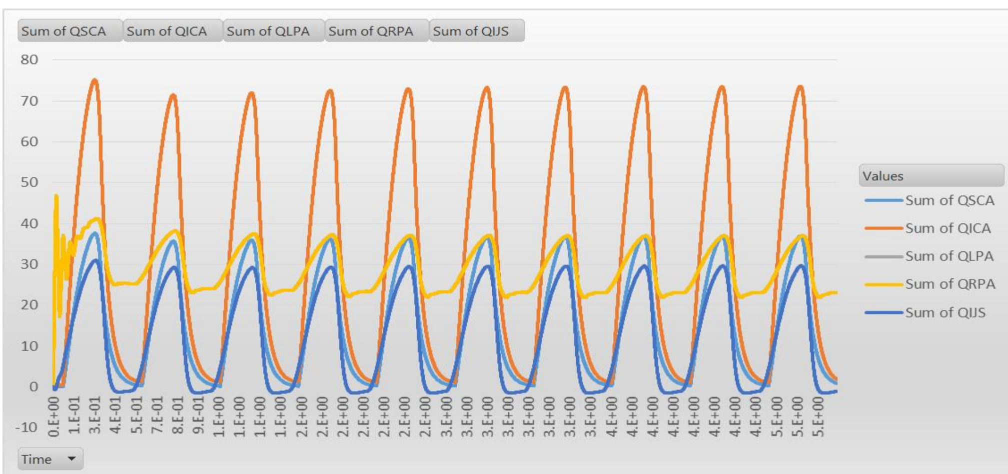

Figure 32 Flow Summary for Maximum Elastance of 0.75, Minimum Elastance of 0.06 and Heart Rate of 120 bpm

When injection jet system is added, the systemic flow is 2.699 mmHg/ml and the pulmonary flow is 3.388 mmHg/ml. The ratio between the pulmonary flow and the systemic flow is 1.255.

Comparison

QSYSTEMIC	2.699	mmHg/ml
QSYSTEMIC (NO IJS)	2.676	mmHg/ml
QPULMONARY	3.388	mmHg/ml
QPULMONARY(NO IJS)	2.674	mmHg/ml
QP/QS	1.255	
QP/QS (NO IJS)	1	
PCAVAL	13.413	mmHg
PCAVAL (NO IJS)	14.621	mmHg
QIJS	0.687	mmHg/ml

Table 11 Heart Rate =120bpm, Maximum Elastance = 0.75, Resistance of IJS = 3

The resistance of Injection Jet is set at 3mmHg. The flow of the systemic circulation is 2.676mmHg/ml and 2.674mmHg/ml without the Injection Jet System. Flow of the systemic circulation is 2.699mmHg/ml and pulmonary circulation is 3.388mmHg/ml with the Injection Jet System. The Injection Jet System added more flow to the systemic circulation as well as the pulmonary circulation. In addition the Injection Jet System had a flow rate of 0.687mmHg/ml. The ratio of the systemic flow to the pulmonary flow resulted to be 1.255 with the injection jet system. However the ratio was 0.999 without the Injection Jet System. The ratio of the systemic flow and pulmonary flow is within the range of 1.20 and 1.50 which is the ideal range.

The caval pressure is 13.413mmHg with the Injection jet system and the caval pressure without the injection jet system is 14.621mmHg. The caval pressure with the injection jet system should be less than the caval pressure without the injection jet system.

RIJS = 2			RIJS = 1		
QSYSTEMIC	2.656	mmHg/ml	QSYSTEMIC	2.54	mmHg/ml
QPULMONARY	3.667	mmHg/ml	QPULMONARY	4.451	mmHg/ml
QP/QS	1.380		QP/QS	1.752	
PCAVAL	13.631	mmHg	PCAVAL	14.219	mmHg
QIJS	1.01	mmHg/ml	QIJS	1.909	mmHg/ml

Table 12 Heart Rate =120bpm, Maximum Elastance = 0.75, Resistance of IJS = 2 (Left) and Heart Rate =120bpm, Maximum Elastance = 0.75, Resistance of IJS = 1(right)

The resistance of the Injection Jet is set at 2mmHg.The flow of the systemic circulation is 2.656 mmHg/ml and the flow of the pulmonary circulation is 3.667mmHg/ml. The ratio of the pulmonary circulation to the systemic circulation is 1.38. The value resides within the range of 1.25 to 1.5. The flow of Injection Jet system is 1.01 mmHg/ml. The caval pressure is 13.631 mmHg which is also within the range between 12.5 and 15.0.

The resistance of the Injection Jet is set at 1mmHg. The flow of the systemic circulation is 2.54 mmHg/ml and the flow of the pulmonary circulation is 4.451. The ratio of the pulmonary circulation to the systemic circulation is 1.75. The value resides above the range of 1.25 and 1.5 which is not good for the patient. The flow of Injection Jet system is 1.909 mmHg/ml. The caval pressure is 15.174 which is also above 15 which is above the range.

Case 3: Heart Rate 100, Maximum Elastance 0.75

Without Injection Jet System

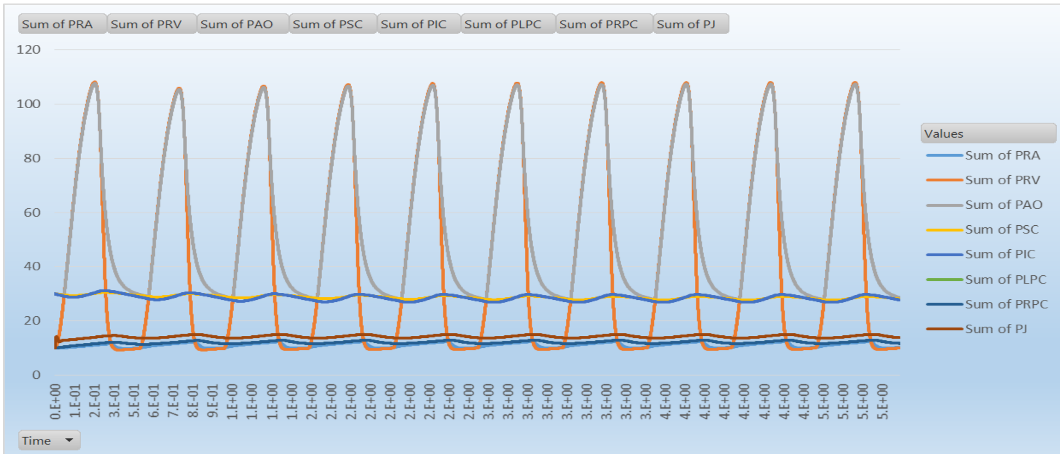

Figure 33 Pressure Summary for Maximum Elastance of 0.75, Minimum Elastance of 0.06 and Heart Rate of 100 bpm

With the change in heart rate to 100bpm, we can tell that the interval between each beat has reduced. However the values and the shape of the function remains identical. The caval pressure is 14.337mmHg.

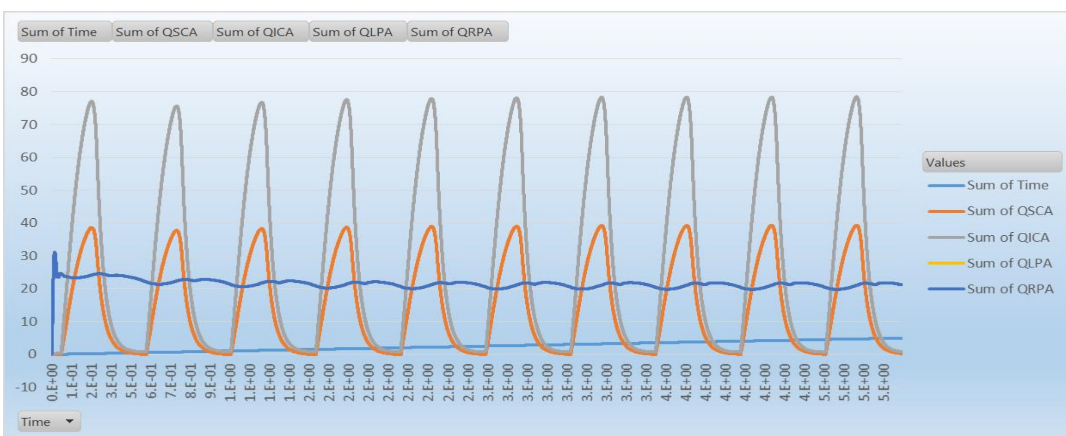

Figure 34 Flow Summary for Maximum Elastance of 0.75, Minimum Elastance of 0.06 and Heart Rate of 100 bpm

The systemic flow is 2.514 mmHg/ml and the pulmonary flow is 2.52 mmHg/ml. The ratio of the systemic pressure over pulmonary pressure is 1.00.

With Injection Jet System

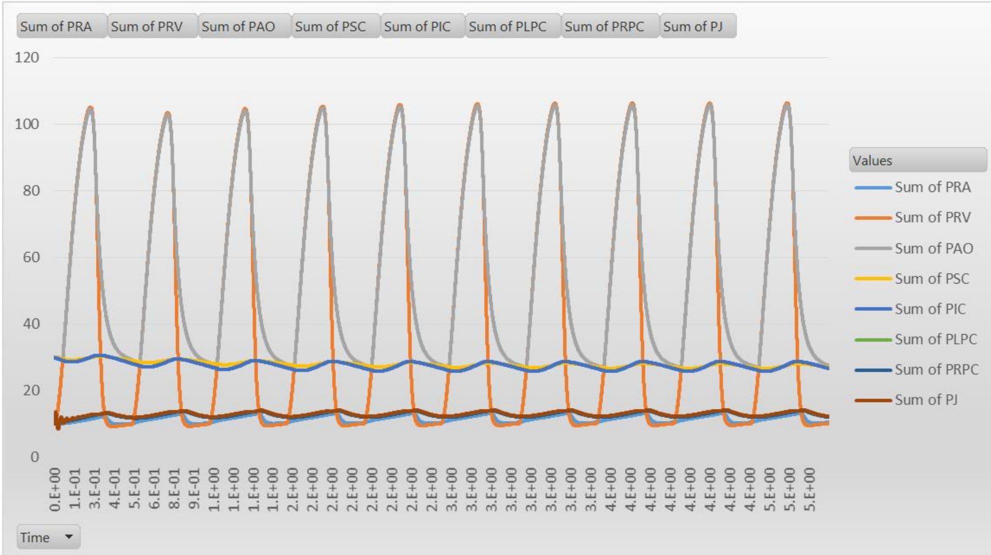

Figure 35 Pressure Summary for Maximum Elastance of 0.75, Minimum Elastance of 0.06 and Heart Rate of 100 bpm

When the injection jet system is added, the caval pressure is 13.164 mmHg.

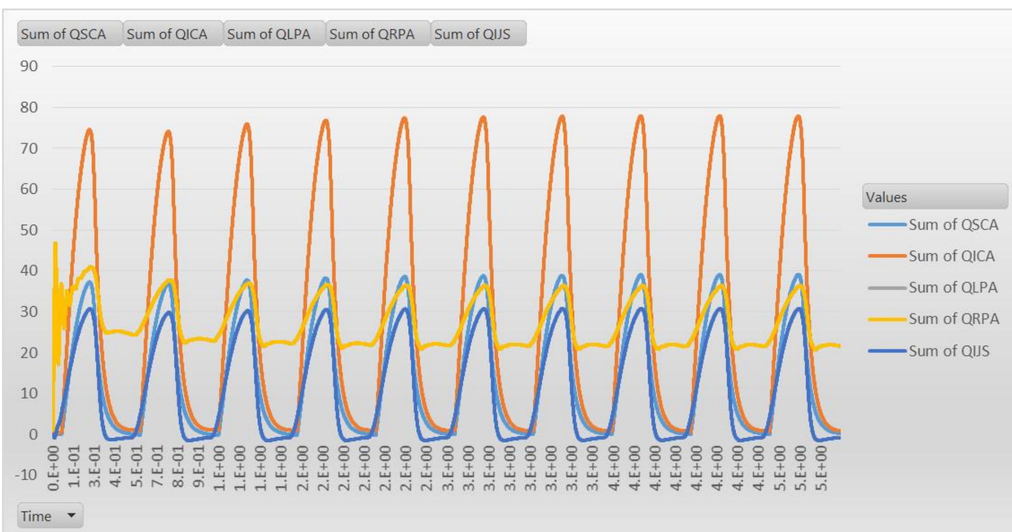

Figure 36 Flow Summary for Maximum Elastance of 0.75, Minimum Elastance of 0.06 and Heart Rate of 100 bpm

When injection jet system is added, the systemic flow is 2.54 mmHg/ml and the pulmonary flow is 3.178 mmHg/ml. The ratio between the pulmonary flow and the systemic flow is 1.251.

Comparison

QSYSTEMIC	2.54	mmHg/ml
QSYSTEMIC (NO IJS)	2.514	mmHg/ml
QPULMONARY	3.178	mmHg/ml
QPULMONARY(NO IJS)	2.52	mmHg/ml
QP/QS	1.25	
QP/QS (NO IJS)	1	
PCAVAL	13.164	mmHg
PCAVAL (NO IJS)	14.337	mmHg
QIJS	0.631	mmHg/ml

Table 13 Heart Rate =100bpm, Maximum Elastance = 0.75, Resistance of IJS = 3

The resistance of Injection Jet is set at 3mmHg. The flow of the systemic circulation is 2.514mmHg/ml and 2.52mmHg/ml without the Injection Jet System. Flow of the systemic circulation is 2.54mmHg/ml and pulmonary circulation is 3.178mmHg/ml with the Injection Jet System. The Injection Jet System added more flow to the systemic circulation as well as the pulmonary circulation. In addition the Injection Jet System had a flow rate of 0.631mmHg/ml. The ratio of the systemic flow to the pulmonary flow resulted to be 1.25 with the injection jet system. However the ratio was 1.002 without the Injection Jet System. The ratio of the systemic flow and pulmonary flow is within the range of 1.20 and 1.50 which is the ideal range. The caval pressure is 13.164mmHg with the Injection jet system and the caval pressure without the injection jet system is

14.337mmHg. The caval pressure with the injection jet system should be less than the caval pressure without the injection jet system.

RIJS = 2			RIJS = 1		
QSYSTEMIC	2.502	mmHg/ml	QSYSTEMIC	2.403	mmHg/ml
QPULMONARY	3.438	mmHg/ml	QPULMONARY	4.172	mmHg/ml
QP/QS	1.374		QP/QS	1.736	
PCAVAL	13.356	mmHg	PCAVAL	13.877	mmHg
QIJS	0.929	mmHg/ml	QIJS	1.762	mmHg/ml

Table 14 Heart Rate =100bpm, Maximum Elastance = 0.75, Resistance of IJS = 2 (Left) and Heart Rate =120bpm, Maximum Elastance = 0.75, Resistance of IJS = 1(right)

The resistance of the Injection Jet is set at 2mmHg.The flow of the systemic circulation is 2.502 mmHg/ml and the flow of the pulmonary circulation is 3.438. The ratio of the pulmonary circulation to the systemic circulation is 1.37. The value resides within the range of 1.25 to 1.5. The flow of Injection Jet system is 0.929 mmHg/ml. The caval pressure is 13.356 mmHg which is also within the range between 12.5 and 15.0.

The resistance of the Injection Jet is set at 1mmHg. The flow of the systemic circulation is 2.403 mmHg/ml and the flow of the pulmonary circulation is 4.172. The ratio of the pulmonary circulation to the systemic circulation is 1.73. The value resides above the range of 1.25 and 1.5 which is not good for the patient. The flow of Injection Jet system is 1.762 mmHg/ml. The caval pressure is 13.877mmHg which is also within 15.

Case 4: Heart Rate 140, Maximum Elastance 0.50

Without Injection Jet System

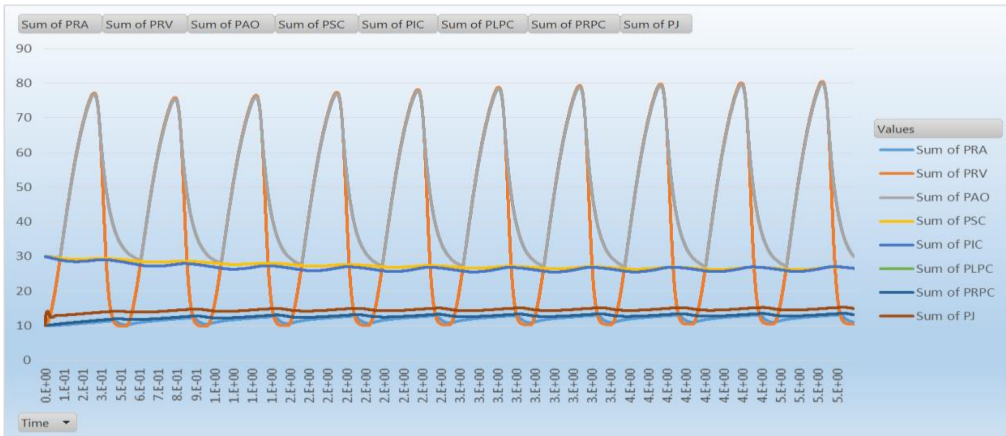

Figure 37 Pressure Summary for Maximum Elastance of 0.50, Minimum Elastance of 0.06 and Heart Rate of 140 bpm

With the change in heart rate to 140bpm as well as maximum elastance of 0.50, we can tell that the interval between each beat has reduced. However the values and the shape of the function remains identical. The caval pressure is 14.867mmHg.

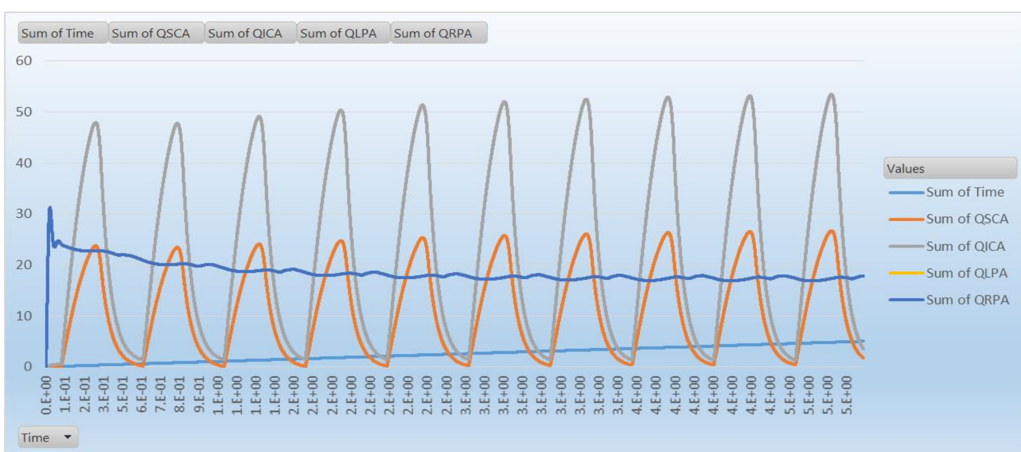

Figure 38 Flow Summary for Maximum Elastance of 0.50, Minimum Elastance of 0.06 and Heart Rate of 140 bpm

The systemic flow is 2.105 mmHg/ml and the pulmonary flow is 2.081 mmHg/ml. The ratio of the systemic pressure over pulmonary pressure is 0.98.

With Injection Jet System

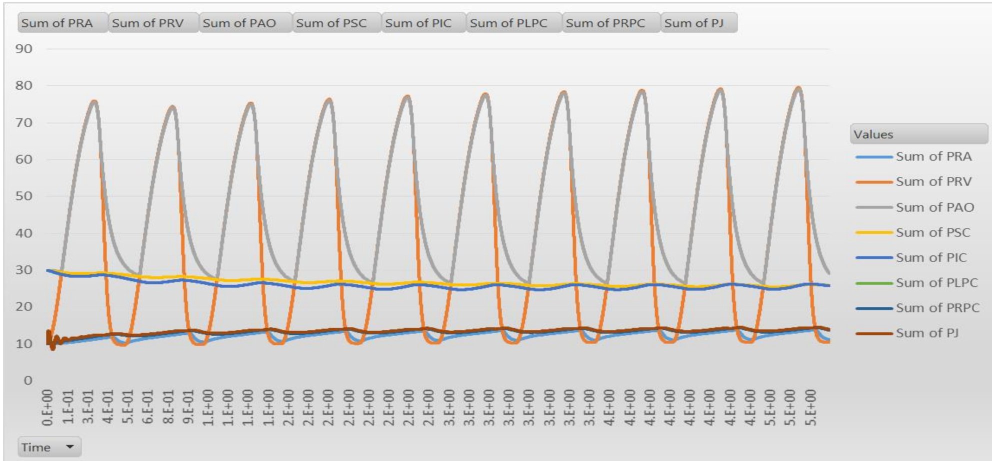

Figure 39 Pressure Summary for Maximum Elastance of 0.50, Minimum Elastance of 0.06 and Heart Rate of 140 bpm

When the injection jet system is added, the caval pressure is 13.972 mmHg.

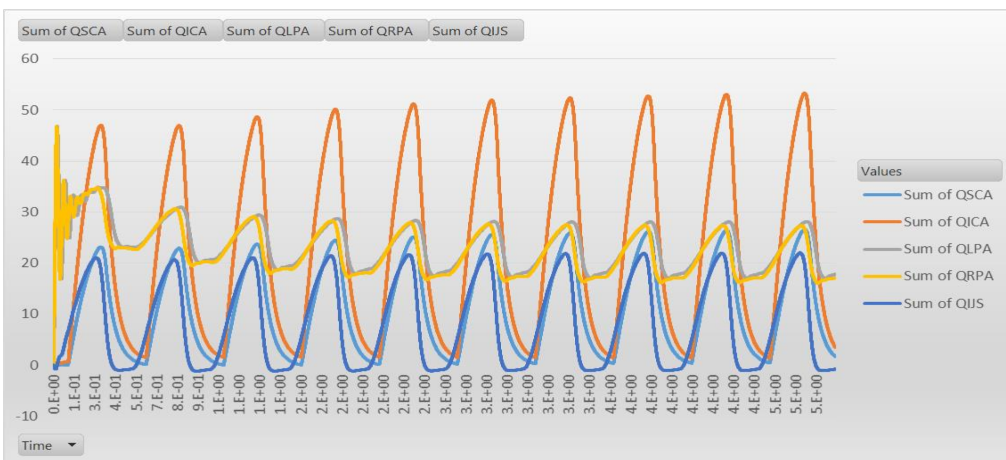

Figure 40 Flow Summary for Maximum Elastance of 0.50, Minimum Elastance of 0.06 and Heart Rate of 140 bpm

When injection jet system is added, the systemic flow is 2.123 mmHg/ml and the pulmonary flow is 2.652 mmHg/ml. The ratio between the pulmonary flow and the systemic flow is 1.249.

Comparison

QSYSTEMIC	2.123	mmHg/ml
QSYSTEMIC (NO IJS)	2.105	mmHg/ml
QPULMONARY	2.652	mmHg/ml
QPULMONARY(NO IJS)	2.081	mmHg/ml
QP/QS	1.24	
QP/QS (NO IJS)	1	
PCAVAL	13.972	mmHg
PCAVAL (NO IJS)	14.867	mmHg
QIJS	0.551	mmHg/ml

Table 15 Heart Rate =140bpm, Maximum Elastance = 0.50, Resistance of IJS = 3

The resistance of Injection Jet is set at 3mmHg. The flow of the systemic circulation is 2.105mmHg/ml and 2.081mmHg/ml without the Injection Jet System. Flow of the systemic circulation is 2.123mmHg/ml and pulmonary circulation is 2.652mmHg/ml with the Injection Jet System. The Injection Jet System added more flow to the systemic circulation as well as the pulmonary circulation. In addition the Injection Jet System had a flow rate of 0.551mmHg/ml. The ratio of the systemic flow to the pulmonary flow resulted to be 1.249 with the Injection Jet System. However the ratio was 0.988 without the Injection Jet System. The ratio of the systemic flow and pulmonary flow is within the range of 1.20 and 1.50 which is the ideal range.

The caval pressure is 13.972mmHg with the Injection jet system and the caval pressure without the injection jet system is 14.867mmHg. The caval pressure with the injection jet system should be less than the caval pressure without the injection jet system.

RIJS = 2			RIJS = 1		
QSYSTEMIC	2.091	mmHg/ml	QSYSTEMIC	2.005	mmHg/ml
QPULMONARY	2.88	mmHg/ml	QPULMONARY	3.519	mmHg/ml
QP/QS	1.377		QP/QS	1.755	
PCAVAL	14.157	mmHg	PCAVAL	14.659	mmHg
QIJS	0.811	mmHg/ml	QIJS	1.535	mmHg/ml

Table 16 Heart Rate =140bpm, Maximum Elastance = 0.75, Resistance of IJS = 2 (Left) and Heart Rate =140bpm, Maximum Elastance = 0.75, Resistance of IJS = 1(right)

The resistance of the Injection Jet is set at 2mmHg.The flow of the systemic circulation is 2.091 mmHg/ml and the flow of the pulmonary circulation is 2.88mmHg/ml. The ratio of the pulmonary circulation to the systemic circulation is 1.377. The value resides within the range of 1.25 to 1.5. The flow of Injection Jet System is 0.811 mmHg/ml. The caval pressure is 14.157 mmHg which is also within the range between 12.5 and 15.0.

The resistance of the Injection Jet is set at 1mmHg. The flow of the systemic circulation is 2.005 mmHg/ml and the flow of the pulmonary circulation is 3.519. The ratio of the pulmonary circulation to the systemic circulation is 1.755. The value resides above the range of 1.25 and 1.5 which is not good for the patient. The flow of Injection Jet System is 1.755 mmHg/ml. The caval pressure is 14.659mmHg which is also within 15.

Case 5: Heart Rate 120, Maximum Elastance 0.50

Without Injection Jet System

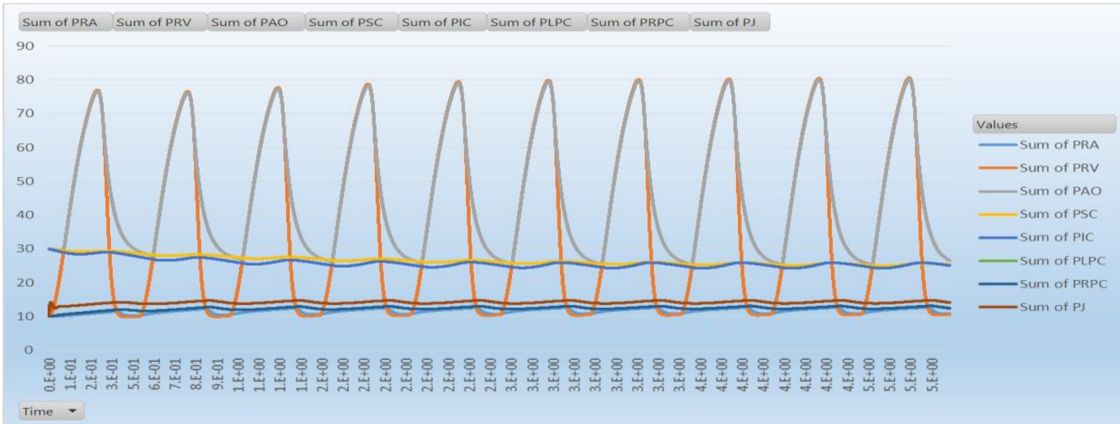

Figure 41 Pressure Summary for Maximum Elastance of 0.50, Minimum Elastance of 0.06 and Heart Rate of 120 bpm

With the change in heart rate to 120 bpm, we can tell that the interval between each beat has reduced. However the values and the shape of the function remains identical. The caval pressure is 14.28mmHg.

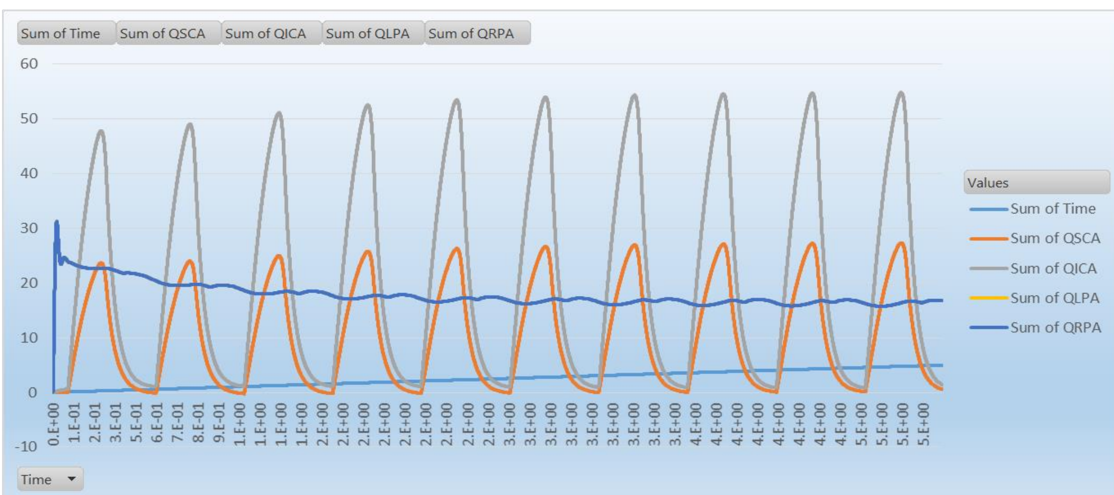

Figure 42 Flow Summary for Maximum Elastance of 0.50, Minimum Elastance of 0.06 and Heart Rate of 120 bpm

The systemic flow is 1.944 mmHg/ml and the pulmonary flow is 1.966 mmHg/ml. The ratio of the systemic pressure over pulmonary pressure is 1.01.

With Injection Jet System

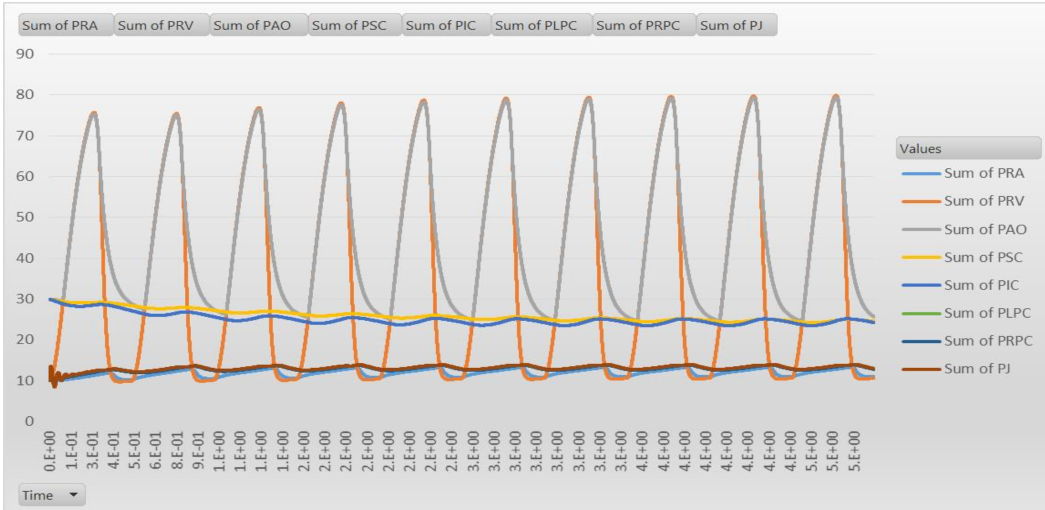

Figure 43 Pressure Summary for Maximum Elastance of 0.50, Minimum Elastance of 0.06 and Heart Rate of 120 bpm

When the injection jet system is added, the caval pressure is 13.388 mmHg.

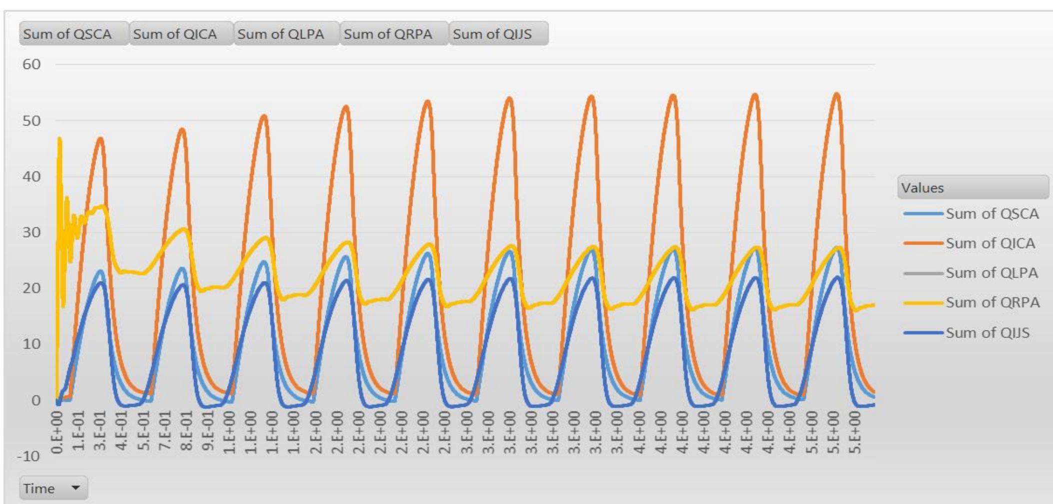

Figure 44 Flow Summary for Maximum Elastance of 0.50, Minimum Elastance of 0.06 and Heart Rate of 120 bpm

When injection jet system is added, the systemic flow is 1.968 mmHg/ml and the pulmonary flow is 2.490 mmHg/ml. The ratio between the pulmonary flow and the systemic flow is 1.265.

Comparison

QSYSTEMIC	1.968	mmHg/ml
QSYSTEMIC (NO IJS)	1.944	mmHg/ml
QPULMONARY	2.49	mmHg/ml
QPULMONARY(NO IJS)	1.966	mmHg/ml
QP/QS	1.26	
QP/QS (NO IJS)	1	
PCAVAL	13.388	mmHg
PCAVAL (NO IJS)	14.28	mmHg
QIJS	0.5	mmHg/ml

Table 17 Heart Rate =120bpm, Maximum Elastance = 0.50, Resistance of IJS = 3

The resistance of Injection Jet is set at 3mmHg. The flow of the systemic circulation is 1.944mmHg/ml and 1.966mmHg/ml without the Injection Jet System. Flow of the systemic circulation is 1.968mmHg/ml and pulmonary circulation is 2.49mmHg/ml with the Injection Jet System. The Injection Jet System added more flow to the systemic circulation as well as the pulmonary circulation. In addition the Injection Jet System had a flow rate of 0.50mmHg/ml. The ratio of the systemic flow to the pulmonary flow resulted to be 1.265 with the injection jet system. However the ratio was 1.011 without the Injection Jet System. The ratio of the systemic flow and pulmonary flow is within the range of 1.20 and 1.50 which is the ideal range.

The caval pressure is 13.388mmHg with the Injection jet system and the caval pressure without the injection jet system is 14.28mmHg. The caval pressure with the injection jet system should be less than the caval pressure without the injection jet system.

RIJS = 2			RIJS = 1		
QSYSTEMIC	1.942	mmHg/ml	QSYSTEMIC	1.873	mmHg/ml
QPULMONARY	2.701	mmHg/ml	QPULMONARY	3.299	mmHg/ml
QP/QS	1.390		QP/QS	1.761	
PCAVAL	13.547	mmHg	PCAVAL	13.978	mmHg
QIJS	0.737	mmHg/ml	QIJS	1.404	mmHg/ml

Table 18 Heart Rate =120bpm, Maximum Elastance = 0.50, Resistance of IJS = 2 (Left) and Heart Rate =120bpm, Maximum Elastance = 0.50, Resistance of IJS = 1(right)

The resistance of the Injection Jet is set at 2mmHg.The flow of the systemic circulation is 1.942 mmHg/ml and the flow of the pulmonary circulation is 2.701mmHg/ml. The ratio of the pulmonary circulation to the systemic circulation is 1.39. The value resides within the range of 1.25 to 1.5. The flow of Injection Jet system is 0.811 mmHg/ml. The caval pressure is 13.547 mmHg which is also within the range between 12.5 and 15.0.

The resistance of the Injection Jet is set at 1mmHg. The flow of the systemic circulation is 1.873 mmHg/ml and the flow of the pulmonary circulation is 3.299. The ratio of the pulmonary circulation to the systemic circulation is 1.761. The value resides above the range of 1.25 and 1.5 which is not good for the patient. The flow of Injection Jet system is 1.404 mmHg/ml. The caval pressure is 13.978mmHg which is also within 15.

Case 6: Heart Rate 100, Maximum Elastance 0.50

Without Injection Jet System

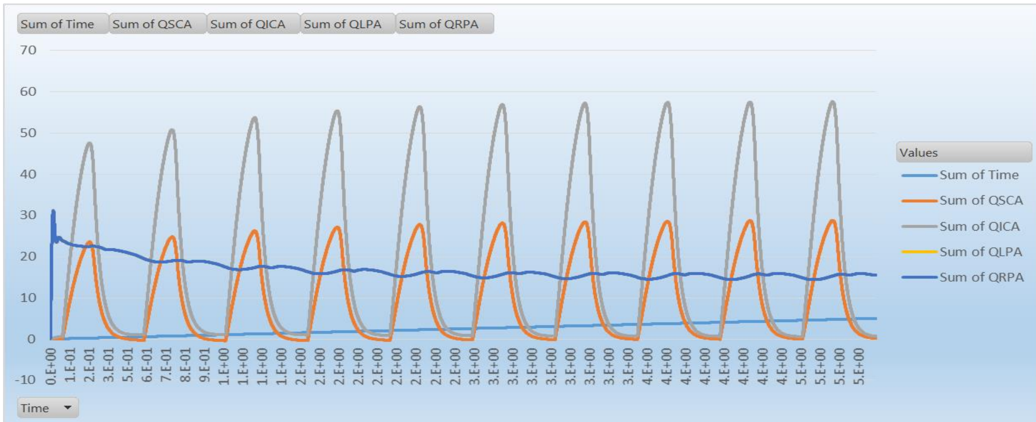

Figure 45 Pressure Summary for Maximum Elastance of 0.50, Minimum Elastance of 0.06 and Heart Rate of 100 bpm

With the change in heart rate to 100 bpm, we can tell that the interval between each beat has reduced. However the values and the shape of the function remains identical. The caval pressure is 14.07mmHg.

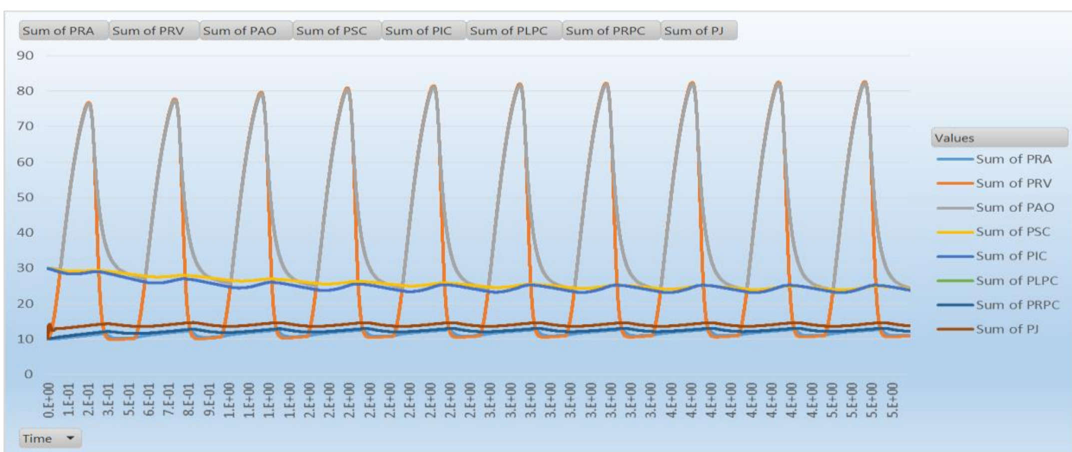

Figure 46 Flow Summary for Maximum Elastance of 0.50, Minimum Elastance of 0.06 and Heart Rate of 100 bpm

The systemic flow is 1.813 mmHg/ml and the pulmonary flow is 1.832 mmHg/ml. The ratio of the systemic pressure over pulmonary pressure is 1.01.

With Injection Jet System

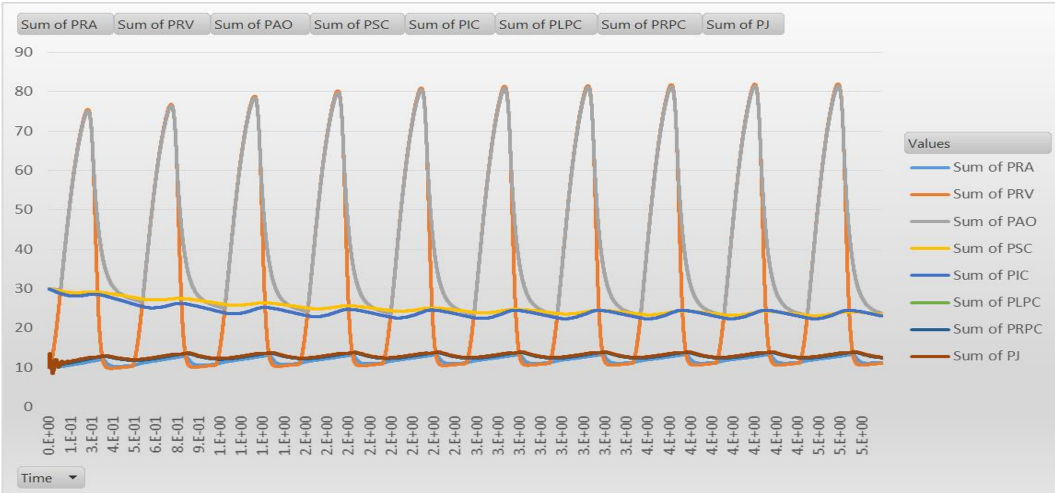

Figure 47Pressure Summary for Maximum Elastance of 0.50, Minimum Elastance of 0.06 and Heart Rate of 120 bpm

When the injection jet system is added, the caval pressure is 13.214 mmHg.

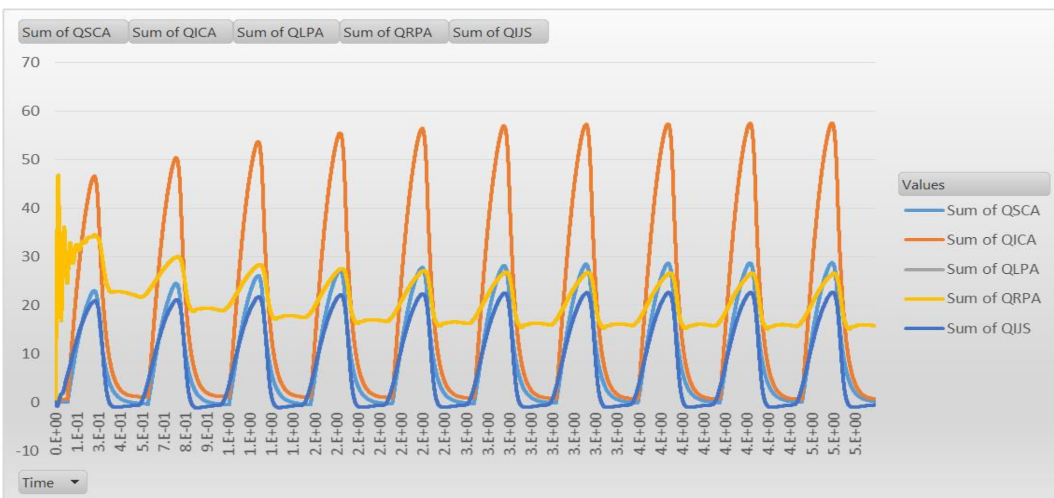

Figure 48 Flow Summary for Maximum Elastance of 0.50, Minimum Elastance of 0.06 and Heart Rate of 120 bpm

When injection jet system is added, the systemic flow is 1.837 mmHg/ml and the pulmonary flow is 2.310 mmHg/ml. The ratio between the pulmonary flow and the systemic flow is 1.257

Comparison

QSYSTEMIC	1.837	mmHg/ml
QSYSTEMIC (NO IJS)	1.813	mmHg/ml
QPULMONARY	2.31	mmHg/ml
QPULMONARY(NO IJS)	1.832	mmHg/ml
QP/QS	1.25	
QP/QS (NO IJS)	1	
PCAVAL	13.214	mmHg
PCAVAL (NO IJS)	14.071	mmHg
QIJS	0.455	mmHg/ml

Table 19 Heart Rate =100bpm, Maximum Elastance = 0.50, Resistance of IJS = 3

The resistance of Injection Jet is set at 3mmHg. The flow of the systemic circulation is 1.837mmHg/ml and 1.966mmHg/ml without the Injection Jet System. Flow of the systemic circulation is 1.813mmHg/ml and pulmonary circulation is 2.31mmHg/ml with the Injection Jet System. The Injection Jet System added more flow to the systemic circulation as well as the pulmonary circulation. In addition the Injection Jet System had a flow rate of 0.455mmHg/ml. The ratio of the systemic flow to the pulmonary flow resulted to be 1.257 with the injection jet system. However the ratio was 1.010 without the Injection Jet System. The ratio of the systemic flow and pulmonary flow is within the range of 1.20 and 1.50 which is the ideal range.

The caval pressure is 13.214mmHg with the Injection jet system and the caval pressure without the injection jet system is 14.07mmHg. The caval pressure with the injection jet system should be less than the caval pressure without the injection jet system.

RIJS = 2			RIJS = 1		
QSYSTEMIC	1.815	mmHg/ml	QSYSTEMIC	1.758	mmHg/ml
QPULMONARY	2.505	mmHg/ml	QPULMONARY	3.059	mmHg/ml
QP/QS	1.380		QP/QS	1.740	
PCAVAL	13.352	mmHg	PCAVAL	13.73	mmHg
QIJS	0.672	mmHg/ml	QIJS	1.741	mmHg/ml

Table 20 Heart Rate =100bpm, Maximum Elastance = 0.50, Resistance of IJS = 2 (Left) and Heart Rate =100bpm, Maximum Elastance = 0.50, Resistance of IJS = 1(right)

The resistance of the Injection Jet is set at 2mmHg.The flow of the systemic circulation is 1.815 mmHg/ml and the flow of the pulmonary circulation is 2.505mmHg/ml. The ratio of the pulmonary circulation to the systemic circulation is 1.38. The value resides within the range of 1.25 to 1.5. The flow of Injection Jet system is 0.672 mmHg/ml. The caval pressure is 13.35 mmHg which is also within the range between 12.5 and 15.0.

The resistance of the Injection Jet is set at 1mmHg. The flow of the systemic circulation is 1.758 mmHg/ml and the flow of the pulmonary circulation is 3.059mmHg/ml. The ratio of the pulmonary circulation to the systemic circulation is 1.74. The value resides above the range of 1.25 and 1.5 which is not good for the patient. The flow of Injection Jet system is 1.741 mmHg/ml. The caval pressure is 13.73mmHg which is also within 15.

Case 7: Heart Rate 140, Maximum Elastance 0.25

Without Injection Jet System

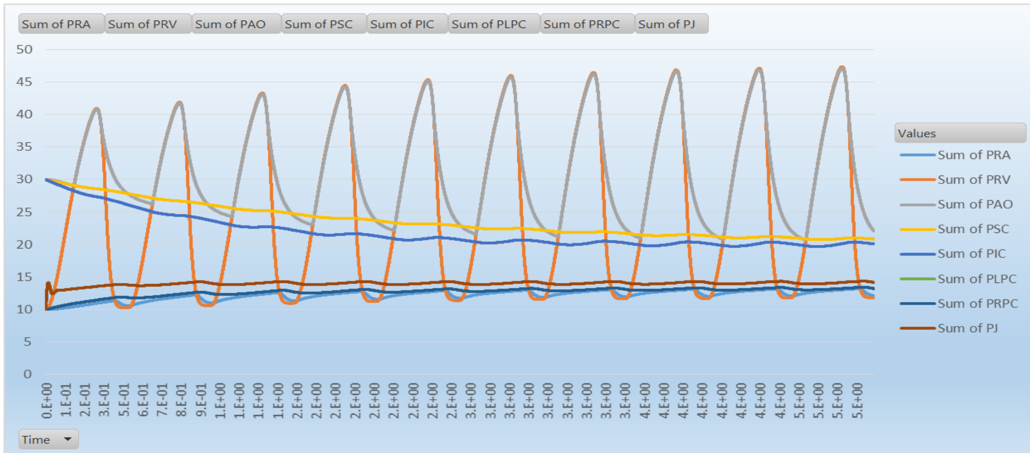

Figure 49 Pressure Summary for Maximum Elastance of 0.25, Minimum Elastance of 0.06 and Heart Rate of 140 bpm

With the change in heart rate to 140 bpm as well as maximum elastance to 0.25, we can tell that the interval between each beat has reduced. However the values and the shape of the function remains identical. The caval pressure is 14.121mmHg.

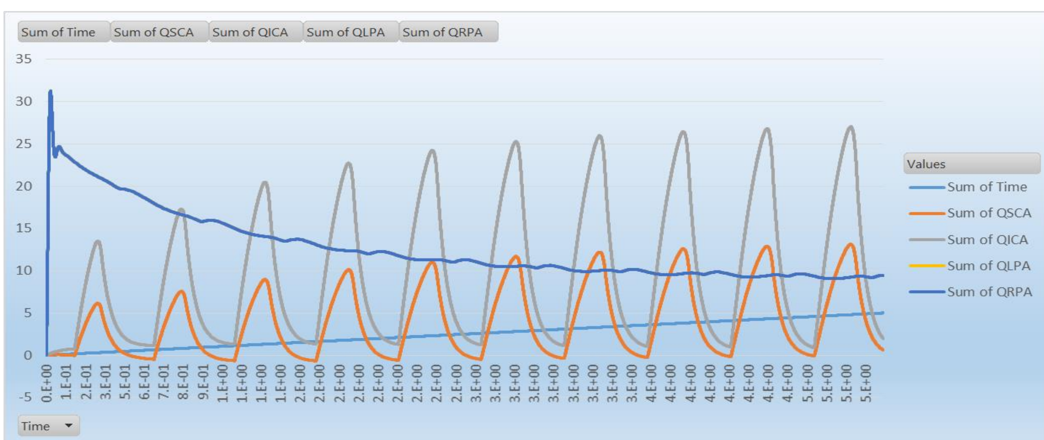

Figure 50 Flow Summary for Maximum Elastance of 0.25, Minimum Elastance of 0.06 and Heart Rate of 140 bpm

The systemic flow is 1.029 mmHg/ml and the pulmonary flow is 1.114 mmHg/ml. The ratio of the systemic pressure over pulmonary pressure is 1.08.

With Injection Jet System

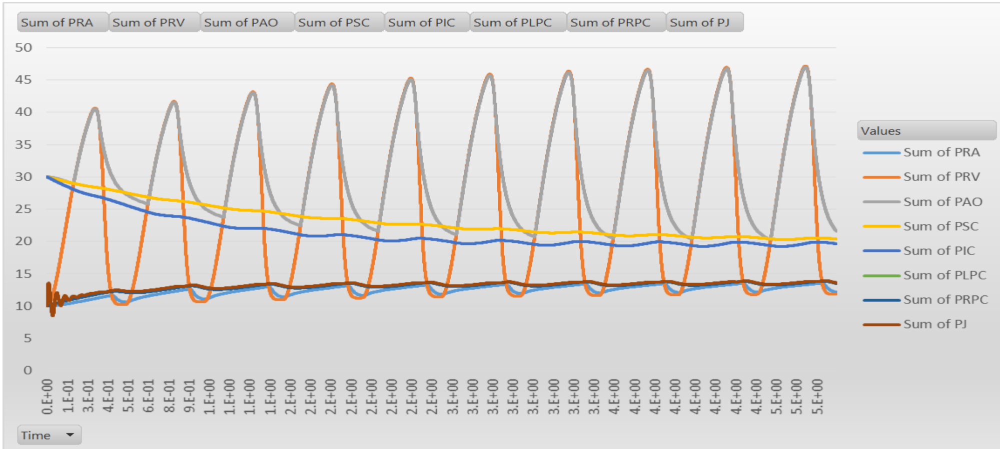

Figure 51 Pressure Summary for Maximum Elastance of 0.25, Minimum Elastance of 0.06 and Heart Rate of 140 bpm

When the injection jet system is added, the caval pressure is 13.63 mmHg.

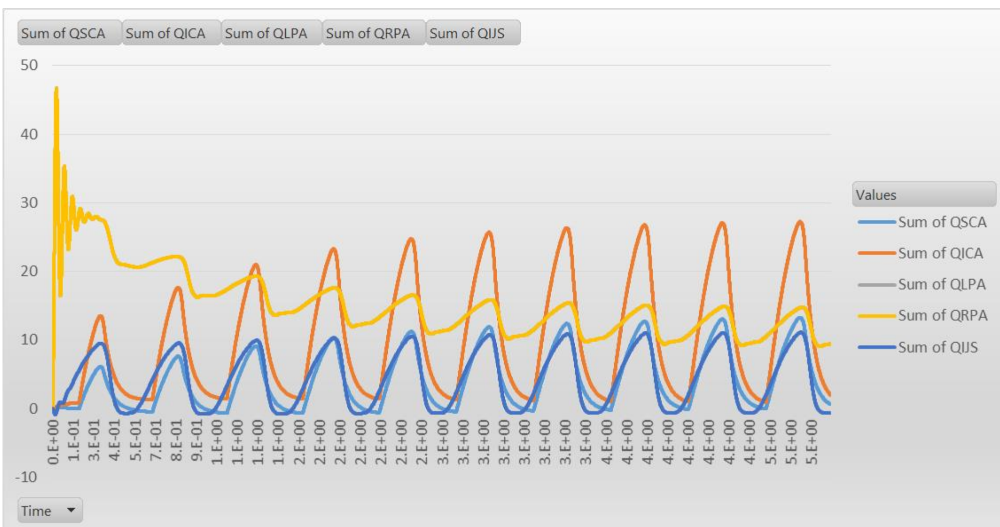

Figure 52 Flow Summary for Maximum Elastance of 0.25, Minimum Elastance of 0.06 and Heart Rate of 140 bpm

When injection jet system is added, the systemic flow is 1.05 mmHg/ml and the pulmonary flow is 1.398 mmHg/ml. The ratio between the pulmonary flow and the systemic flow is 1.33.

Comparison

QSYSTEMIC	1.049	mmHg/ml
QSYSTEMIC (NO IJS)	1.029	mmHg/ml
QPULMONARY	1.398	mmHg/ml
QPULMONARY(NO IJS)	1.114	mmHg/ml
QP/QS	1.33	
QP/QS (NO IJS)	1	
PCAVAL	13.63	mmHg
PCAVAL (NO IJS)	14.121	mmHg
QIJS	0.276	mmHg/ml

Table 21 Heart Rate =140bpm, Maximum Elastance = 0.25, Resistance of IJS = 3

The resistance of Injection Jet is set at 3mmHg. The flow of the systemic circulation is 1.029mmHg/ml and 1.114mmHg/ml without the Injection Jet System. Flow of the systemic circulation is 1.049mmHg/ml and pulmonary circulation is 1.398mmHg/ml with the Injection Jet System. The Injection Jet System added more flow to the systemic circulation as well as the pulmonary circulation. In addition the Injection Jet System had a flow rate of 0.276mmHg/ml. The ratio of the systemic flow to the pulmonary flow resulted to be 1.332 with the injection jet system. However the ratio was 1.082 without the Injection Jet System. The ratio of the systemic flow and pulmonary flow is within the range of 1.20 and 1.50 which is the ideal range.

The caval pressure is 13.630mmHg with the Injection jet system and the caval pressure without the injection jet system is 14.121mmHg. The caval pressure with the injection jet system should be less than the caval pressure without the injection jet system.

RIJS = 2			RIJS = 1		
QSYSTEMIC	1.038	mmHg/ml	QSYSTEMIC	1.007	mmHg/ml
QPULMONARY	1.518	mmHg/ml	QPULMONARY	1.86	mmHg/ml
QP/QS	1.462		QP/QS	1.847	
PCAVAL	13.724	mmHg	PCAVAL	13.982	mmHg
QIJS	0.407	mmHg/ml	QIJS	0.781	mmHg/ml

Table 22 Heart Rate =140bpm, Maximum Elastance = 0.25, Resistance of IJS = 2 (Left) and Heart Rate =140bpm, Maximum Elastance = 0.25, Resistance of IJS = 1(right)

The resistance of the Injection Jet is set at 2mmHg.The flow of the systemic circulation is 1.038 mmHg/ml and the flow of the pulmonary circulation is 1.518mmHg/ml. The ratio of the pulmonary circulation to the systemic circulation is 1.462. The value resides within the range of 1.25 to 1.5. The flow of Injection Jet system is 0.407 mmHg/ml. The caval pressure is 13.724 mmHg which is also within the range between 12.5 and 15.0.

The resistance of the Injection Jet is set at 1mmHg. The flow of the systemic circulation is 1.007 mmHg/ml and the flow of the pulmonary circulation is 1.86mmHg/ml. The ratio of the pulmonary circulation to the systemic circulation is 1.847. The value resides above the range of 1.25 and 1.5 which is not good for the patient. The flow of Injection Jet system is 0.781mmHg/ml. The caval pressure is 13.982mmHg which is also within 15.

Case 8: Heart Rate 120, Maximum Elastance 0.25

Without Injection Jet System

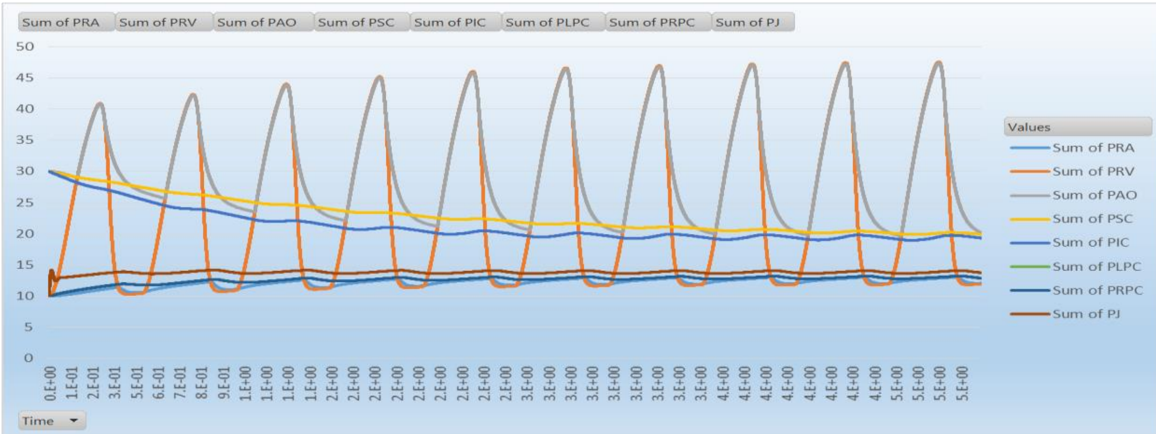

Figure 53 Pressure Summary for Maximum Elastance of 0.25, Minimum Elastance of 0.06 and Heart Rate of 120 bpm

With the change in heart rate to 120 bpm, we can tell that the interval between each beat has reduced. However the values and the shape of the function remains identical. The caval pressure is 13.832mmHg.

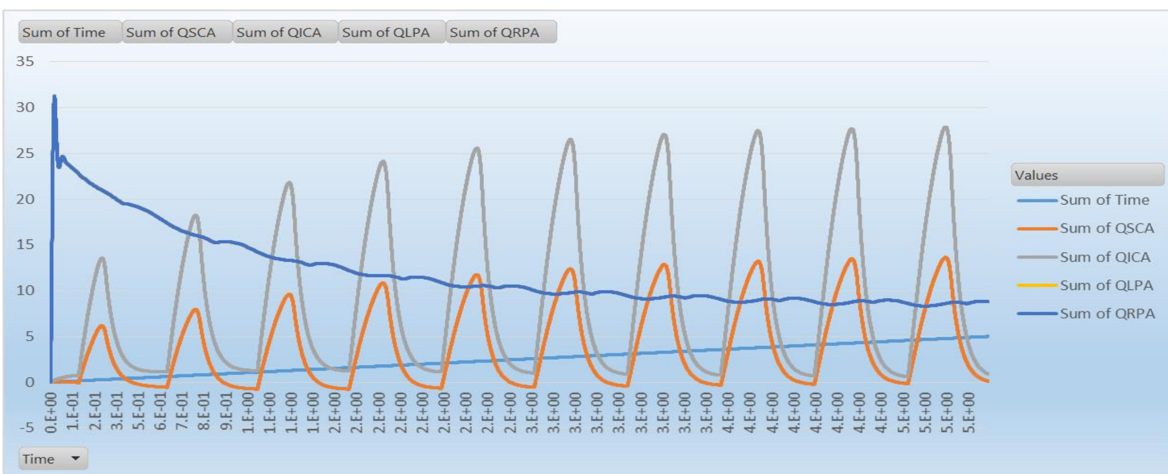

Figure 54 Flow Summary for Maximum Elastance of 0.25, Minimum Elastance of 0.06 and Heart Rate of 120 bpm

The systemic flow is 0.96 mmHg/ml and the pulmonary flow is 1.035 mmHg/ml. The ratio of the systemic pressure over pulmonary pressure is 1.07.

With Injection Jet System

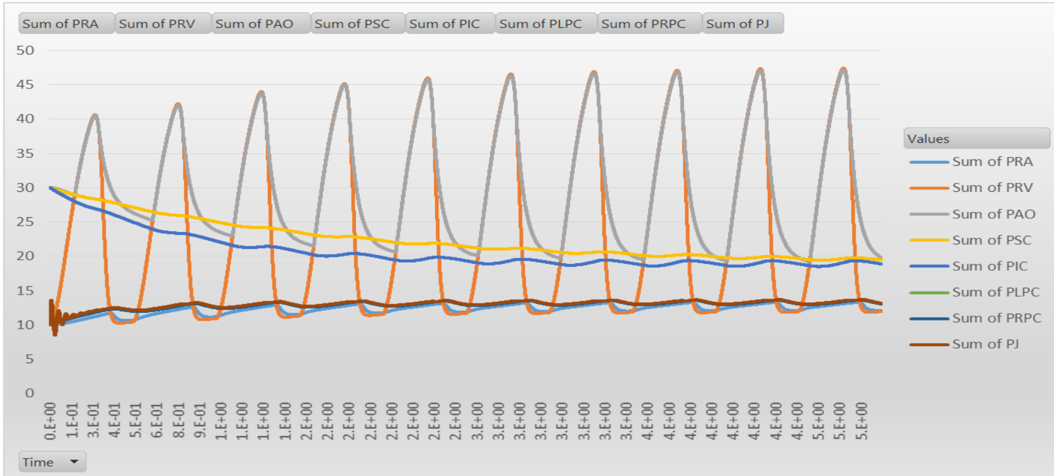

Figure 55 Pressure Summary for Maximum Elastance of 0.25, Minimum Elastance of 0.06 and Heart Rate of 120 bpm

When the injection jet system is added, the caval pressure is 13.35 mmHg.

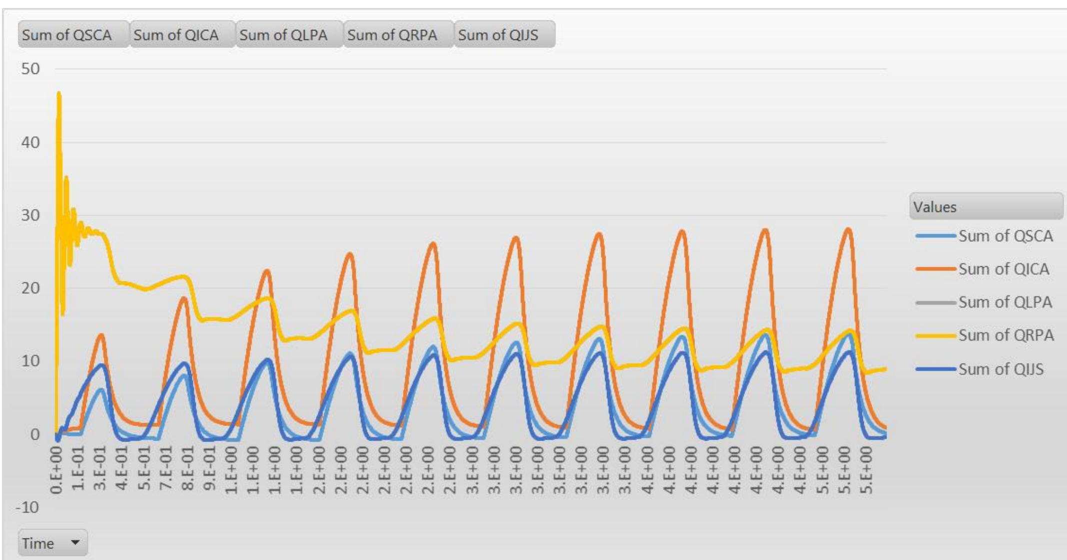

Figure 56 Flow Summary for Maximum Elastance of 0.25, Minimum Elastance of 0.06 and Heart Rate of 120 bpm

When injection jet system is added, the systemic flow is 0.98 mmHg/ml and the pulmonary flow is 1.295 mmHg/ml. The ratio between the pulmonary flow and the systemic flow is 1.32.

Comparison

QSYSTEMIC	0.98	mmHg/ml
QSYSTEMIC (NO IJS)	0.96	mmHg/ml
QPULMONARY	1.295	mmHg/ml
QPULMONARY(NO IJS)	1.035	mmHg/ml
QP/QS	1.32	
QP/QS (NO IJS)	1	
PCAVAL	13.356	mmHg
PCAVAL (NO IJS)	13.832	mmHg
QIJS	0.251	mmHg/ml

Table 23 Heart Rate =120bpm, Maximum Elastance = 0.25, Resistance of IJS = 3

The resistance of Injection Jet is set at 3mmHg. The flow of the systemic circulation is 0.96mmHg/ml and 1.035mmHg/ml without the Injection Jet System. Flow of the systemic circulation is 0.98mmHg/ml and pulmonary circulation is 1.295mmHg/ml with the Injection Jet System. The Injection Jet System added more flow to the systemic circulation as well as the pulmonary circulation. In addition the Injection Jet System had a flow rate of 0.251mmHg/ml. The ratio of the systemic flow to the pulmonary flow resulted to be 1.321 with the injection jet system. However the ratio was 1.078 without the Injection Jet System. The ratio of the systemic flow and pulmonary flow is within the range of 1.20 and 1.50 which is the ideal range.

The caval pressure is 13.356mmHg with the Injection jet system and the caval pressure without the injection jet system is 13.832mmHg. The caval pressure with the injection jet system should be less than the caval pressure without the injection jet system.

RIJS = 2			RIJS = 1		
QSYSTEMIC	0.971	mmHg/ml	QSYSTEMIC	0.947	mmHg/ml
QPULMONARY	1.406	mmHg/ml	QPULMONARY	1.724	mmHg/ml
QP/QS	1.447		QP/QS	1.820	
PCAVAL	13.436	mmHg	PCAVAL	13.655	mmHg
QIJS	0.371	mmHg/ml	QIJS	0.714	mmHg/ml

Table 24 Heart Rate =120bpm, Maximum Elastance = 0.25, Resistance of IJS = 2 (Left) and Heart Rate =120bpm, Maximum Elastance = 0.25, Resistance of IJS = 1(right)

The resistance of the Injection Jet is set at 2mmHg.The flow of the systemic circulation is 0.971 mmHg/ml and the flow of the pulmonary circulation is 1.406mmHg/ml. The ratio of the pulmonary circulation to the systemic circulation is 1.448. The value resides within the range of 1.25 to 1.5. The flow of Injection Jet system is 0.371 mmHg/ml. The caval pressure is 13.436 mmHg which is also within the range between 12.5 and 15.0.

The resistance of the Injection Jet is set at 1mmHg. The flow of the systemic circulation is 0.947 mmHg/ml and the flow of the pulmonary circulation is 1.724mmHg/ml. The ratio of the pulmonary circulation to the systemic circulation is 1.82. The value resides above the range of 1.25 and 1.5 which is not good for the patient. The flow of Injection Jet system is 0.714 mmHg/ml. The caval pressure is 13.6555mmHg which is also within 15.

Case 9: Heart Rate 100, Maximum Elastance 0.25

Without Injection Jet System

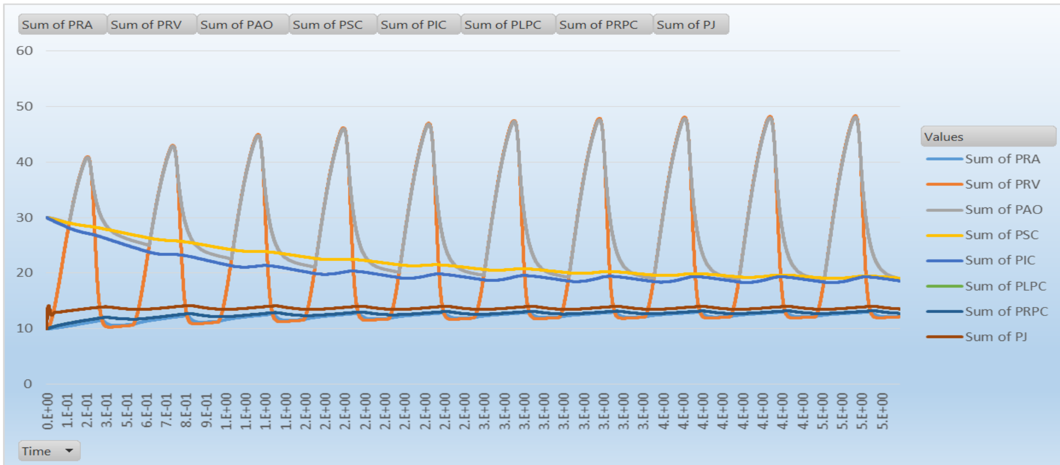

Figure 57 Pressure Summary for Maximum Elastance of 0.25, Minimum Elastance of 0.06 and Heart Rate of 100 bpm

With the change in heart rate to 100 bpm, we can tell that the interval between each beat has reduced. However the values and the shape of the function remains identical. The caval pressure is 13.724mmHg.

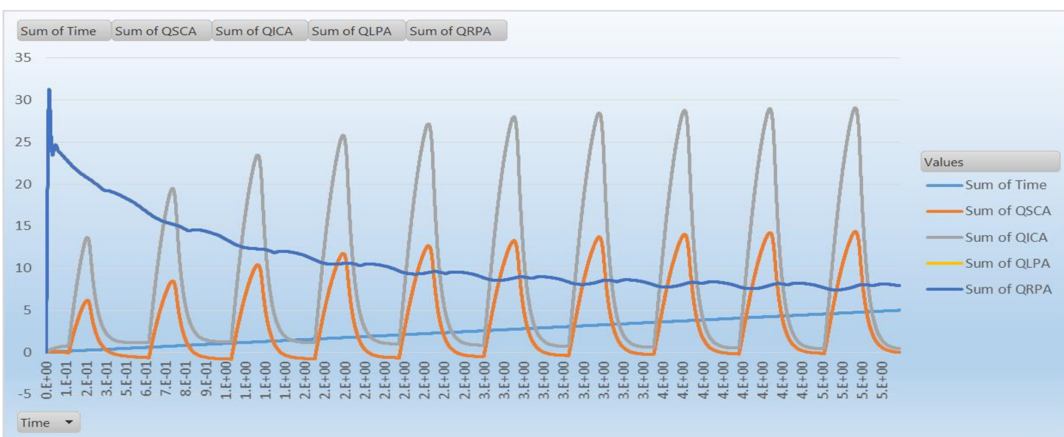

Figure 58 Flow Summary for Maximum Elastance of 0.25, Minimum Elastance of 0.06 and Heart Rate of 100 bpm

The systemic flow is 0.892 mmHg/ml and the pulmonary flow is 0.94 mmHg/ml. The ratio of the systemic pressure over pulmonary pressure is 1.05.

With Injection Jet System

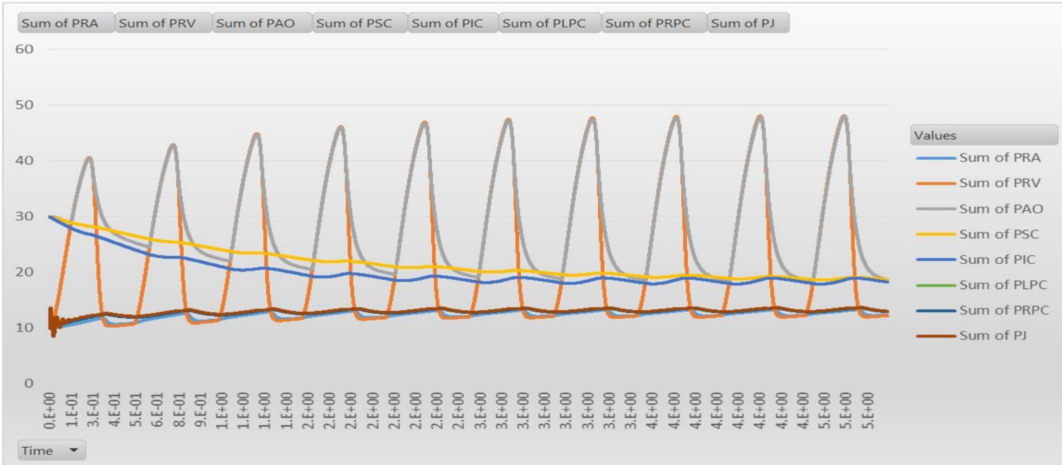

Figure 59 Pressure Summary for Maximum Elastance of 0.25, Minimum Elastance of 0.06 and Heart Rate of 100 bpm

When the injection jet system is added, the caval pressure is 13.28 mmHg.

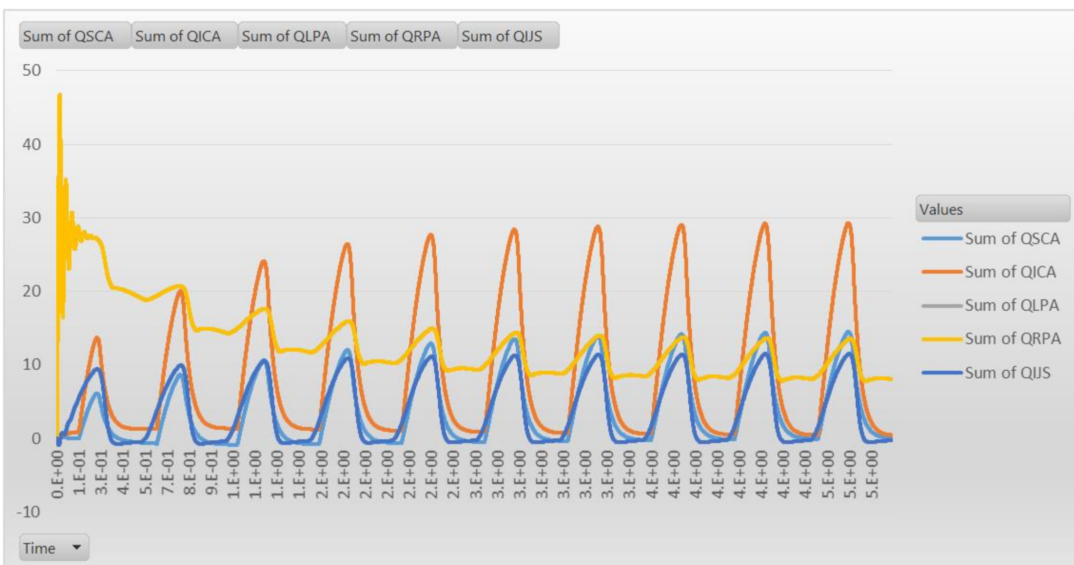

Figure 60 Flow Summary for Maximum Elastance of 0.25, Minimum Elastance of 0.06 and Heart Rate of 100 bpm

When injection jet system is added, the systemic flow is 0.909mmHg/ml and the pulmonary flow is 1.175 mmHg/ml. The ratio between the pulmonary flow and the systemic flow is 1.29.

Comparison

QSYSTEMIC	0.909	mmHg/ml
QSYSTEMIC (NO IJS)	0.892	mmHg/ml
QPULMONARY	1.175	mmHg/ml
QPULMONARY(NO IJS)	0.94	mmHg/ml
QP/QS	1.29	
QP/QS (NO IJS)	1	
PCAVAL	13.282	mmHg
PCAVAL (NO IJS)	13.724	mmHg
QIJS	0.226	mmHg/ml

Table 25 Heart Rate =100bpm, Maximum Elastance = 0.25, Resistance of IJS = 3

The resistance of Injection Jet is set at 3mmHg. The flow of the systemic circulation is 0.892mmHg/ml and 0.940mmHg/ml without the Injection Jet System. Flow of the systemic circulation is 0.909mmHg/ml and pulmonary circulation is 1.175mmHg/ml with the Injection Jet System. The Injection Jet System added more flow to the systemic circulation as well as the pulmonary circulation. In addition the Injection Jet System had a flow rate of 0.226mmHg/ml. The ratio of the systemic flow to the pulmonary flow resulted to be 1.292 with the injection jet system. However the ratio was 1.053 without the Injection Jet System. The ratio of the systemic flow and pulmonary flow is within the range of 1.20 and 1.50 which is the ideal range.

The caval pressure is 13.282mmHg with the Injection jet system and the caval pressure without the injection jet system is 13.724mmHg. The caval pressure with the injection jet system should be less than the caval pressure without the injection jet system.

RIJS = 2			RIJS = 1		
QSYSTEMIC	0.902	mmHg/ml	QSYSTEMIC	0.883	mmHg/ml
QPULMONARY	1.277	mmHg/ml	QPULMONARY	1.568	mmHg/ml
QP/QS	1.4157		QP/QS	1.775	
PCAVAL	13.35	mmHg	PCAVAL	13.539	mmHg
QIJS	0.335	mmHg/ml	QIJS	0.646	mmHg/ml

Table 26 Heart Rate =100bpm, Maximum Elastance = 0.25, Resistance of IJS = 2 (Left) and Heart Rate =100bpm, Maximum Elastance = 0.25, Resistance of IJS = 1(right)

The resistance of the Injection Jet is set at 2mmHg.The flow of the systemic circulation is 0.902 mmHg/ml and the flow of the pulmonary circulation is 1.277mmHg/ml. The ratio of the pulmonary circulation to the systemic circulation is 1.415. The value resides within the range of 1.25 to 1.5. The flow of Injection Jet system is 0.335 mmHg/ml. The caval pressure is 13.35 mmHg which is also within the range between 12.5 and 15.0.

The resistance of the Injection Jet is set at 1mmHg. The flow of the systemic circulation is 0.883 mmHg/ml and the flow of the pulmonary circulation is 1.568mmHg/ml. The ratio of the pulmonary circulation to the systemic circulation is 1.775. The value resides above the range of 1.25 and 1.5 which is not good for the patient. The flow of Injection Jet system is 0.646 mmHg/ml. The caval pressure is 13.539mmHg which is also within 15.

Discussion

Throughout the simulation, the systemic flow, pulmonary flow, the ratio between the pulmonary flow to systemic flow, caval pressure is important since it explains whether the IJS is being beneficial throughout the circulation or not. These values are determined by change in maximum elastance, heart rate and resistance of the injection jet system.

When there is an increase in maximum elastance, there is an increase in caval pressure and when the maximum elastance decreases, the caval pressure decreases, Therefore the caval pressure is directly affected by the maximum elastance. The caval pressure is directly proportional to the maximum elastance. The systemic and pulmonary flows also increases as the maximum elastance increases. However, the ratio between the pulmonary flow and systemic flow decreases as the maximum elastance increases. The flow also increase inside the IJS as the maximum elastance increases.

When the heart rate changes and the heart rate increases, there is an increases in the systemic flow, pulmonary flow. However, the ratio between the two acts differently. When the heart rate increases, the ratio decreases and when the heart rate decreases the ratio decreases as well. However, when IJS is not in the circulation the lower the heart rate, the ratio gets bigger. The caval pressure increases as the heart rate increases and the flow increases as the heart rate increases. As the heart rate increases, all the values are proportional besides the ratio of the pulmonary flow and the systemic flow.

When the resistance of the injection jet system increases, the systemic flow increases but the pulmonary flow decreases. Thus the ratio between the two flows decreases as the resistance is bigger. The caval pressure is increased when the resistance is higher but also is increased when the resistance is lower. The flow in the injection jet system increases as the resistance decreases.

Since the problem was solved in one dimensional problem, even with the general parameters of the resistance, compliance and the inductance value set, there are a lot of limitations compared to a computational fluid dynamics model. However, the values of the flow and pressure can be estimated and provide a general idea of range of flow and pressure mathematically.

Conclusion

The important physiological parameters are given below.

Emax	0.75	0.5	0.25
HR (bpm)	140	140	140
RIJS(mmHg)	3	3	3
Physiological Parameters			
Q systemic(mmHg/ml)	2.924	2.123	1.049
Q pulmonary mmHg/ml)	3.598	2.652	1.398
Qp/Qs	1.2305	1.2492	1.3327
Pcaval(mmHg)	14.243	13.972	13.63

Table 27 Physiological parameters when Emax changes, HR = 140 and RIJS is 3

Emax	0.75	0.5	0.25
HR (bpm)	120	120	120
RIJS(mmHg)	3	3	3
Physiological Parameters			
Q systemic(mmHg/ml)	2.699	1.968	0.98
Q pulmonary mmHg/ml)	3.388	2.490	1.295
Qp/Qs	1.255	1.265	1.321
Pcaval(mmHg)	13.413	13.388	13.356

Table 28 Physiological parameters when Emax changes, HR = 120 and RIJS is 3

Emax	0.75	0.5	0.25
HR (bpm)	100	100	100
RIJS(mmHg)	3	3	3
Physiological Parameters			
Q systemic(mmHg/ml)	2.5400	1.8370	0.9090
Q pulmonary mmHg/ml)	3.1780	2.3100	1.1750
Qp/Qs	1.2512	1.2575	1.2926
Pcaval(mmHg)	13.164	13.214	13.630

Table 29 Physiological parameters when Emax changes, HR = 100 and RIJS is 3

The caval pressure is below 15mmHg for all cases as desired as well as Qp/Qs values residing within the range of 1.2-1.5. Therefore, all the physiological parameters are within the range for all of the cases when RIJS is 3 for different heart rate and maximum elastance.

Emax	0.75	0.5	0.25
HR (bpm)	140	140	140
RIJS(mmHg)	2	2	2
Physiological Parameters			
Q systemic(mmHg/ml)	2.869	2.091	1.038
Q pulmonary mmHg/ml)	3.899	2.88	1.518
Qp/Qs	1.359	1.377	1.462
Pcaval(mmHg)	14.49	14.15	13.72

Table 30Physiological parameters when Emax changes, HR = 140 and RIJS is 2

Emax	0.75	0.5	0.25
HR (bpm)	120	120	120
RIJS(mmHg)	2	2	2
Physiological Parameters			
Q systemic(mmHg/ml)	2.656	1.942	0.971
Q pulmonary mmHg/ml)	3.667	2.701	1.406
Qp/Qs	1.380	1.390	1.447
Pcaval(mmHg)	13.63	13.54	13.43

Table 31 Physiological parameters when Emax changes, HR = 120 and RIJS is 2

Emax	0.75	0.5	0.25
HR (bpm)	100	100	100
RIJS(mmHg)	2	2	2
Physiological Parameters			
Q systemic(mmHg/ml)	2.502	1.815	0.902
Q pulmonary mmHg/ml)	3.438	2.505	1.277
Qp/Qs	1.374	1.380	1.415
Pcaval(mmHg)	13.35	13.35	13.35

Table 32 Physiological parameters when Emax changes, HR = 120 and RIJS is 2

The caval pressure is below 15mmHg for all cases as desired as well as Qp/Qs values residing within the range of 1.2-1.5. Therefore, all the physiological parameters are within the range for all of the cases when RIJS is 2 for different heart rate and maximum elastance. However, there was an increase in caval pressure when the resistance of IJS decreased.

Emax	0.75	0.5	0.25
HR (bpm)	140	140	140
RIJS(mmHg)	1	1	1
Physiological Parameters			
Q systemic(mmHg/ml)	2.726	2.005	1.007
Q pulmonary mmHg/ml)	4.735	3.519	1.860
Qp/Qs	1.736	1.755	1.847
Pcaval(mmHg)	15.17	14.66	13.98

Table 33 Physiological parameters when Emax changes, HR = 140 and RIJS is 1

Emax	0.75	0.5	0.25
HR (bpm)	120	120	120
RIJS(mmHg)	1	1	1
Physiological Parameters			
Q systemic(mmHg/ml)	2.54	1.873	0.947
Q pulmonary mmHg/ml)	4.451	3.299	1.724
Qp/Qs	1.752	1.761	1.820
Pcaval(mmHg)	14.22	13.97	13.65

Table 34 Physiological parameters when Emax changes, HR = 120 and RIJS is 1

Emax	0.75	0.5	0.25
HR (bpm)	100	100	100
RIJS(mmHg)	1	1	1
Physiological Parameters			
Q systemic(mmHg/ml)	2.403	1.758	0.883
Q pulmonary mmHg/ml)	4.172	3.059	1.568
Qp/Qs	1.736	1.740	1.775
Pcaval(mmHg)	13.87	13.73	13.53

Table 35 Physiological parameters when Emax changes, HR = 120 and RIJS is 1

The caval pressure is below 15 mmHg for all cases besides when the Emax is 0.75, HR is 140bpm and RIJS is 1mmHg. However, the Qp/Qs for all cases are above the range of 1.2-1.5. This means that there are too much flow that are being cycled which means the circulation of the blood is not efficient. Therefore, when RIJS is 1, there is no benefit for adding IJS into the system.

References

1. Mondésert B, Marcotte F, Mongeon FP, Dore A, Mercier LA, Ibrahim R, Asgar A, Miro J, Poirier N, Khairy P. Fontan circulation: success or failure? Can J Cardiol. 2013;29(7):811-20.

2. Ovroutski S, Ewert P, Miera O, Alexi-Meskishvili V, Peters B, Hetzer R, Berger F. Long-term cardiopulmonary exercise capacity after modified Fontan operation. Eur J Cardiothorac Surg. 2010;37(1):204-9.

3. Caruthers RL, Kempa M, Loo A, Gulbransen E, Kelly E, Erickson SR, Hirsch JC, Schumacher KR, Stringer KA. Demographic characteristics and estimated prevalence of Fontan-associated plastic bronchitis. Pediatr Cardiol. 2013;34(2):256-61.

4. Rao PS. Protein-losing enteropathy following the Fontan operation. J Invasive Cardiol. 2007;19(10):447-8.

5. Khanna G, Bhalla S, Krishnamurthy R, Canter C. Extracardiac complications of the Fontan circuit. Pediatr Radiol. 2012;42(2):233-41.

6. Diller GP, Giardini A, Dimopoulos K, Gargiulo G, Müller J, Derrick G, Giannakoulas G, Khambadkone S, Lammers AE, Picchio FM, Gatzoulis MA, Hager A. Predictors of morbidity and mortality in contemporary Fontan patients: results from a multicenter study including cardiopulmonary exercise testing in 321 patients. Eur Heart J. 2010;31(24):3073-83.

7. Gentles TL, Gauvreau K, Mayer JE, Jr., Fishberger SB, Burnett J, Colan SD, Newburger JW, Wernovsky G. Functional outcome after the Fontan operation: factors influencing late morbidity. J Thorac Cardiovasc Surg. , 1997;114:392-403; discussion 404-5.

8. Gentles TL, Mayer JE, Gauvreau K, Newburger JW, Lock JE, Kupferschmid JP, Burnett J, Jonas RA, Castaneda AR, Wernovsky G. Fontan operation in five hundred consecutive patients: factors influencing early and late outcome. J Thorac Cardiovasc Surg. 1997;114:376-391.

9. Sen S, Bandyopadhyay B, Eriksson P, Chattopadhyay A. Functional capacity following univentricular repair--midterm outcome. Congenit Heart Dis. 2012;7(5):423-32.

10. John A, Johnson J, Khan M, Driscoll D, Warnes C, Cetta F. Clinical outcomes and improved survival in patients with protein-losing enteropathy after the Fontan operation. J Am Coll Cardiol., 64: 54-62, 2014.

11. Deal BJ, Jacobs ML. Management of the failing Fontan circulation. Heart. 2012;98(14):1098-104.

12. Hebert A, Jensen AS, Idorn L, Sørensen KE, Søndergaard L. The effect of Bosentan on exercise capacity in Fontan patients; rationale and design for the TEMPO study. BMC Cardiovasc Disord. 2013;13:36.

13. Hraška V. Decompression of thoracic duct: new approach for the treatment of failing Fontan. Ann Thorac Surg. 2013;96(2):709-11.

14. Albal PG, Menon PG, Kowalski W, Undar A, Turkoz R, Pekkan K. Novel fenestration designs for controlled venous flow shunting in failing Fontans with systemic venous hypertension. Artif Organs. 2013;37(1):66-75.

15. Koçyıldırım E, Dur O, Soran O, Tüzün E, Miller MW, Housler GJ, Wearden PD, Fossum TW, Morell VO, Pekkan K. Pulsatile venous waveform quality in Fontan circulation-clinical implications, venous assists options and the future. Anadolu Kardiyol Derg. 2012;12(5):420-6.

16. Valdovinos J, Shkolyar E, Carman GP, Levi DS. In Vitro Evaluation of an External Compression Device for Fontan Mechanical Assistance. Artif Organs. 2013; available online ahead of print.

17. Durham LA 3rd, Dearani JA, Burkhart HM, Joyce LD, Cetta F Jr, Cabalka AK, Phillips SD, Sundareswaran K, Farrar D, Park SJ. Application of Computer Modeling in Systemic VAD Support of Failing Fontan Physiology. World J Pediatr Congenit Heart Surg. 2011;2(2):243-8.

18. Thacker D, Patel A, Dodds K, et al. Use of oral budesonide in the management of protein-losing enteropathy after the Fontan operation. Ann Thorac Surg ; 89:837-42, 2010.

19. Davies RR, Sorabella RA, Yang J, Mosca RS, Chen JM, Quaegebeur JM. Outcomes after transplantation for "failed" Fontan: a single-institution experience. J Thorac Cardiovasc Surg. 2012;143(5):1183-1192.e4.

20. Backer CL, Russell HM, Pahl E, Mongé MC, Gambetta K, Kindel SJ, Gossett JG, Hardy C, Costello JM, Deal BJ. Heart transplantation for the failing Fontan. Ann Thorac Surg. 2013;96(4):1413-9.

21. Backer CL, Russell HM, Pahl E, Mongé MC, Gambetta K, Kindel SJ, Gossett JG, Hardy C, Costello JM, Deal BJ. Heart transplantation for the failing Fontan. Ann Thorac Surg. 2013;96(4):1413-9.

22. Veldtman G, Webb G. Improved survival in Fontan-associated protein-losing enteropathy. J Am Coll Cardiol 64:63-64, 2014.

23. Throckmorton AL, Lopez-Isaza S, Downs EA, Chopski SG, Gangemi JJ, Moskowitz W. A viable therapeutic option: mechanical circulatory support of the failing Fontan physiology. Pediatr Cardiol. 2013;34(6):1357-65.

24. Throckmorton AL, Lopez-Isaza S, Moskowitz W. Dual-pump support in the inferior and superior vena cavae of a patient-specific fontan physiology. Artif Organs. 2013;37(6):513-522.

25. Giridharan GA, Koenig SC, Kennington J, Sobieski MA, Chen J, Frankel SH, Rodefeld MD. Performance evaluation of a pediatric viscous impeller pump for Fontan cavopulmonary assist. J Thorac Cardiovasc Surg. 2013;145(1):249-57.

26. Rodefeld MD, Coats B, Fisher T, Giridharan GA, Chen J, Brown JW, Frankel SH. Cavopulmonary assist for the univentricular Fontan circulation: von Kármán viscous impeller pump. J Thorac Cardiovasc Surg. 2010;140(3):529-36.

27. Throckmorton AL, Ballman KK, Myers CD, Frankel SH, Brown JW, Rodefeld MD. Performance of a 3-bladed propeller pump to provide cavopulmonary assist in the failing Fontan circulation. Ann Thorac Surg. 2008;86(4):1343-7.

28. Throckmorton AL, Ballman KK, Myers CD, Litwak KN, Frankel SH, Rodefeld MD. Mechanical cavopulmonary assist for the univentricular Fontan circulation using a novel folding propeller blood pump. ASAIO J. 2007;53(6):734-41.

29. Yamada A, Shiraishi Y, Miura H, Yambe T, Omran MH, Shiga T, Tsuboko Y, Homma D, Yamagishi M. Peristaltic hemodynamics of a new pediatric circulatory assist system for Fontan circulation using shape memory alloy fibers. Conf Proc IEEE Eng Med Biol Soc. 2013;2013:683-6.

30. Rodefeld MD, Frankel SH, Giridharan GA. Cavopulmonary assist: (em)powering the univentricular fontan circulation. Semin Thorac Cardiovasc Surg Pediatr Card Surg Annu. 2011;14(1):45-54.

31. Strickland L. Kneass , Practice and Theory of the Injector, 1984, John Wiley & Sons, New York.

32. CD-Adapco, StarCCM+ 3.04.009 User Guide, 2008.

33. Long, C.C., Hsu, M-C., Bazilevs Y., Feinstein, J.A., and Marsden, A., Fluid–structure interaction simulations of the Fontan procedure using variable wall properties, Int. J. Numer. Meth. Biomed. Engng., 2012, Vol. 28, pp. 513–527.

34. Greenfield, J.C. and Fry, D.L., Relationship Between Instantaneous Aortic flow and the Pressure Gradient, Circulation Research, Vol. 17, 1965.

35. Suga H, Sagawa K. Instantaneous pressure-volume relationships and their ratio in the excised, supported canine left ventricle. Circulation Research. 1974;35(1):117-26.

36. Simaan MA, Ferreira A, Chen S, Antaki JF, Galati DG. A dynamical state space representation and performance analysis of a feedback-controlled rotary left ventricular assist device. IEEE Transactions on Control Systems Technology. 2009;17(1):15-28.

37. Simaan, M., Faragallah, G., Wang, Y., and Divo, E., “Left Ventricular Assist Devices: Engineering Design Considerations,” Chapter 2 in New Aspects of Ventricular Assist Devices, G. Reyes (ed.), InTech Open Access Publisher, Croatia, 2011.

38. Ceballos, A., Argueta-Morales, I.R., Divo, E., Osorio, R., Caldarone, C., Kassab, A.J. and DeCampli, W.M., "Computational Analysis of Hybrid Norwood Circulation with Distal Aortic Arch Obstruction and Reverse Blalock-Taussig Shunt," Annals of Thoracic Surgery, 94(5), 2012, p. 1540-1546.

39. A. Ceballos, E. Divo, I. Argueta-Morales, C. Calderone, A. Kassab, and W. Decampli, "A Multi-Scale CFD Analysis of the Hybrid Norwood Palliative Treatment for Hypoplastic Left Heart Syndrome: effect of the reverse Blalock-Taussig shunt diameter," ASME Paper IMECE 2013- 66856 , Proceedings of the 2013 International Congress and Exposition IMECE 2013, November 15-21, San Diego, California, USA.

40. William M. DeCampli, I. Ricardo Argueta-Morales, Eduardo Divo, and Alain J. Kassab, "Computational Fluid Dynamics in Congenital Heart Disease," Cardiology in the Young, 2012, Vo. 22, pp. 800–808. (doi: 10.1017/S1047951112002028).

41. Ceballos, A. , Osorio, R. Divo, E., Argueta-Morales, I.R., Caldarone, C., Kassab, A. and DeCampli, W., A Multiscale Model of the Neonatal Circulatory System Following Hybrid Norwood Palliation, Proceedings of 11th International Symposium of the Computer Methods in Biomechanics and Biomedical Engineering Conference (CMBBE), April 3-7, 2013, Salt Lake City, Utah, Abstract and Poster presentation.

42. Ceballos, A., Osorio, R., Divo, E., Clark, W., Argueta-Morales, I.R., Kassab, A., and Decampli, W., "A Multiscale Model of the Neonatal Circulatory System Following Hybrid Norwood Palliation," Junior Investigator Selected Presentation (one of four) Presented by A. Ceballos at the The 3rd International Conference on Engineering Frontiers in Pediatric and Congenital Heart Disease, held at Stanford Medical School, May 1-2, 2012, (also selected poster presentation).

43. Ceballos, A. Kassab,A., Osorio, R., Divo, E., Argueta-Morales, I.R., Caldarone, C., Decampli, W., "A Multiscale Model of the Neonatal Circulatory System Following Hybrid Norwood Palliation," Abstract 172, Society of Thoracic Surgeons (STS) 48th Annual Meeting, Fort Lauderdale, Florida, January 30 – February 1, 2012. (also poster presentation).

44. Ceballos, A., Osorio, R., Kassab, A., Divo, E., Argueta-Morales, I.R., and DeCampli, W., "A Multiscale Model of the Circulatory System in Infants Undergoing Hybrid Norwood Palliation," Abstract in Proc. of 2011Coupled Problems in Science and Engineering (Coupled 2011 ECCOMAS Conf., 20-22 June, 2011, Kos, Greece), Papadrakakis, M., Onates, E., and Schefler, B. (eds.), CMINE, Barcelona, 2011 (CD ROM).

45. Andres Ceballos, Lauren Blanchette, Eduardo Divo, Ricardo Argueta-Morales, Christopher A. Caldarone, Alain Kassab, and William M. DeCampli, "A multi-scale CFD analysis of the hybrid, “Norwood palliative treatment for hypoplastic left heart syndrome: effect of reverse Blalock-Taussig Shunt (RBTS) diameter,"

4th International Conference on Engineering Frontiers in Pediatric and Congenital Heart Disease, Paris, May 21-22, 2014. (Abstract and Poster Presentation).

46. Marsden, A.L., Vignon-Clementel, I.E., Chan, F.P., Feinstein, J.A., Taylor, C.A., Effects of exercise and respiration on hemodynamic efficiency in CFD simulations of the total cavopulmonary connection. Annals of Biomedical Engineering, 2007, Vol. 35, 250–263.

47. Diane A. de Zélicourt, Alison Marsden, Mark A. Fogel, Ajit P. Yoganathan, Imaging and patient-specific simulations for the Fontan surgery: Current methodologies and clinical applications , Progress in Pediatric Cardiology, 2010, Vol. 30, pp. 31–44.

48. Ethan Kung, Alessia Baretta, Catriona Baker, Gregory Arbia, Giovanni Biglino, Chiara Corsini, Silvia Schievano, Irene E.Vignon-Clementel, Gabriele Dubini, Giancarlo Pennati, AndrewTaylor, AdamDorfman, Anthony M.Hlavacek, Alison L. Marsden, Tain-YenHsia, Fancesco Migliavacca, for the Modeling Of Congenital Hearts Alliance (MOCHA) Investigators, Predictive modeling of the virtual Hemi-Fontan operation for second stage single ventricle palliation: Two patient-specific cases, Journal of Biomechanics 46 (2013) 423–429.

49. Hjortdal, V. E., K. Emmertsen, E. Stenbøg, T. Fru¨ nd, M. Rahbek Schmidt, O. Kromann, K. Sørensen, and E. M. Pedersen. Effects of exercise and respiration on blood flow in total cavopulmonary connection: A real-time magnetic resonance flow study. Circulation 108:1227–1231, 2003.

50. Itatani, K., Miyaji, K., Tomoyasu, T., Nakahata, Y., Ohara, K., Takamoto, S., and Ishii, M., Optimal Conduit Size of the Extracardiac Fontan Operation Based on Energy Loss and Flow Stagnation, Ann Thorac Surg 2009, Vol. 88, pp. 565–573.

51. Argueta-Morales, I.R., Tran, R., Ceballos, A., Osorio, R., Clark, W., Divo, E., Kassab, A., William M. DeCampli, Mathematical modeling of patient-specific ventricular assist device implantation to reduce particulate embolization rate to cerebral vessels, ASME Journal of Bioengineering, 2014, Vo. 136, No. 7, pp. 071008-1 - 071008-8.

52. Moghadam, M., Migliavacca, F., Vignon-Clementel, I., Hsia, T.Y., and Marsden, A., Optimization of Shunt Placement for the Norwood Surgery Using Multi-Domain Modeling, ASME Journal of Biomechanical Engineering, May 2012, Vol. 134, pp. 051002-1-12.

53. Migliavacca, Pennati, G., Dubinin, G., Fumero, R., Pietrabissa, R., Urcelay, G., Bove, E., HSIA, T.Y., and De Leval, M., Modeling of the Norwood circulation: effects of shunt size, vascular resistances, and heart rate, Am. J. Physiol. Heart Circ. Physiol., 280: H2076–H2086, 2001.

54. Waite L, Fine J. Applied Biofluid Mechanics. The McGraw-Hill Companies, Inc; 2007.

55. Szabo, G., Soans, D., Graf, A., Beller, C. J., Waite, L., and Hagl, S., A New Computer Model of Mitral Valve Hemodynamics During Filling, European J. of Cardio-Thoracic Surgery, 2004, Vol. 26, pp. 239-247.

56. Vukicevic M, Conover T, Chiulli J, Pennati G., Hsia TY, Figliola RS. Mock Circulatory System of the Fontan Circulation to Study Respiration Effects on Venous Flow Behavior, ASAIO J, 2013; 59(3).

57. Biglino G, Schievano S, Baker C, Giardini A., Figliola RS, Taylor A., Hsia TY, In-vitro study of the Norwood palliation: a patient-specific mock circulatory system, ASAIO Journal, 2012;58(1):25-31

58. Figliola RS, Giardini A, Conover T, Camp TA, Biglino G, Chiulli J, Hsia TY. In vitro simulation and validation of the circulation with congenital heart defects. Progress in Pediatric Cardiology 30 (2010) 71–80.

59. William Clark, (M.S. 2012), A Bench Top Study of the Optimization of the LVAD Cannula Implantation to Reduce Risk of Cerebral Embolism, M.S. Thesis, UCF, 2012.

60. Secasanu V, Argueta-Morales IR, Cox K, Ionan C, Kassab AJ, DeCampli WM. Systemic-to-pulmonary artery shunt counterpulsation prevents diastolic coronary blood flow runoff. J. Am. Coll. Surg. 2013; 217(3S):36. Presented at the Surgical Forum of the American College of Surgeons 99th Annual Clinical Congress on Oct, 2013. Washington, DC.

61. Goldberg DJ, Shaddy RE, Ravishankar C, Rychik J. The failing Fontan: etiology, diagnosis and management. Expert Rev Cardiovasc Ther. 2011;9(6):785-93.

62. Hebson CL, McCabe NM, Elder RW, Mahle WT, McConnell M, Kogon BE, Veledar E, Jokhadar M, Vincent RN, Sahu A, Book WM. Hemodynamic phenotype of the failing Fontan in an adult population. Am J Cardiol. 2013;112(12):1943-7.

63. Senzaki H, Masutani S, Ishido H, Taketazu M, Kobayashi T, Sasaki N, Asano H, Katogi T, Kyo S, Yokote Y. Cardiac rest and reserve function in patients with Fontan circulation. J Am Coll Cardiol. 2006;47(12):2528-35.

64. Lunze FI, Lunze K, McElhinney DB, Colan SD, Gauvreau K, Lange PE, Schmitt B, Berger F. Heterogeneity of regional function and relation to ventricular morphology in patients with fontan circulation. Am J Cardiol. 2013;112(8):1207-13.

65. Lambert E, d'Udekem Y, Cheung M, Sari CI, Inman J, Ahimastos A, Eikelis N, Pathak A, King I, Grigg L, Schlaich M, Lambert G. Sympathetic and vascular dysfunction in adult patients with Fontan circulation. Int J Cardiol. 2013;167(4):1333-8.

66. de Leval MR. The Fontan circulation: a challenge to William Harvey? Nat Clin Pract Cardiovasc Med. 2005;2(4):202-8.

67. La Gerche A, Gewillig M. What Limits Cardiac Performance during Exercise in Normal Subjects and in Healthy Fontan Patients? Int J Pediatr. 2010;2010. pii: 791291.

68. David J. Goldberg, MD Hypoplastic Left Heart Syndrome The Children Hospital of Philadelphia 2013 http://www.chop.edu/conditions-diseases/hypoplastic-left-heart-syndrome-hlhs/about#.VgCeX99VhBc

69. Shahabuddin S[1], Fatimi S, Atiq M, Amanullah M. Kawashima operation: functional modification of bidirectional Glen shunt with left superior vena cava in single ventricular morphology. J Pak Med Assoc. 2009 Jan;59(1):43-5.

70. Krishan B. Chandran, Stanley E. Rittgers, Ajit P.Yoganathan Biofluid Mechanics: The Human Circulation, Second Ddition ISBN-13: 978-1439845165

71. Sadao Isotani, Walter Maigon Pontuschka , Seiji Isotani An Algorithm to Optimize the Calculation of the Fourth Order Runge-Kutta Method Applied to the Numerical Integration of Kinetics Coupled Differential Equations July 3, 2012

72. Tong Joe Lin, Harold G. Donnelly Gas bubble entrainment by plunging laminar liquid jets May 1966

73. Richard P. Brent SIAM Journal on Numerical Analysis - 10(2):pp. 327-344; Some Efficient Algorithms for Solving Systems of Nonlinear Equations

74. MATLAB version R2013A Massachusetts: The MathWorks Inc., 2015.

Figure References

[1] Hypoplastic left heart syndrome – Figure 1

http://bionews-tx.com/news/2013/07/29/ut-southwestern-researcher-contributes-to-study-identifying-genetic-mutation-linked-to-congenital-heart-disease/

[2]Norwood – Figure 2

http://www.severinbrenny.com/norwood_operation.html

[3]Fontan external internal and normal comparison - Figure 2

http://www.heartbabyhome.com/

[4] Fontan – Figure 2

http://www.severinbrenny.com/fontan_proceedure.jpg

[5] Entrainment – Figure 14

https://media.lanecc.edu/users/driscolln/RT112/Air_Flow_Fluidics/Air_Flow_Fluidics7.html

Appendix

A. A Equations